IDŐJÁRÁS

QUARTERLY JOURNAL
OF THE HUNGARIAN METEOROLOGICAL SERVICE

CONTENTS

****

http://www.met.hu/Journal-Idojaras.php

VOL. 118 * NO. 1 * JANUAR – MARCH 2014

IDŐJÁRÁS

Quarterly Journal of the Hungarian Meteorological Service

Editorial Office: Kitaibel P.u. 1, H-1024 Budapest, Hungary
P.O. Box 38, H-1525 Budapest, Hungary
E-mail: journal.idojaras@met.hu
Fax: (36-1) 346-4669

Indexed and abstracted in Science Citation Index Expanded™ and Journal Citation Reports/Science Edition
Covered in the abstract and citation database SCOPUS®

Subscription by mail:
IDŐJÁRÁS, P.O. Box 38, H-1525 Budapest, Hungary
E-mail: journal.idojaras@met.hu

IDŐJÁRÁS

Quarterly Journal of the Hungarian Meteorological Service
Vol. 118, No. 1, January – March, 2014, pp. 1–17

Risk analysis of the first and last frost occurrences during growing season of vegetables in the Elbe River lowland

Vera Potop[1]*, **Pavel Zahraniček**[2], **Luboš Türkott**[1], **Petr Štěpánek**[2], and **Josef Soukup**[1]

[1]*Czech University of Life Sciences Prague, Faculty of Agrobiology, Food and Natural Resources, Department of Agroecology and Biometeorology, Kamycka 129, 165 21 Prague 6 – Suchdol, Czech Republic*

[2]*Global Change Research Centre AS CR, Bědila 986/4a, 603 00 Brno, Czech Republic*

**Corresponding author E-mail: potop@af.czu.cz*

(Manuscript received in final form May 17, 2013)

Abstract–This study has, for the first time, analyzed in detail the risk occurrences of the last spring frost, first fall frost, and the length of the frost-free period during the growing season of vegetable crops at a high horizontal resolution of 10 km (CZGRIDS, ALADIN-Climate/CZ) in the Elbe River lowland. The daily minimum air temperature from 116 grid points throughout the studied area for the period 1961–2011 was used. The daily values of minimum air temperature ranges of 0 °C to −1.1 °C, −1.2°C to −2.2 °C, and below −2.2 °C were considered to constitute mild, moderate, and severe frosts intensities, respectively. Firstly, comprehensive analysis of the spatio-temporal variability of the date of the last spring frost, the date of the first fall frost, and the length of the frost-free period in the Elbe River lowland were provided. Secondly, a catalogue of the mean dates of the spring and fall frosts for the three frost severities (mild, moderate, and severe) and degrees of earliness (early, mean, and late ending/beginning), as well as the length of the frost-free period over the Elbe River lowland, was developed. Thirdly, to identify the areas with high-risk occurrences of damaging last spring frosts during the sowing/planting period of vegetables in the Elbe River Lowland.

According to the regional catalogue of frosts, an earlier ending of spring and a later beginning of fall frosts, simultaneous with the latest ending of the frost-free period, were recorded during the 1990s, 2000s, and 2010s. The severe spring frosts in the period of 1981–2011 ended earlier than in the period of 1961–1980; consequently, the end of the 20th and the beginning of the 21st century are suitable periods for the growth extension of species and varieties of vegetables with longer growing seasons and higher demands on temperature. Whereas the latest spring frost has ended on an earlier date across the Elbe lowland, the first frost date in the fall has generally been delayed to a later date.

Key-words: thermophilic, cold-resistant, frost-resistant vegetables, late spring frost, early fall frost, frost-free period

1. Introduction

Most of Europe experienced increases in the surface air temperature from 1901 to 2005, which amounts to a 0.9 °C increase in annual mean temperature over the entire continent (*Alcamo et al.*, 2007). In the mean temperature series for the Czech Republic determined for the period 1848–2000, the significant linear trend for the increase reached 0.69°C/100 years (*Brazdil et al.*, 2009). In context of global warming, *Karl et al.* (1993) noted an asymmetrical rise in temperature extremes that manifests as a swifter rise in minimum temperatures than in maxima, which resulted in a decrease in the diurnal temperature range. For example, in Australia and New Zealand, the frequency of days below 0 °C decreased with warming in daily minimum temperatures (*Plummer et al.*, 1999). *Easterling et al.* (2000) concluded that the number of frost days has decreased in every country (Australia, China, central and northern Europe, New Zealand, USA) where it has been examined.

For central Europe, *Menzel et al.* (2003) found a greater change in the frost-free period, most likely also due to the greater increase in daily minimum temperatures. Consequently, trees may not take advantage of the frost-free period as before but may profit from a reduced risk of damage by late spring frosts. *Scheifinger et al.* (2003) indicated that the occurrence date of the last spring frost in central Europe has been increasingly early during the last few decades.

Numerous studies have evaluated the variability in the frost events and associated statistics (e.g., *Thom,* 1959; *Easterling et al., 2000; Robeson,* 2002; *Tait* and *Zheng*, 2003; *Menzel et al., 2003; Scheifinger et al.*, 2003; *Rahimi et al.,* 2007; *Didari* et al., 2012). Nearly all of the studies in the previous decades have reported increases of the frost-free period. For example, *Bootsma* (1994) and *Shen et al.*, (2005) noticed an increased frost-free period, a later growing season end, and an increase in growing degree days for most of Canada. *Robeson* (2002) determined a trend toward earlier spring frosts in Illinois but no consistent trends in autumn frosts.

Variations in the frost-free period length and the timing of frost events can also be an important indicator of climatic change that may not be represented in mean conditions (*Robeson,* 2002; *Easterling et al.,* 2000). There are a large variety of extreme events, and their impacts can be highly variable. Our research examines the variations in the last spring frost, the first fall frost, and the frost-free period length for the Elbe River lowland in the Czech Republic as an indicator of climate variations in this region. Vegetable crops are the most sensitive to the timing of extreme cold events at the beginning and end of the growing season. Damage caused by late frosts in spring (or early frosts during fall) is a limiting factor, particularly in the case of fruits and vegetables in central Europe.

In the Czech Republic, research focusing on the risks of late spring and early autumn frosts and their impacts on agricultural production gained considerable attention during the 1960s and 1970s (*Stibral*, 1966; *Forgáč* and *Molnar*, 1967; *Pejml*, 1955, 1973). This subject has remained in the background of interest to climatologists, although frost is one of the most devastating weather events that diminishes agriculture productivity in the Czech Republic.

Therefore, there were three main objectives in this study: (i) comprehensive analysis of the spatio-temporal variability of the date of the last spring frost (LSF), the date of the first fall frost (FFF), and the length of the frost-free period (FFP) in the Elbe River lowland; (ii) estimation of the tendency of the last spring frost, the first fall frost, and the length of the frost-free period; and (iii) the evaluation of the risk occurrences of damaging last spring frosts during sowing/planting for thermophilic, cold-resistant, and frost-resistant vegetables.

2. *Methods and materials*

2.1. Quality control and homogenization of gridded datasets

Monthly and daily series of temperatures (mean, minimum, and maximum), rainfall and sunshine duration for period 1961–2011 were analyzed. A regular gridded network with a high horizontal resolution of 10 km (CZGRIDS, ALADIN-Climate/CZ) from the Czech Hydrometeorological Institute (CHMI) was applied (*Fig. 1a*). High-density gridded datasets allow very precise and detailed delimitation of the area in which frosts occur in comparison with the station network datasets. The station network in the Elbe River lowland has significantly fewer units located primarily in non-agricultural areas, and their data series are not complete. The gridded network was created using the technical series from 268 climatological and 784 rain-gauge stations of the CHMI network. From these technical series, new values for the regular 10×10 km grid network (ALADIN-Climate/CZ RCM outputs) were interpolated (*Štěpánek et al.* 2011a, 2011b). The spatial interpolation of the agroclimatological characteristics ranges between longitudes 13.7°E and 16.5°E and latitudes 49.6°N and 50.8°N. The lowest and highest altitudes of the gridded dataset were 169 m and 573 m above sea level, respectively.

In our approach, data quality control is carried out by combining several methods: (i) by analyzing difference series between candidate and neighbouring stations, i.e., pairwise comparisons (ii) by applying limits derived from interquartile ranges (this can be applied either to individual series, i.e., absolutely or to difference series between candidate and reference series, i.e., relatively), and (iii) by comparing the series values tested with "expected" (theoretical) values – technical series created by means of statistical methods for spatial data (e.g., IDW, kriging).

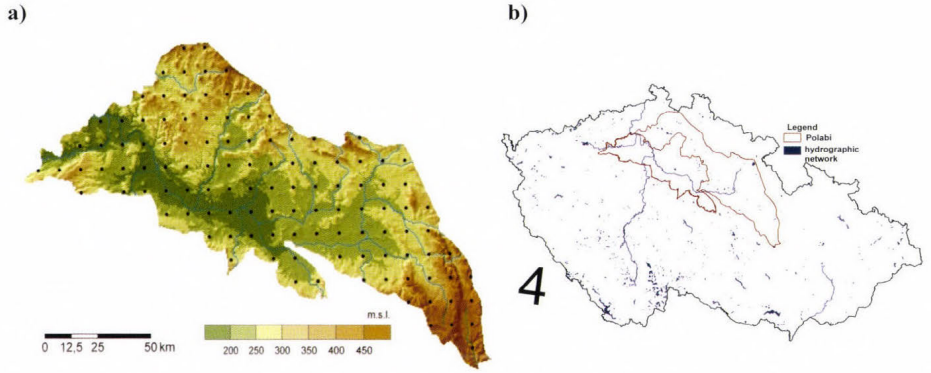

Fig. 1. (a) Location of the 116 grid points and their elevation (m a.s.l.) situated in the Elbe River lowland and (b) geographic boundaries of the Elbe River lowland.

The relative homogeneity tests applied were: the standard normal homogeneity test (SNHT) developed by *Alexandersson* (1986, 1995), the Maronna and Yohai bivariate test (*Potter*, 1981), and the *Easterling* and *Peterson* test (1995). The reference series were calculated as a weighted average from five nearest stations (with the same period of observations as the candidate series) with statistically significant correlation. The power of weights (inverse distance) for temperature was taken as 1 and for precipitation as 3. All the procedures for quality control and homogenization have been carried out with the ProClimDB and AnClim softwares (*Štěpánek,* 2010). More details on quality control and homogenization procedures are provided in *Štěpánek et al.* (2011a, 2011b).

2.2. Study region

The Elbe River lowland is the traditional and informal name for a lowlands region located in the Central Bohemian Region of the Czech Republic (*Fig. 1a-b*). The gridded data of the annual and growing season temperatures (mean, minimum, and maximum), rainfall, and sunshine duration were spatially averaged using ArcGIS Spatial Analyst extension over the Elbe River lowland. The results are presented in *Table 1*. In the Elbe River lowland, the mean long-term annual precipitation total was 591.6 mm compared with the 674 mm average for the entire territory of the Czech Republic. This precipitation primarily falls in the summer (40% of annual totals). In the growing season, the mean precipitation totals are 365 mm (*Table 1*). A significant excess of precipitation during some periods can result in catastrophic flooding (e.g., as in the year 2002), whereas a long-term lack of precipitation can contribute to extreme drought incidences (*Tolasz* et *al.*, 2007; *Potop,* 2010, *Potop et al.*, 2011).

Table 1. Areal averages of the basic agroclimatological characteristics determined using ArcGIS Spatial Analyst extension over the Elbe River lowland for the period 1961–2000. These averages are over all 116 grids (λ=13.7°E – 16.5°E; φ=49.6°N – 50.8°N, h=169 to 573 m a.s.l.)

	T_{mean} °C	T_{max} °C	T_{min} °C	Rainfall mm	Sunshine hours
Growing season					
Mean	14.5	20.5	8.9	365.0	1160.0
Minimum	12.7	17.8	7.4	304.7	1002.0
Maximum	15.6	21.4	10.0	461.1	1257.6
Range	2.9	3.6	2.6	156.4	255.6
Annual					
Mean	8.4	13.1	3.9	591.6	1574.2
Minimum	6.6	10.6	2.6	460.5	1327.2
Maximum	9.4	14.0	4.9	849.7	1730.3
Range	2.8	3.4	2.3	389.2	403.1

The annual mean temperature (T_{mean}) at the Elbe River lowland and in the country is 8.4 °C and 7.5 °C, respectively. The mean temperature during the growing season is 14.5 °C. The mean annual maximum (T_{max}) and minimum (T_{min}) temperatures are 13.1 °C and 3.9 °C, respectively. The average T_{max} and T_{min} during the growing season are 20.5 °C and 8.9 °C, respectively. The mean annual sunshine totals reach 1574.2 hours, whereas, in the growing season, the total is 1160 hours (*Table 1*).

The T_{mean} during the growing season ranges between 12.7 °C and 15.6 °C. The majority of the Elbe River lowland area had T_{mean} values from 14.5 °C to 15.0 °C. In terms of the mean T_{min}, the lowest values (less than 7.5 °C) were centered in the northern part of the Elbe River lowland, which has an altitude higher than 450 m (*Fig. 2a*). The mean T_{min} varies from 7.4 °C to 10.0°C over the Elbe River lowland territory. The mean T_{max} during the growing season ranged between 17.6 °C and 21.4 °C, while a small area had T_{max} values less than 18.5 °C (*Fig. 2b*). The mean precipitation total in the growing season fluctuates between 304 and 461 mm, but in a large portion of the Elbe River lowland, total precipitation is less than 350 mm. The mean sunshine duration total ranges from 1000 to 1257 hours, but the maximum value is received in the central portion of the Elbe River lowland. The warmest and longest duration of sunshine and the lowest precipitation totals during the growing season occur in the middle to lower reaches of the Elbe River, between Poděbrady and Litoměřice. As a practical recommendation, the authors suggest that this region may be suitable for cultivation of thermophile vegetable crops in combination with an irrigation system that would assure the qualitative yields (*Potop et al.*, 2012; *Potop et al.*, 2013).

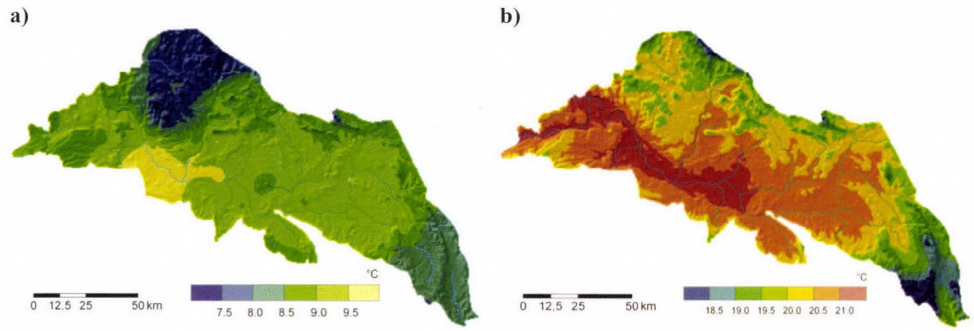

Fig. 2. Spatial distribution of the minimum (a) and maximum (b) temperatures during the growing season (April-September) for the period 1961–2000 over the Elbe River lowland.

2.3. *Determining the dates of the last spring first fall frosts, and the length of the frost-free period*

The daily minimum air temperature from 116 grid points throughout the studied area for the period 1961–2011 was used (*Fig. 1a*). For each grid point and for each year, the first and the last frost day and the frost-free period (i.e., the number of consecutive days from the date of the last frost with minimum air temperature greater than 0 °C) were identified. The LSF day is defined as the last date in a year on or before July 15 on which the daily minimum temperature $T_{min} \leq 0°C$. The FFF day is defined as the first date in a year after July 16 on which $T_{min} \leq 0°C$. The FFP is the number of days between the LSF and FFF.

The three degrees of frost severity were defined with regard to the physiological requirements of the vegetable types. The daily values of minimum air temperature ranges of 0 °C to −1. 1°C, −1.2 °C to −2.2 °C, and below −2.2 °C were considered to constitute mild, moderate, and severe frosts intensities, respectively (*WMO*, 1963). Using these definitions, the last three spring and first three fall frosts were specified for the spring and fall of each year. After determining the frost dates, it was necessary to transform them into a form that we could analyse statistically. For this purpose, Julian days (calendar days of the year) were used. These values were statistically processed, and we identified the mean, standard deviation, latest occurrence, earliest occurrence, and the length of the frost-free period. The extreme values were the latest beginning/ending, the earliest beginning/ending of spring and fall frosts and the shortest/longest FFP. The ending of the spring frost and beginning of the fall frost were classified into three categories: early, mean, and late. In this study, percentiles of date of spring and fall frosts for the fitted Gaussian distribution from 25 to 75% correspond to mean date of beginning/ending of frosts,

percentiles less than 25% are qualified as early date, and percentiles above 75% correspond to late date (*Table 2*).

*Table 2.*Classification of the timing of ending of the spring frost and beginning of the fall frost. The units used are Julian days

Categories	Percentile %	Last mild spring frost	Last moderate spring frost	Last severe spring frost	First mild fall frost	First moderate fall frost	First severe fall frost
early	< 25	< 102	< 92	< 86	< 284	< 290	< 294
mean	25–75	102–121	92–113	86–111	284–303	290–313	294–317
late	>75	>121	>113	>111	>303	>313	>317

3. Results and discussion

3.1. Statistical characteristics of the variability of frost series from 116 grid points

The mean, standard deviation, latest and earliest occurrence of the LSF and FFF, and length of the FFP are given in *Table 3*. The mean date of occurrence of the last mild spring frosts in the Elbe River lowland is on day 112 (April 22). The mean dates of the last spring frost with moderate and severe intensity were April 13 and April 8, respectively. The earliest last mild spring frost occurred on day 74 (March 15) in the period 1961–2011. The latest mild frosts occurred on day 164 (June 13). According to these results, the highest risk for field vegetables is a late spring frost.

Table 3. Statistical characteristics of the average frost series (at 116 grid points) of the studied area. The units used are dates and Julian days

	Last mild spring frost	Last moderate spring frost	Last severe spring frost	First mild fall frost	First moderate fall frost	First severe fall frost	Frost-free period
mean	112 (Apr 22)	103 (Apr 13)	98 (Apr 8)	293 (Oct 20)	302 (Oct 29)	305 (Nov 1)	180
STDev	15	16	14	15	17	16	25
earliest	74 (Mar 15)	59 (Feb 28)	65 (Mar 6)	260 (Sep 17)	270 (Sep 27)	276 (Oct 3)	93
latest	164 (Jun 13)	135 (May 15)	125 (May 5)	329 (Nov 25)	344 (Dec 10)	345 (Dec 11)	284

The earliest first mild fall frosts occurred on September 17, and the latest onset was November 25. Frosts with higher intensity occurred later, and the earliest beginnings of the moderate and severe frosts were on September 27 and October 3, respectively, whereas the latest onsets of moderate and severe frosts fell in the winter period on December 10 and 11, respectively. In the studied region, there were years with a possible extension of the growing season for frost-resistant vegetables, allowing distribution of the harvest. From the climatological point of view, this phenomenon indicates a delay in the onset of winter. The average length of the frost-free period was 180 days, almost half of the year.

3.2. Temporal evaluation of the frosts characteristic

3.2.1. Date of the last spring frost

Catalogues of the spring and fall frost dates of the three severities (mild, moderate, and severe), degrees of earliness (early, mean, and late ending/beginning), and the lengths of the frost-free periods were developed (*Table 4*). According to the timing (*Table 2*), the ending of the LSF and the beginning of the FFF, we can divide the earliness into three categories: early, mean, and late ending (beginning) to evaluate the impact of frost on the production of vegetables, where the highest risk is a late spring ending and early fall beginning of frosts. The mean dates of spring and fall frosts for three frost severities (mild, moderate, and severe) and earliness (early, mean, and late ending/beginning) and the length of the frost-free period was averaged over the Elbe River lowland for the period 1961–2011 (*Table 4*). As shown in *Table 4*, in the last two decades, the last mild spring frosts were concentrated into categories of early and mean ending, whereas in May they did not occur. Conversely, in the period from 1961 to 1980, the majority of cases were recorded in the mean and late ending categories of LSF. We observed that in the coolest decade of the 1970s (the lowest negative deviation of mean temperature since 1961), the majority of LSF and FFF events were concentrated in the late ending category. In this respect, the regional average of the late ending of mild spring frosts occurred in the first half of May in five consecutive years (1976, 1977, 1978, 1979, and 1980). At the same time, the years of 1977, 1979, and 1980 had shorter frost-free periods of 143, 152, and 156 days, respectively. Moreover, an extreme year in terms of the termination of the spring frost was 1976 with the latest end of the mild (May 4), moderate (April 25), and severe (April 30) frosts. This year, however, had an average length of the frost-free period (177 days), which was caused by the delayed onset of mild (October 30), moderate (November 17), and severe (November 26) fall frosts. The exceptionality of this year was also confirmed by a persistent extreme summer drought, and as a result, the yield was reduced for all vegetable types as well as for cereals in the

Czech Republic and central Europe (*Potop et al.*, 2011; *Potop et al.*, 2012; *Potop*, 2013).

Table 4. Mean dates of spring and fall frosts for three frost severities (mild, moderate, and severe) and earliness (early, mean, and late ending/beginning) and the length of frost-free period over the Elbe River lowland (1961–2011)

Year	Mild spring frost			Moderate spring frost			Severe spring frost			Frost-free period, days	Mild autumn frost			Moderate autumn frost			Severe autumn frost		
	Early	Mean	Late	Early	Mean	Late	Early	Mean	Late		Early	Mean	Late	Early	Mean	Late	Early	Mean	Late
1961	1 Apr			28 Mar			18 Mar			217			5 Nov			21 Nov			20 Nov
1962		28 Apr			22 Apr			9 Apr		173		19 Oct			25 Oct			26 Oct	
1963		28 Apr			17 Apr			8 Apr		169		14 Oct			23 Oct			9 Nov	
1964		23 Apr			2 Apr			27 Mar		167	8 Oct				25 Oct			1 Nov	
1965		28 Apr			3 Apr			29 Mar		166		12 Oct		15 Oct			18 Oct		
1966	11 Apr			2 Apr				28 Mar		202			30 Oct		3 Nov			31 Oct	
1967		28 Apr			19 Apr			4 Apr		177		23 Oct			4 Nov				14 Nov
1968		17 Apr			10 Apr			14 Apr		194		28 Oct			24 Oct			2 Nov	
1969		18 Apr			17 Apr			21 Apr		178		15 Oct				12 Nov		7 Nov	
1970		1 May			18 Apr			7 Apr		147	26 Sep			15 Oct				8 Nov	
1971		29 Apr			20 Apr			13 Apr		149	26 Sep			9 Oct			7 Oct		
1972	10 Apr				10 Apr				26 Apr	180	8 Oct			11 Oct			7 Oct		
1973			6 May		20 Apr			9 Apr		161		15 Oct			24 Oct		13 Oct		
1974		22 Apr		2 Apr				18 Apr		171	11 Oct				26 Oct			5 Nov	
1975		25 Apr			8 Apr			30 Mar		172		15 Oct			29 Oct			28 Oct	
1976			4 May			25 Apr			30 Apr	177			30 Oct			17 Nov			26 Nov
1977			12 May			24 Apr		19 Apr		143	3 Oct				25 Oct				24 Nov
1978			4 May			3 May		13 Apr		176		28 Oct			5 Nov				13 Nov
1979			7 May			6 May		3 Apr		152	7 Oct			15 Oct			18 Oct		
1980			12 May			7 May			26 Apr	156		15 Oct			23 Oct			28 Oct	
1981		30 Apr				24 Apr		20 Apr		176		24 Oct			3 Nov			9 Nov	
1982		30 Apr				26 Apr		20 Apr		182		30 Oct			8 Nov			6 Nov	
1983	9 Apr			2 Apr				28 Mar		190		17 Oct			28 Oct			28 Oct	
1984		26 Apr			20 Apr			19 Apr		184		28 Oct				13 Nov			29 Nov
1985		25 Apr			11 Apr			16 Apr		179		22 Oct			21 Oct			24 Oct	
1986	3 Apr				4 Apr			14 Apr		190	11 Oct				31 Oct				18 Nov
1987		24 Apr			8 Apr			27 Mar		184		26 Oct			4 Nov			3 Nov	
1988		22 Apr			15 Apr				25 Apr	190			29 Oct		30 Oct			27 Oct	
1989	10 Apr			30 Mar			23 Mar			190		18 Oct			7 Nov				16 Nov
1990		26 Apr			5 Apr			11 Apr		183		27 Oct			31 Oct			26 Oct	
1991			6 May		21 Apr			13 Apr		167		21 Oct			27 Oct			23 Oct	
1992		16 Apr			14 Apr			13 Apr		179		13 Oct		16 Oct			12 Oct		
1993	11 Apr				8 Apr			10 Apr		187		16 Oct			18 Oct			27 Oct	
1994		22 Apr			11 Apr			4 Apr		167	8 Oct			12 Oct			7 Oct		
1995		28 Apr			9 Apr			1 Apr		180		26 Oct			25 Oct			30 Oct	
1996		18 Apr			16 Apr			11 Apr		200			4 Nov		5 Nov				20 Nov
1997		24 Apr			20 Apr				23 Apr	170		12 Oct			21 Oct		20 Oct		
1998	11 Apr				2 Apr			6 Apr		199		28 Oct			6 Nov			12 Nov	
1999		15 Apr			14 Apr			28 Mar		186		19 Oct			26 Oct			21 Oct	
2000	4 Apr				3 Apr		16 Mar			210			31 Oct			28 Nov			18 Nov
2001		16 Apr			14 Apr			2 Apr		208			10 Nov			11 Nov		7 Nov	
2002	8 Apr				6 Apr			10 Apr		194		21 Oct			3 Nov			4 Nov	
2003		14 Apr			5 Apr			12 Apr		180		12 Oct			19 Oct		17 Oct		
2004		18 Apr			9 Apr		19 Mar			187		23 Oct			20 Oct			24 Oct	
2005		28 Apr			10 Apr				22 Apr	190			5 Nov			11 Nov		22 Oct	
2006	11 Apr				4 Apr			6 Apr		197		27 Oct			31 Oct			30 Oct	
2007		28 Apr			17 Apr			9 Apr		176		22 Oct		15 Oct				6 Nov	
2008		13 Apr			12 Apr			30 Mar		192		23 Oct			4 Nov			7 Nov	
2009	2 Apr			27 Mar			26 Mar			205		25 Oct			2 Nov				20 Nov
2010		18 Apr			10 Apr			28 Mar		175	11 Oct			15 Oct				23 Oct	
2011		29 Apr				28 Apr		5 Apr		171		19 Oct		17 Oct			20 Oct		

As we approach summer, the risk of the last spring frosts occurring after May 15 decreases. Extremely late occurrences of moderate spring frosts, reaching up to the month of June, were observed in 1975 and 1977 (June 6) and 1962 (June 3) (not shown). Severe frosts in June with intensities greater than –2.2 °C did not occur in any of the grid points during the entire study period.

3.2.2. Date of the first fall frost and the length of the frost-free period

The late onset of fall frosts extends the growing season of field vegetables. The longest lasting FFPs occurred in 1961 (217 days), 2000 (210 days), and 2009 (205 days) (*Table 4*). The shortest lasting FFPs occurred in 1977 (143), 1970 (147), and 1971 (149) (*Table 4*). In these years, the early beginnings of the mild fall frosts were on September 26. From 1970–1980, there were 6 years recorded with early beginnings of mild fall frosts, 4 years with early beginnings of moderate and severe frosts, and 9 years where the length of FFP was below average (180 days). According to the timing of frosts in 1980–1990, a mean fall frost beginning prevailed for all intensities, except for 1986, when mild frosts occurred on October 11 (early category) (*Table 4*). However, the severe fall frosts in 1986 had a late onset 38 days later (November 18). Usually, the first severe and moderate fall frosts occur closer to winter, after the mild ones. The period of the 1990s had a large number of years in which the severe fall frosts began earlier than mild frosts. In 1994, the FFP ended earlier due to the early beginning of the severe fall frosts (October 7), which occurred the day before the first mild frost. Similarly, in 1992, the severe fall frosts began on October 12, and the mild frosts began on October 13 (*Table 4*). In the first decade of the 21st century, such a situation occurred in 2001, when the severe fall frosts began approximately three days earlier than the mild frosts. This year also had the latest ending of the FFP (208 consecutive days, from April 10 to November 10) for the entire study period. The years with sudden commencement of the severe fall frosts are associated with the occurrence of an uncharacteristic synoptic situation for the fall season. The years 2010 and 2011 had an early beginning of fall frosts that occurred during the harvest period of root vegetables (*Table 4*).

An early ending of spring, together with the late onset of fall frosts in, e.g., 1961 (November 5) and 2000 (October 31), provides suitable conditions for sowing/planting of field vegetables, as well as their ripening and harvesting. However, our regional average frost date series suggests that the FFP exhibits a large amount of interannual variability, and it is also apparent that the region's average FFP has lengthened over the preceding two decades.

3.3. *Trends of changes in the last spring frost, first fall frost, and length of the frost-free period*

The change trends in the dates of the last and first frosts of the three severities, as well as the length of the frost-free period from 1961 to 2011 and their statistical significance according to a t-test (α=0.05) were evaluated. To study the mean tendency in the lowlands region, the results of individual grid points were averaged. For all thresholds, the linear trends of the start, end, and length of the frost-free period are plotted in *Fig. 3*. Overall, the last spring frosts display a decreasing trend, whereas the first fall frosts display an increasing tendency. The early start of the FFP and the consequent lengthening of the FFP also suggest an early ending of the spring frost for the last 51 years. This conclusion is confirmed by the results in *Fig. 3*, which indicate that, for the entire study region, the last mild spring frosts have shifted to an earlier date, and there is a trend of a 2-day earlier shift per decade on average. The last moderate and severe spring frosts have also shifted to an earlier date with a decadal trend of 1.5 days per 10 years. An early ending of spring frost is consistent with the increase of the region's daily minimum temperatures in the recent decades (*Potop et al.*, 2013).

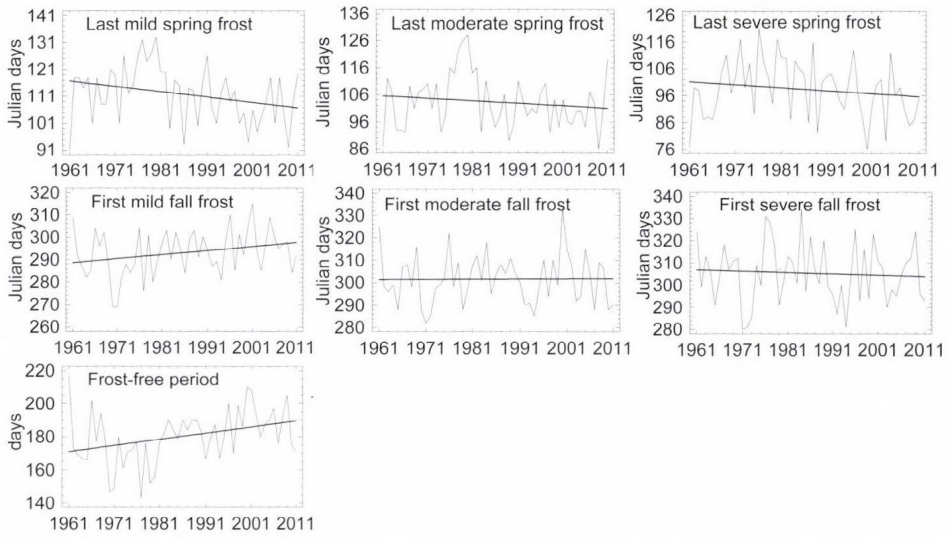

Fig. 3. Date change trends for the last spring frost and first fall frost of the three frost severities and length of frost-free period over the Elbe River lowland for the period 1961–2011.

The increases in the mean minimum temperatures have been demonstrated to have affected the length of the frost-free period (*Easterling et al.*, 1997; *Easterling et al.*, 2000). A pronounced trend towards higher daily minimum

temperatures can be observed, often coincidently with a decrease of the number of frost days over central Europe (*Scheifinger et al.*, 2003; *Menzel et al.* 2003), Australia, and New Zealand (*Plummer et al.,* 1999), the US (*Feng* and *Hu*, 2004) and large portions of the Earth's continents (*Easterling et al.,* 1997).

Whereas the latest spring frost has ended on an earlier date across the Elbe lowland, the first frost date in the fall has generally been delayed to a later date (*Fig. 3*). The delay of the first fall frost date exhibits a trend of 1.8 days per 10 years. There has been a general increase in the length of the frost-free period. The FFP is lengthening by up to 3.7 days per 10 years on average. The trend for the frost-free season displays two distinct periods: a shortening of the FFP in the 1960s and an intensified lengthening of the FFP since the 1980s. These changes are consistent with the global, European, and national temperature changes. For the first period, including the 1960s–1970s, the temperatures do not exhibit conspicuous changes, whereas in the second, beginning with the 1980s, significant warming is evident (*Brazdil et al.*, 2009).

The lengthening FFP in lowlands was primarily a result of an earlier start of the growing season. The consequences to agriculture from these changes include a reduced risk of spring and fall frost damage to crops and a lengthened growing season for vegetable crops. The earlier LSF implies that consecutive warm days in the spring occur earlier and, hence, allow spring melts to occur earlier too. These conditions raise soil temperature earlier for seed germination and, thus, reduce the frost risk for spring crops. The delay of consecutive cold days in the fall improves the chances for crops to mature to a higher-quality yield (*Shen et al.,* 2005).

These changes in the last spring and the first fall frosts are also in general agreement with those in *Feng* and *Hu* (2004), *Menzel et al.* (2003), and *Shen et al.*, (2005). For example, in Germany (1951–2000), the dates of the last spring frost have advanced by 0.24 days per year on average. The respective fall dates are delayed up to 0.25 days per year, whereas the frost-free period is lengthening by up to 0.49 days per year (*Menzel et al.,* 2003).

3.4. Risk occurrences of damaging last spring frosts during sowing/planting for thermophilic, cold-resistan,t and frost-resistant vegetables

The aim here is to identify the areas with high-risk occurrences of damaging LSF during the sowing/planting period of vegetables in the Elbe River lowland. A wide assortment of vegetables grown in the studied region has been divided into three basic types according to their sensitivity to low temperatures: *thermophilic vegetables* (heavy damage to plants in all development stages), *cold-resistant vegetables* (can tolerate a short period of decreasing temperature slightly below 0°C), and *frost-resistant vegetable* (can tolerate a frost less than –2.2°C depending on development stage) (*WMO*, 1997). The per cent risk values of LSF occurrence during the sowing/planting of thermophilic (*Fig. 4a*), cold-

resistant (*Fig. 4b*), and frost-resistant vegetables (*Fig. 4c*) in the Elbe River lowland for the period 1961–2011 are given in *Table 5* and *Fig. 4*. According to the per cent values for frost occurrences, four types of frost risk areas were defined: low, moderate, high, and critical (*Fig. 4*).

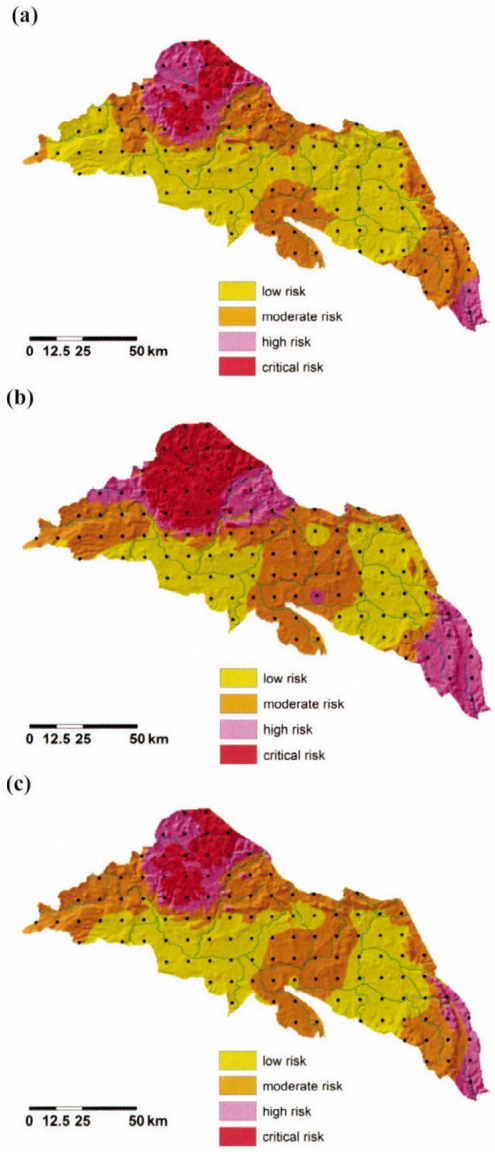

Fig. 4. Frost risk maps for last spring frosts during sowing/planting of thermophilic (a), cold-resistant (b), and frost-resistant (c) vegetables over the Elbe River lowland (1961–2011). Red indicates critical-risk areas, pink indicates high-risk areas, orange indicates moderate-risk areas and yellow indicates low-risk areas.

Table 5. Risk occurrences (%) of the last spring frosts during sowing/planting of thermophilic, cold-resistant, and frost-resistant vegetables in the Elbe River lowland (1961–2011)

Altitude m a.s.l.	Thermophilic t_{min} <–0.1 after May 15			Cold-resistant t_{min} <–2.2 after April 15			Frost-resistant t_{min} <–2.2 after April 1		
	mean	min	max	mean	min	max	mean	min	max
below 250	4.5	0	15.4	30.6	19.2	48.1	56.9	38.5	73.1
251–300	11.3	0	38.5	41	15.4	82.7	67.4	40.4	94.2
above 300	15.4	1.9	34.6	46.2	32.7	67.3	74.3	61.5	90.4

Thermophilic vegetables (e.g., tomato, pepper, pumpkins, and cucumber) from an agronomic point of view should be planted before May 15, considering risk (*Maly et al.*, 1998). The critical temperature after May 15 for thermophilic vegetables is Tmin $\leq$–0.1°C (*Table 5*). In areas with an altitude below 250 m, the risk of critical temperature occurrence is as high as 4.5%; at altitudes from 251 to 300 m, the risk is as high as 11.3%; and at altitudes above 300 m, the risk is as high as 15.4% (*Table 5*). The risk level of frost after May 15 in the traditional grown vegetable regions (up to 250 m) is low (*Fig. 4a*). At higher altitudes (251–300 m), areas with zero incidences of negative temperatures were found, which may allow for the possible expansion of thermophilic vegetable growth. The critical and high risks after May 15 are related to high altitudes in the region (higher than 300 m) and frost hollows, whereas low frost risk is observed in the lower areas (lower than 250 m) (*Fig. 4a*).

During the sowing/planting of *cold-resistant vegetables* (e.g., early kohlrabi, summer savoy cabbage, late cauliflower, late cabbage, late carrots, and celeriac), a severe LSF after April 15 has occurred every second year at higher altitudes. The risk levels for severe LSF occurrence (up to 250 m) are moderate (30.6%) at lower altitudes and high (46.2%) at higher altitudes (*Table 5*). Most vegetable growing areas fall within the low and moderate risk categories for severe spring frosts (*Fig. 4b*). It will be possible to extend the areas suitable for the growing of cold-resistant vegetables (i.e., mostly Brassicas) towards the north-east in the middle Elbe lowland.

Typically, the date of planting/sowing of *frost-resistant vegetables* (e.g., onion, root parsley) in the Czech Republic corresponds with the end of March, and a gradual shift occurs from the hottest regions of south Moravia towards the Elbe region. *Fig. 4c* defines two main areas with a low risk of severe frosts after April 1. The occurrence of severe frosts during the planting of frost-resistant vegetables in the growing area of the Elbe lowland is, on average, 56.9% (*Table 5*). It follows that, despite the considerable resistance of these vegetables to low temperatures, it is necessary to choose lands with southern exposure (or cover plants with non-woven textile). Utilizing resistant varieties and hardening seedlings before planting are advisable.

4. Summary and conclusions

This study has, for the first time, analyzed in detail the risk occurrences of the last spring frost, first fall frost, and the length of the frost-free period during the growing season of vegetable crops at a high horizontal resolution of 10 km in the Elbe River lowland. The main results for the period of 1961–2011 can be summarized as follows:

(i) The most frosts occurring during the vegetable growing season are the spring frosts in the last third of April. According to the frost series averaged over the Elbe River lowland region, the earliest and latest dates of the spring frost range have been March 15 and May 27, respectively. The earliest and latest dates of the fall frost range have been September 17 and November 25, respectively. The latest endings of the spring frost were recorded in 1973 (May 6), 1976 (May 4), 1977 (May 12), 1978 (May 4), 1979 (May 7), 1980 (May 12) and 1991 (May 6). Conversely, the earliest beginnings of the first frost were in 1970 and 1971 (September 26).

(ii) A catalogue of the mean dates of the spring and fall frosts for the three frost severities (mild, moderate, and severe) and degrees of earliness (early, mean, and late ending/beginning), as well as the length of the frost-free period over the Elbe River lowland, was developed. According to the regional catalogue of frosts, an earlier ending of spring and a later beginning of fall frosts, simultaneously with the latest ending of the frost-free period, were recorded during the 1990s, 2000s, and 2010s. The shortest frost-free periods were recorded in 1961–1970 and 1971–1980. The severe spring frosts in the period of 1981–2011 ended earlier than in the period, of 1961–1980; consequently, the end of the 20th and the beginning of the 21st century are suitable periods for the growth extension of species and varieties of vegetables with longer growing seasons and higher demands on temperature. These results agree with other studies conducted at a European scale (*Menzel et al.,* 2003, *Scheifinger et al.*, 2003).

(iii) The real risk of late frost damage for vegetable crops have been lower during the last three decades (1990s, 2000s, and 2010s) than estimated in the previous decades (1970s and 1980s). These results corroborate other research, indicating that spring frost is a critical period for detecting recent climatic changes and their impacts (*Robeson*, 2002; *Easterling et al.*, 2000; *Scheifinger et al.*, 2003).

Acknowledgements: This research was supported by S grant of MSMT CR and projects 6046070901 and CZ.1.07/2.3.00/20.0248.

References

Alcamo, J., Moreno, J.M., Nováky, B., Bindi, M., Corobov, R., Devoy, R.J.N., Giannakopoulos, C., Martin, E., Olesen, J.E. and *Shvidenko, A.*, 2007: Europe. In: Parry, M.L., Canziani, O.F., Palutikof, J.P., van der Linden, P.J., Hanson, C.E. (Eds.), *Climate Change 2007: Impacts, Adaptation and Vulnerability*. Contribution of Working Group II to the Fourth Assessment Report of the Intergovernmental Panel on Climate Change. Cambridge University Press, Cambridge, UK, 541–580.

Alexandersson, A., 1986: A homogeneity test applied to precipitation data. *J. Climatol. 6*, 661–675.

Alexandersson, A., 1995: Homogenity testing, multiple breaks and trends. In: *Proc. 6th Int. Meeting on Stat. Climatology*, Galway, Ireland. 439–441.

Brazdil, R., Chroma, K., Dobrovolny, P. and *Tolasz, R.*, 2009: Climate fluctuations in the Czech Republic during the period 1961-2005. *Int. J. Climatol. 29*, 223–242.

Bootsma, A., 1994: Long term (100yr) climatic trends for agriculture at selected locations in Canada. *Climatic Change 26*, 65–88.

Didari, S., Zand-Parsa, S., Sepaskhah A.R., Kamgar-Haghighi, A.A. and *Khalili, D.*, 2012: Preparition of frost atlas using different interpolation methods in a semiarid region of south of Iran. *Theor. Appl. Climatol. 108*,159–171.

Easterling, D.R. and *Peterson, T.C.*, 1995: A new method for detecting undocumented discontinuities in climatological time series. *Int. J. Climatol. 15*, 369–377.

Easterling, D.R., Horton, B., Jones P.D., Peterson, T.C., Karl, R.R., Parker, D.E., Salinger, M.J., Razuvayev, V., Plummer N., Jamason, P. and *Folland C.K.*, 1997: Maximum and minimum temperature trends for the globe. *Science 277*, 364–367.

Easterling, D.R., Evans, J.L., Groisman, P.Y.A., Karl, T.R., Kunkel, K.E. and *Ambenje, P.*, 2000: Observed variability and trends in extreme climate events: a brief review. *B. Am. Meteorol. Soc. 81*, 417–425.

Forgač, P. and *Molnar, F.*, 1967: Spring frost in Western Slovakia region. In: *Proccedings of HMÚ*, Bratislava: SHMU, 9, 31–86.

Feng, S. and *Hu, Q.*, 2004: Changes in agro-meteorlogoical indicators in the contiguous United States: 1950-2000. *Theor. Appl. Climatol. 78*, 247–264.

Karl T.R., Knight R.W., Gallo, K.P. and *Peterson T.C.* 1993: A New Perspective on Recent Global Warming: Asymmetric Trends of Daily Maximum and Minimum Temperature. *B. Am. Meteorol. Soc. 74*, 1007–1023.

Maly, I., Bartos, J., Hlusek, J., Kopec, K., Petrikova, K., Rod, J. and *Spistitz, P.*, 1998: Field Vegetable Growing. Prague, Czech Republic. *Agrospoj* 64. (in Czech)

Menzel, A., Gert, J., Rein, A., Helfried, S. and *Nicole, E.* 2003: Variations of the climatological growing season (1951–2000) in Germany compared with other countries. *Int. J. Climatol. 23*, 793–812.

Pejml, K., 1955: Development and current status of predictions night frosts during the growing season. *Meteorol. B. 8*, 8–42. (in Czech)

Pejml, K., 1973: Secular evolution of frequency and intensity of spring frosts. In*: Proceedings of HMÚ. 19*, 8–42. (in Czech)

Plummer, N., Salinger, M.J., Nicholls, N., Suppiah, R., Hennessy, K.H., Leighton, R.M., Trewin, B., Page, Ch.M. and *Lough, J.M.*, 1999: Changes in climates extremes over the Australian region and New Zealand during the Twentieth Century. *Climatic Change 42*, 183–202.

Potter, K.W., 1981: Illustration of a New Test for Detecting a Shift in Mean in Precipitation Series. *Mon. Weather Rev. 109*, 2040–2045.

Potop, V., 2010: Temporal variability of daily climate extremes of temperature and precipitation in the middle Polabí (Elbeland) lowland region. *Scientia Agriculturae Bohemica. 41*, 140–148.

Potop, V., Koudela, M. and *Možný, M.*, 2011: The impact of dry, wet and heat episodes on the production of vegetable crops in Polabí (River Basin). *Scientia Agriculturae Bohemica. 42*, 93–101.

Potop, V., Možný, M. and *Soukup, J.*, 2012: Drought evolution at various time scales in the lowland regions and their impact on vegetable crops in the Czech Republic. *Agr. Forest Meteorol. 156*, 121–133.

Potop, V., 2013: The evolution of the assortment and yield of vegetable crops in relation to climate in Polabí. In *Proceedings of influence of abiotic and biotic stresses on properties of plants 2013*. Praha 13.–14.2.2013, 198–201. (in Czech)

Potop, V., Türkott, L., Zahradníček, P. and *Štěpánek, P.*, 2013: Evaluation of agro-climatic potential of Bohemian plateau (České tabule) for growing vegetables. *Meteorol. B.. 66*, 42–48. (in Czech)

Rahimi, M., Hajjam, S., Khalili, A., Kamalid, G.A. and *Stigter, C.J.*, 2007: Risk analysis of first and last frost occurrences in the Central Alborz Region, Iran. *Int. J.f Climatol. 27*, 349–356.

Robeson, S.M., 2002: Increasing growing-season length in Illinois during the 20th century. *Climatic Change 52*, 219–238.

Shen, S. S. P., Yin, H., Cannon, K., Howard A., Chetner S. and *Karl, T.R.*, 2005: Temporal and Spatial Changes of the Agroclimate in Alberta, Canada, from 1901 to 2002. *J. Appl. Meteorol. 44*, 1090–1105.

Scheifinger, H., Menzel, A., Koch, E. and Peter, Ch., 2003: Trends of spring time frost events and phenological dates in Central Europe. *Theor. Appl. Climatol. 74*, 41–51.

Stibral, J., 1966. Frequency of frosts during flowering apple trees. *Meteorol. B. 19*, 177–179. (in Czech)

Štěpánek, P. 2010: ProClimDB – software for processing climatological datasets. CHMI, regional office Brno. http://www.climahom.eu/ProcData.html

Štěpánek, P., Zahradníček, P., Brazdil, R. and *Tolasz, R.*, 2011a: Methodology of data quality control and homogenization of time series in climatology. Praha. 118.

Štěpánek, P., Zahradníček, P. and *Huth, R.*, 2011b: Interpolation techniques used for data quality control and calculation of technical series. An example of Central European daily time series. *Időjárás 115*, 87–98.

Tait, A. and *Zheng, X.* 2003: Mapping frost occurrence using satellite data. *J. Appl. Meteorol. 42*, 193–203.

Tolasz, R., Brazdil, R., Bulir, O., Dobrovolny, P., Dubrovsky, M., Hajkova, L., Halasova, O., Hostynek, J., Janouch, M., Kohut, M., Krska, K., Krivancova, S., Kveton, V., Lepka, Z., Lipina, P., Mackova, J., Metelka, L., Mikova, T., Mrkvica, Z., Mozny, M., Nekovar, J., Nemec, L., Pokorny, J., Reitschlager, J.D., Richterova, D., Roznovsky, J., Repka, M., Semeradova, D., Sosna, V., Striz, M., Serlc, P., Skachova, H., Stepanek, P., Stepankova, P., Trnka, M., Valerianova, A., Valter, J., Vanicek, K., Vavruska, F., Vozenilek, V., Vrabik, T., Vysoudil, M., Zahradnicek, J., Zuskova, I., Zak, M. and *Zalud, Z.*, 2007: Atlas podnebí Česka. *Climate Atlas of Czechia*. ČHMÚ Praha, Univerzita Palackého v Olomouci, Praha-Olomouc, 254.

Thom, H.C.S., 1959: The distribution of freeze-date and freeze-free period for climatological series with freeze less years. *Mon. Weather Rev. 87*, 136–144.

WMO, 1963. Protection Against Frost Damage, WMO-No. 133. WMO, Geneva, Switzerland.

WMO, 1997. Definition of agrometeorological information required for vegetable crops. WMO-No. 866. WMO, Geneva, Switzerland. 110.

IDŐJÁRÁS

Quarterly Journal of the Hungarian Meteorological Service
Vol. 118, No. 1, January – March, 2014, pp. 19–40

Seasonality and geographical occurrence of West Nile fever and distribution of Asian tiger mosquito

Attila Trájer*[1,2], Ákos Bede-Fazekas[3], János Bobvos[4], and Anna Páldy[4]

[1] *Department of Limnology, University of Pannonia*
Egyetem u. 10, Veszprém 8200, Hungary

[2] *MTA-PE Limnoecology Research Group*
Egyetem u. 10, Veszprém 8200, Hungary

[3] *Corvinus University of Budapest, Faculty of Landscape Architecture*
Department of Garden and Open Space Design
Villányi út 29-43, H-1118 Budapest, Hungary

[4] *National Institute of Environmental Health*
Gyáli u. 2-6, Budapest 1097, Hungary

**Corresponding author E-mail: atrajer@gmail.com*

(Manuscript received in final form April 16, 2013)

Abstract—The importance and risk of emerging mosquito borne diseases is going to increase in the European temperate areas due to climate change. The present and upcoming climates of Transdanubia seem to be suitable for the main vector of Chikungunya virus, the Asian tiger mosquito, *Aedes albopictus* Skuse (syn. *Stegomyia albopicta*). West Nile fever is recently endemic in Hungary. We used climate envelope modeling to predict the recent and future potential distribution/occurrence areas of the vector and the disease. We found that climate can be sufficient to explain the recently observed area of *A. albopictus*, while in the case of West Nile fever, the migration routes of reservoir birds, the run of the floodplains, and the position of lakes are also important determinants of the observed occurrence.

Key-words: climate change, climate envelope model, vector-borne diseases, *Culex*, mosquitoes, *Aedes albopictus*, West Nile fever, Chikungunya disease

1. Introduction

1.1. Climate change and emerging mosquito-borne diseases

Within the class Insecta, the order Diptera has the greatest vectorial potential (e.g., flies, sand flies, mosquitoes) as vectors of important human infectious diseases. The most important family is Culicidae with such important genera as *Aedes* and *Culex*. Vector-borne diseases are sensitive to climatic conditions (*Githeko et al.*, 2000; *Harwell et al.*, 2002; *Hunter*, 2003; *Rogers* and *Randolph*, 2006). While the length of every development stages varies among species, it is common that it is greatly affected by the ambient temperature (*Rueda et al.*, 1990; *Bayoh* and *Lindsay*, 2003, 2004; *Teng* and *Apperson*, 2000). Global warming can cause the expansion and the increasing abundance of insect populations (e.g., pests of plants) by changing the length of vegetation period and moderation of the winter colds throughout Europe (*Cannon*, 2004; *Dukes* and *Mooney*, 1999; *Ladányi* and *Horváth*, 2010). Climate change can facilitate the migration of these arthropod vectors to north (*De la Roque et al.*, 2008). The projected warmer conditions are favored by mosquitoes and their parasites (*Epstein et al.*, 1998; *Reiter*, 2001). Since the adult mosquitoes have good flying ability, their expansion can be rapid. They are vectors of many serious viral infection, such as West Nile fever (hence: WNF) and Chikungunya disease which are re-emerging or emerging diseases in the Northern Hemisphere (*Meckenzie et al.*, 2004; *Reiter et al.*, 2006). The transmitters and main sources of the disease are *Culex* species.

While the potential mosquito vectors of West Nile virus (hence: WNV) live in the entire holarctic ecozone, theoretically West Nile virus may be endemic in every part of Eurasia and North America. In contrast to the theoretical investigations, the historical presence of WNF was less abundant. From this reason we aimed to study the climatic requirements of the disease itself and not those of the potential vectors. According to *Spielman* (2001), *Culex* mosquito populations begin to proliferate when the water temperature exceeds 15 °C during June, so the first stable week, when the ambient temperature reaches the 15 °C, can be used as the start of the WNF season.

Many of the potential vectors of WNV are native in Europe. As it is expected, the climate in the Carpathian Basin will be warmer, more arid, and will have extreme rainfalls more frequently in the colder half-year (*Bartholy et al.*, 2007). The increased frequency of heavy rainfall events, with consequential floodings may increase the incidence of mosquitoe-borne diseases and water-borne diseases (*Hunter*, 2003).

Chikungunya virus belongs to the family Togaviridae and is usually transmitted to humans by *Aedes* mosquitoes (e.g., the Asian tiger mosquito, *Aedes albopictus* Skuse (1894). Before 2006, Chikungunya disease and the *Aedes* mosquitoes were mainly reported from the sub-saharan Africa, the

Hindustan Peninsula, and Southeast Asia, but now the vector, *Ae. albopictus*, is presents widely in the Mediterranean Basin (in Spain, France, Italy, Slovenia, Croatia, Serbia, Bosnia and Herzegovina, Albania, and Greece).

Our aim was to study the influence of the ambient temperature and floods on WNF case number and to create a model to take into consideration the potential future distribution of West Nile virus and *Ae. albopictus* mosquito.

1.2. Climate envelope modeling

Ecological modeling methods are utilized in ecology to predict how species, diseases, or ecological structures will response to global warming or other changes of the ecological environment. To project the possible impact of climate change on the distribution of the selected vector, *Ae. albopictus*, and the occurrence of the disease WNF we used climate envelope modeling (CEM) method (*Hijmans* and *Graham*, 2006). *Fischer et al.* (2001) also used CEM to model the future expansion of *Ae. albopictus*. CEM is based on statistical correlations between the observed distributions of species (e.g., *Aedes albopictus* mosquito) or occurrences of diseases (e.g., WNF) and environmental variables to define the tolerance, the limiting ecological factors (e.g., minimum/maximum of temperature, precipitation, length of the vegetation season) of the species or the disease (*Guisan* and *Zimmermann*, 2000; *Elith* and *Leathwick*, 2009). Based on this bioclimatic envelope, using a selected climate scenario, one can predict the probable future range of the species/disease. The hidden and sometimes arguable idea of the CEM is assuming that climate plays primary role on the present and future distribution of the species (*Czúcz,* 2010). For example, in the case of a vector-borne infectious disease, the long-distance transport, the migrating workers and traveling can play a very important role as the determinant of the real geographical occurrence (*Walther et al.,* 2009; *Neghina et al.,* 2009).

1.3. Migrating birds, rivers, wetlands, and West Nile virus

Not only climatic factors determine the distribution of WNF. The principal vectors of the West Nile virus are *Culex pipiens* complex and *Culex modestus* (in Europe, *Culex* species and ticks in Russia also ticks, while migrating birds are the most important reservoirs and propagators of WNV) (*McLean et al.,* 2001; *Reed et al.,* 2003). Mosquitoes transmit the virus to birds, and then the next generation of the virus will infect the biting mosquitoes.

The mean water level and the changes of the water level of the rivers may have an important influence on the mosquito season.

WNV (a member of Flaviviridae) originally was autochthonous in Africa before the 1990's and it was first isolated in 1937, in the Sub-Saharan West Nile territory of Uganda. Then the virus was isolated from humans, birds, and mosquitoes in Egypt (Nile delta) in the early 1950s (*Hubálek* and *Halouzka*,

1999). In Europe it appeared at first, in Albania, 1958 (*Bárdos et al.,* 1959) and many of the early larger outbreaks were reported from the river deltas: from the Rhone delta in 1963 (*Hannoun et al.,* 1964), the Rumanian Danube delta in 1971 (*Topciu et al.,* 1971), and the Volga Delta in 1964 (*Chumakov et al.*, 1964).

Bird migration is the most important way of WNF/WNV introduction to the temperature areas (*Malkinson et al.,* 2002; *Reed et al.,* 2003). It is clear that rivers and riverbanks, coastal plains and deltas are the gathering and feeding places of migrating birds (*Malkinson et al.,* 2002). In Hungary also most of the cases occurred near to riversides, mainly between the riverbank of Tisza, Zagyva, and Rába, as it was seen in 2008. (*Krisztalovics et al.*, 2008).There are 3 main migration routes between Africa and Eurasia (via Gibraltar, via Sicily, via Sinai) (*Fig. 1A*), and one of them (*Fig. 1B*, red lines) makes connection between Eurasia and the eastern sub-saharan part of Africa, e.g., the West Nile territory (*Fig. 1B*), which is the most important migration route of white stork (*Ciconia ciconia* Linnaeus (1758) (*Berthold*, 2004), which bird species itself an important introducer of WNF (*Malkinson et al.,* 2002). It seems that migratory birds are the most important introductory hosts for the virus (*Rappole* and *Hubálek*, 2003). According to *Jourdain et al.* (2007), the risk for introduction of African pathogens, such as WNF into Mediterranean wetlands may be the highest from March to July, which is in accordance with the spring migration and breeding for birds.

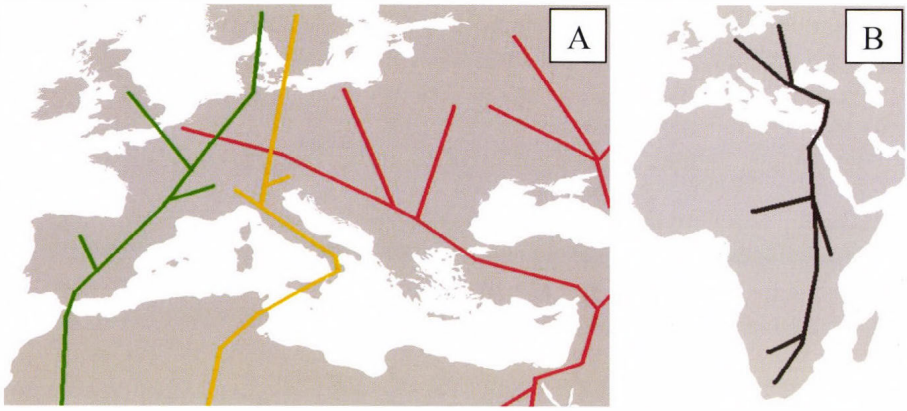

*Fig. 1.***A**: The simplified scheme of the main migration routes of birds between Africa and Europe. Red: Via Sinai per the Middle East from East Africa to Central and Eastern Europe, Yellow: Via Sicily per the Apennine Peninsula, Green: Via Gibraltar per the Hispanic Peninsula. The composite figure mainly was based on the migration routes of different birds of the homepage Global Register of Migratory Species. **B**: The right picture shows the eastern migration scheme route of white stark (Global Register of Migratory Species, *Ciconia ciconia*). Note, that the West Nile territory is an important part of their migration route.

1.4. The threshold minimum temperature of West Nile season

Since according to *Kilpatrick et al.* (2008), *Reisen et al.* (2006), and *Spielman* (2001) the temperature derived transmission of WNV from *Culex* mosquitoes to humans may be between 14–15 °C, we handle the 15 °C as the minimum temperature limit of the WNF season.

2. Materials and methods

2.1. Data sources

2.1.1. West Nile data of Hungary for the period of 2004–2010

The Hungarian WNF data was derived from the Hungarian Epidemiological and Surveillance System and Epinfo (2010A), Epinfo (2010B), and *Krisztalovics et al.* (2008). We could gain the geographical distribution data of the years 2008, 2010, 2011, and 2012.

2.1.2. The hydrological data of the river Tisza

The hydrological data of the river Tisza in the period of 2007–2012 were retrieved from the National Water Warning Network of Hungary (Hydroinfo). We averaged the monthly water levels of May to September. To depict the annual amplitude of the water regime, we used the difference between the annual maximum and minimum water levels.

2.1.3. Climate data

We used the REMO climate model (ENSEMBLES, 2013), which is nested into the ECHAM5 global climate model *(Roeckner et al.*, 2003, 2004) and is based on the IPCC SRES A1B scenario. The A1 scenarios suppose rapid economic and population growth, and rapid global transfer of technologies and knowledge (*Nakicenovic et al.*, 2000).

1961–1990 is the reference period of the REMO model, and the periods of 2011–2040 and 2041–2070 are the selected prediction periods. REMO has 25 km horizontal resolution and the entire Europe is within its domain. In our model we used about the 80% of the points of REMO.

2.1.4. Distribution and occurrence data

Since the model studied the climate requirements only of the European populations – the North African distribution segments were excluded –, it was able to project the shift of this part only. The distribution data of *A. albopictus* was derived from the VBORNET database of the European Centre for Disease

Prevention and Control according to stage in September 2012 (*Medlock et al.*, 2012).

The occurrence of WNF was also derived from European Centre for Disease Prevention and Control homepage and from the European Disease and European Centre for Disease Prevention and Control (ECDC) homepage (ECDC West Nile Fever Maps 2012 and 2011). Furthermore, we also used a publication of the Eurosurveillance journal (*Krisztalovics et al.*, 2008).

The Chironomidae (family Chironomidae) mosquito geographical presence data was derived from *Móra* and *Dévai* (2004). The original checklist and map was based on the review of the faunistical data in the period of 1990–2004. In these 104 years long period, 228 species were observed in Hungary and 98 species are expected to occur (*Móra* and *Dévai*, 2004).

We did not use weighting process, the distribution/occurrence maps of the mosquito and WNF was reduced to simple presence-absence maps. The regions entitled as 'indigenous' and 'recently present' of *Aedes albopictus* while in the case of WNF, the 'area reporting cases in 2012', 'area reporting cases in 2011', 'area reporting cases in 2010' were selected to be digitized. All the data were based on the NUTS3 regions, which are the third level public administration territories of the European Union. After a georeferencing process with third order polynomial transformation, the digitization of the bitmap-format distribution maps were realized with the assistance of the digital NUTS3 polygon borders (GISCO, 2013).

2.1.5. Population of the Hungarian regions

While we studied the regional WNF incidence rate of 2008, 2010, 2011, and 2012 (5-year-long short interval), we could use the population numbers of the year 2012. We retrieved the statistical data from the Central Statistical Office of Hungary (KSH, 2012).

2.2. Statistics

We applied descriptive statistics using SPSS 10.0 and Excel 2010 softwares.

2.3. Modeling method

According to *Thuiller et al.* (2004), climate has the greatest influence on forming the geographical distribution of the species in Europe. We used three physical (climate) factors averaged in the 30-year periods: the monthly mean temperature (T_{mean}, °C), the monthly minimum temperature (T_{min}, °C), and the monthly precipitation (P, mm) of the 12 months. This means 3×12 factors in the model.

Cumulative distribution functions were calculated by PAST statistic analyzer (*Hammer et al.*, 2001) for the selected 3×12 climatic parameters (T_{mean},

T_{min}, P). 10–10% from the extrema in the case of *Ae. albopictus* and 5–5% from the extrema in the case of WNF were neglected from the climatic values found within the observed distribution/occurrence. The selection of the amount of percentiles to be left from the climatic values was based on our former studies. The aim was to restrict the false positive error of the model result in a reasonably degree. We refined the climatic data by the inverse distance weighted interpolation method of ESRI ArcGIS 10 software. The modeling steps were the follows: first, the grid points within the distribution were quoted; second, the percentile points of the climatic parameters were calculated; third, the suitable percentiles of the climatic parameters were chosen; fourth, modeling phrases (3 strings) were created by string functions of Microsoft Excel 2007 for the three modeling periods; fifth, the ranges were selected where all the climatic values of the certain period were between the extrema selected in step 3.

3. Results

3.1. West Nile fever in the period of 2004–2012 in Hungary

3.1.1. Statistics

In Hungary, West Nile fever is recently endemic; 34 cases were reported in the period of 2004–2009 (*Krisztalovics et al.,* 2011; Epinfo, 2010A), 11 cases in 2010 (Epinfo, 2010B), 4 cases in 2011 and 12 cases in 2012 (ECDC, West Nile fever maps 2012). In the period of 2004–2012 WNF showed an increasing trend, but the annual incidence was low and highly variable (0–19/10 million) from year to year (*Fig. 2*), so the trend was not significant at 5% significance level.

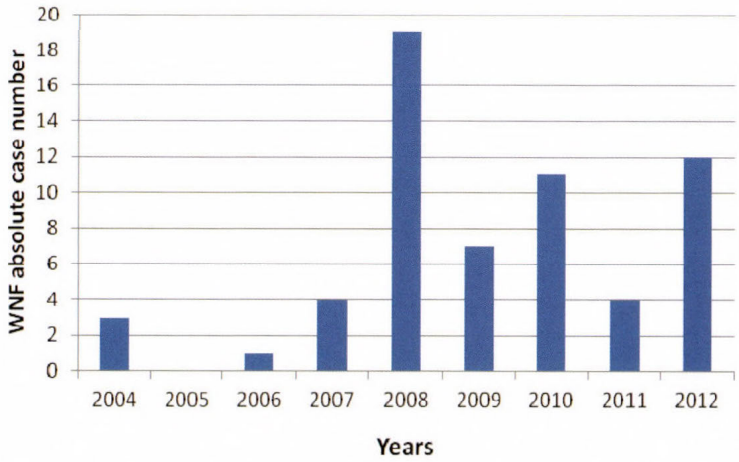

Fig. 2. The absolute annual WNF case number in the period of 2004–2012 in Hungary.

3.1.2. Regional distribution of the WNF incidences

The Hungarian regions correspond to the NUTS 2 statistical regions of the European Union. In 2008 and 2010–2012 (the geographical data of 2009 is missing), the highest WN incidence rates were observed in northern Great Plain (NGP; $6.6*10^{-6}$), southern Great Plain (SGP; $5.24*10^{-6}$), southern Transdanubia (STD; $5.2*10^{-6}$), and western Transdanubia (WTD; $5.01*10^{-6}$). In central Transdanubia (CTD; $3.62*10^{-6}$), northern Hungary (NH; $2.48*10^{-6}$), and central Hungary (CH; $2.41*10^{-6}$), the WNF average incidence of this 3 regions were about the half of the average incidence rate of NGP, SGP, STD, and WTD. The changing WNF incidence rate did not show any significant trends, and the geographic distribution of the cases showed that the focuses of occurrence changed from year to year (*Fig. 3*).

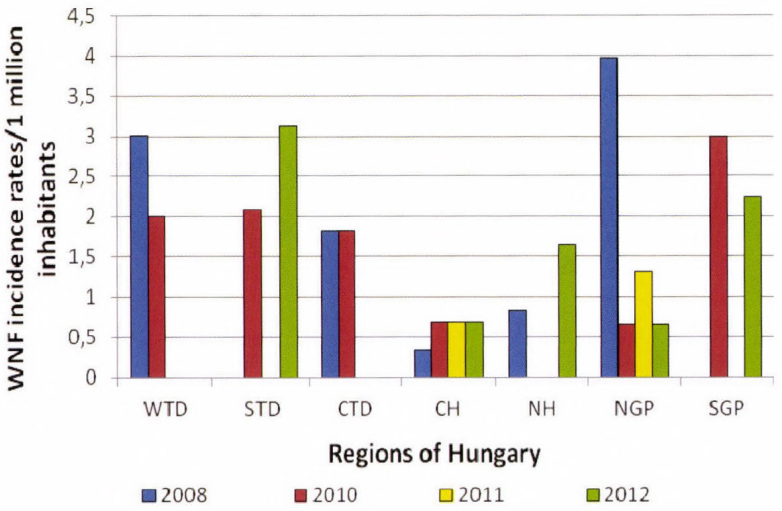

Fig. 3. WNF incidence rates per 1 million inhabitants in the different Hungarian regions in 2008 and 2010–2012 according to the population numbers of 2012. WTD=western Transdanubia, STD=southern Transdanubia, CTD=central Transdanubia, CH=central Hungary, NH=northern Hungary, NGP=northern Great Plain, SGP=southern Great Plain.

3.1.3. Seasonality

WNF showed a clear seasonality (*Fig. 4*). About the ¾ of the cases occurred in August and September. In most of the years the season started in late July (e.g.,

in the 30th week in 2010) or August (e.g., in 2007, 2008). No cases were recorded between December and March and in June.

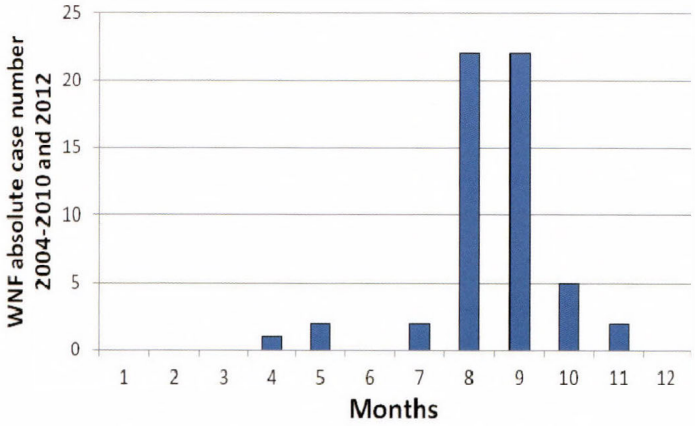

Fig. 4. The seasonal distribution of the WNF cases in Hungary in the period of 2004–2010 and 2012.

3.1.4. Ambient mean weekly temperature and WNF

In 2004–2010 and 2012, the 66.66% of the first symptoms of the disease cases occurred above 19 °C and 84,84% above 16 °C. The highest case numbers were observed between 21–21.9 °C weekly mean ambient temperatures (*Fig. 5*). No cases were observed under 10 °C. Note, that the incubation period of the infection with WNV is thought to range from 3 to 14 days (CDC), but the probability distribution of the latency interval is not known.

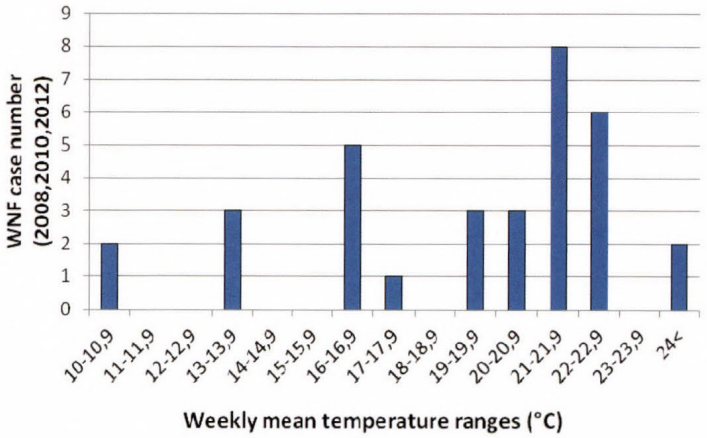

Fig. 5. The frequency histogram of weekly ambient temperatures of 2008, 2010, and 2012, and the number of the WNF cases.

3.1.5. West Nile season

The averaged ambient weekly temperature of the 4 previous weeks before the first WNF case was 21.6 °C in 2008 (*Fig. 4*), 23.82 °C in 2010 (*Fig. 5*), and 23.65 °C in 2012 (*Fig. 6*). 78.6% of the cases in the period of 2004–2010 and 2012 (the weekly data of 2011 is missing) occurred in August and September. In 2008 and 2010 the WNF cases terminated, when the weekly mean temperature dropped below 14.3–13.7 °C. In 2012 after the penultimate case, the ambient temperature dropped below 13.7 °C and the last case occurred, when the mean temperature was 7.5 °C. 19 weeks passed from the first stable week with 15 °C or more ambient temperature to the first WNF case 2008, 14 in 2010, and 13 in 2012.

As we mentioned in Section 2, we selected the weeks of the mean ambient temperature more than 15 °C as the season of *Culex* mosquitoes. According to these observations, we practically handled the period of May to September as the main time of the *Culex* season.

The *Culex* season started in the 18th week of the year (in mid-April) in 2008 and terminated in the 37th week in the first quarter of September. In 2008 the observed WNF season exceeded the theoretical *Culex* season by 2 weeks (*Fig. 6*).

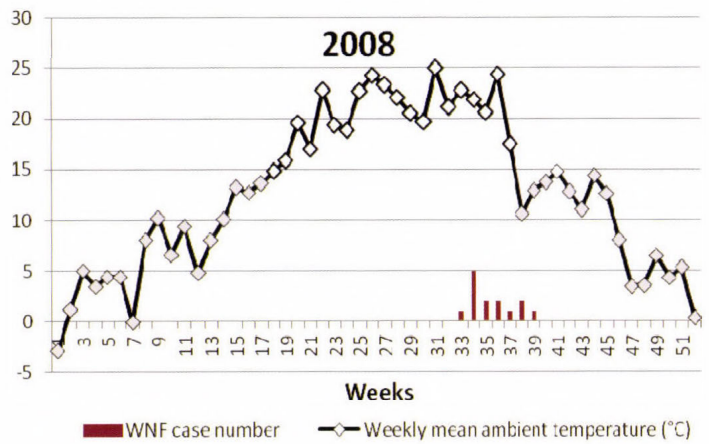

Fig. 6. The weekly ambient temperatures in 2008 and the absolute number of WNF cases. Light gray points mark the weeks, when the ambient temperature was less than 5 °C.

In 2010, the *Culex* season started in the 20th week in the start of May and terminated in the 35th week in late August. In 2009, the last case occurred in the last week of the theoretical season (*Fig. 7*).

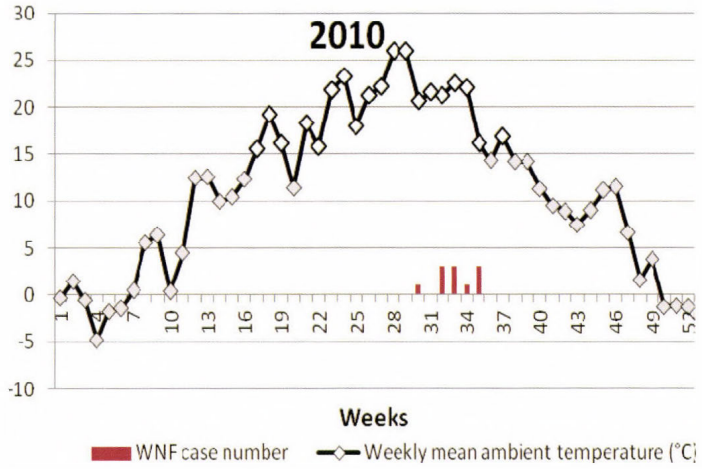

Fig. 7. The weekly ambient temperatures in 2010 and the absolute number of WNF cases. Light gray points mark the weeks, when the ambient temperature was less than 5 °C.

In 2012, the season started in the 16th week and terminated in the 43rd week in late October. In 2012, the last observed case exceeded the theoretical season by 4 weeks, the previous case occurred 1 week before the theoretical end of the mosquito season (*Fig. 8*).

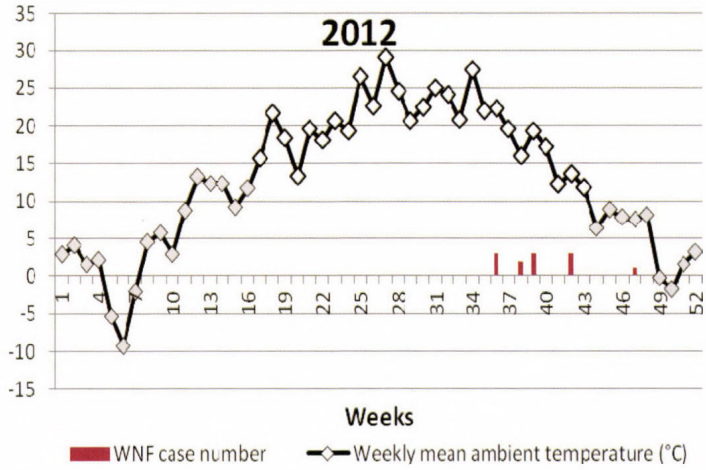

Fig. 8. The weekly ambient temperatures in 2012 and the absolute number of WNF cases. Light gray points mark the weeks, when the ambient temperature was less than 15 °C.

3.2. Floods and WNF in Hungary

3.2.1. Presence of Chironomidae mosquitoes as wetland indicators and WNF

From the first observed human WNF in Hungary in 2004 most of the cases were tied to the rivers Tisza, Raba, Drava, Zagyva, Körös, and Hernád channels (e.g., East Main Channel), and lake Balaton. The river Danube had a less importance. For example from January 2008 to September 2008, 8 WNF cases occurred in the Tisza valley and only 2 cases were observed in the Danube valley. Only 1–2 cases per year were matched to the river Danube. Since before 2007 the WNF level were very low (in the period 2004–2006 only 4 cases were observed), we used the period 2007–2012.

Despite the fact, that Chironomidae (non-biting) mosquitoes are not the vectors of WNF, this species are tied to wetlands, rivers in Hungary since the larvae live in aquatic or semi-aquatic habitats (*Móra* and *Dévai*, 2004). They are good water quality indicators as well, while the larvae can live in polluted waters (*Lindegaard*, 1995). The larvae of *Culex* mosquitoes are also live in aquatic habitats. In 2008, most of the WNF cases between May and September were linked to similar habitats (rivers, lakes, channels) as non-biting mosquitoes (*Fig. 9*).

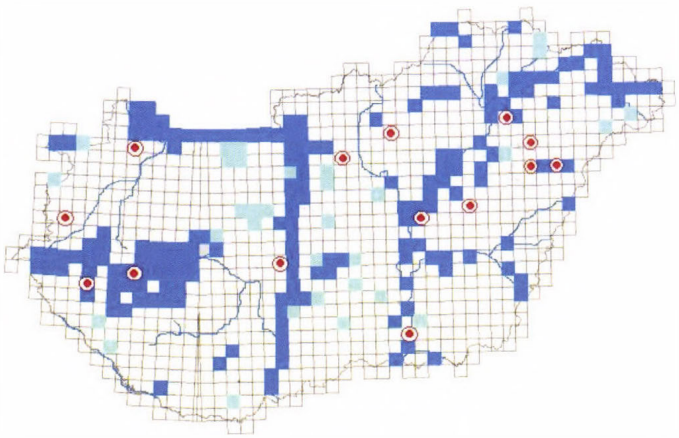

Fig. 9. The confirmed presence of Chironomidae mosquitoes (dark blue), the non-confirmed, but expected presence of Chironomidae mosquitoes (light blue) (according to *Móra* and *Dévai*, 2004), and the occurrence of WNF in 2008 between May and September (n=14) in 2008, Hungary (red circles within red spots; according to *Krisztalovics et al.*, 2008).

3.2.2. Amplitude of the water level changes of the rivers Tisza and Danube

The mean of the annual maximum and minimum water levels of river Danube was Δ=556 cm, since in the case of river Tisza it was 1.6 times higher: Δ=899 cm. (*Fig. 10*).

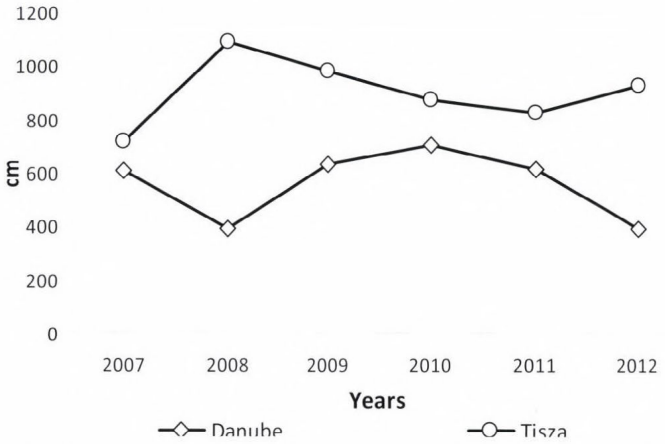

Fig. 10. Differences between the annual maximum and minimum water levels of the rivers Danube and Tisza in the period of 2007–2010.

3.2.3. Water level of the river Tisza at Szolnok (2007–2012)

Since over the Danube the number of the observed WNF cases was negligible under the studied period, we selected the river Tisza as a typical representative of the rivers in the Carpathian Basin, while the entire drainage basin of Tisza is within the Carpathian Basin, and the water regime of the Tisza is the consequence of the previous and the same year's precipitation patterns of the Carpathian Basin.

The average water level of Tisza between May and September in Szolnok (according to the long-time average, *l*) was the following: –71 cm in, 118.6 cm in 2008, –108 cm in 2009, 454.6 cm in 2010, –40.2 cm in 2011, and –99.6 cm in 2012. We calculated the own mean of the 6-year-long period, which was 42.4 cm. Thereafter, we calculated the water level differences from the mean: –113.4 cm in 2007, 76.2 cm in 2008, –150.4 cm in 2009, 412.2 cm in 2010, –82.6 cm in 2011, and –142 cm in 2012. After this process we calculated the percent values according to the absolute range –150.4 cm in 2009, 412.2 cm in 2010, absolute range 562.6 cm as 100%: –20.16% in 2007, 13.54% in 2008, –26.73% in 2009, 73.26% 2010, –14,68% in 2011, and –25.28% in 2012.

3.2.4. Changes in the WNF case number (2007-2012)

The case numbers of the years were the following: n=4 in 2007, n=19 in 2008, n=7 in 2009, n=11 in 2010, n=4 in 2011 and n=12 in 2012. The mean of the WNF case numbers was 9.5 cases per year in the period. We calculated the differences of the cases from the mean: –5.5 in 2007, 9.5 in 2008, –2.5 in 2009, 1.5 in 2010, –5.5 in 2011 and 2.5 in 2012. After this process we calculated the percent values of the differences according to the absolute range of the maxima and the minima of the WNF cases (–5.5 [2007, 2011]; 9.5 [2008]; absolute range)=15 as 100%): 36.6% in 2007, 63.3% in 2008, –16.6% in 2009, 10% in 2010, –36% in 2011 and 16.6% in 2012.

The comparison of the changes of the water level of the Tisza in Szolnok and the WNF cases- showed that five years from the six the sign (less or more than the mean, 0%) of this percent values changed simultaneously except the year 2012 (*Fig. 11*). The relative risk to the above-average number of WNF cases was 4 times higher when the mean level of the river Tisza was higher than the mean of the studied six years (WNF>mean and water level>mean: 2 years, WNF<mean and water level>mean: 0 year, WNF>mean and water level<mean: 1 year, WNF<mean and water level<mean: 3 years).

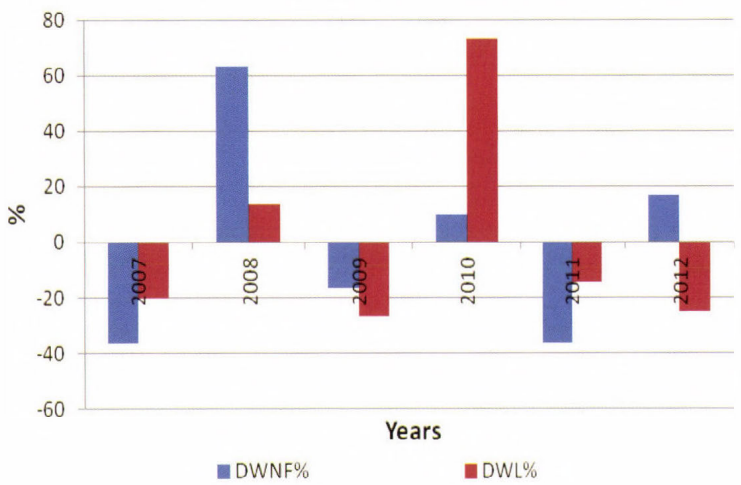

Fig. 11. The percent difference of the May-September mean water level of the period 2007–2012 within the absolute water level range of the river Tisza at Szolnok (DWL%) and the percent difference of the annual WNF case number in Hungary within the absolute water level range of the maxima and minima of the case inerval (DWNF%) in the period of 2007–2012.

3.3. Model results

3.3.1. The predicted occurrence of West Nile fever

The observed and predicted potential distributions of the WNF are shown in *Fig. 12*. The recent occurrence of visceral WNF is mostly restricted to the eastern Mediterranean areas and Eastern Europe. The model predicted the potential occurrence of WNF with the sporadic cases in the reference period to be greater than the observed current occurrence. The major difference can be seen in Spain. Future expansion is expected principally in Asia Minor, the Carpathian Basin, and the Balkan Peninsula, but the set of the affected countries is much larger: Spain, France and Hungary (mainly in the far future period), Serbia, Macedonia, Bulgaria, Romania, Ukraine, and Turkey. Considering the current occurrence and the model result, east-southeast Europe and the Carpathian Basin are highly vulnerable areas. In the western parts of Europe, the primary limiting value is the minimum temperature in July (T_{min} of July more than 20.9 °C). It seems that the continental climate with warm summers and September are favor of West Nile disease (T_{mean} from June to September should be more than about 22 °C). WNF need for moderate summer precipitation (P in July is less than about 80 mm).

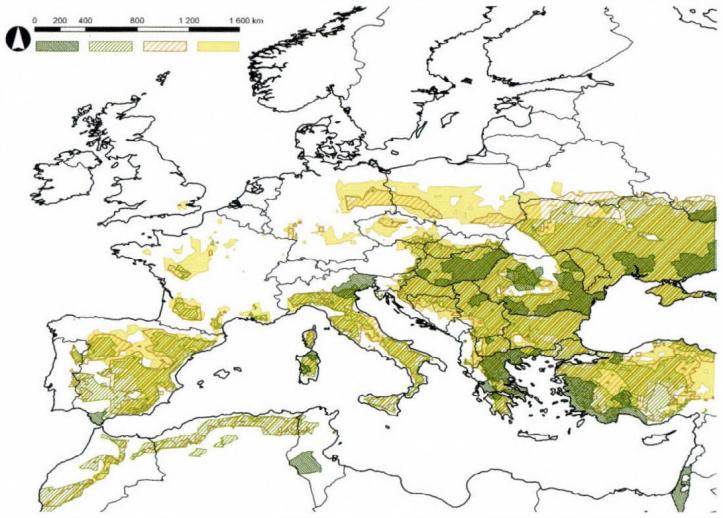

Fig. 12. The recent (2010–2012) distribution of WNF (dark green according to the VBORNET database), the potential distribution area for the reference period (1961–1990, light green), and the projected future distribution for the periods of 2011–2040 (orange) and 2041–2070 (yellow)

3.3.2. Predicted distribution of the Ae. albopictus mosquito

Observed and predicted potential distribution of the aggregation of the Asian tiger mosquito species are shown in *Fig. 13*. The Mediterranean, most of the territories of Italy, and some regions of the Balkan and Spain with Mediterranean climate are included in the observed distribution. The modeled potential distribution seems to be greater in Western Europe and in the north Balkan, and some parts of the Carpathian Basin. In the near future period expansion is predicted mainly in France, Spain, Croatia, Serbia, and Hungary. In the period of 2041–2070, significant expansion is projected in the northern parts of France. The primary limiting value is the minimum temperature in January (T_{min} should be more than about –2 °C), *Ae. albopictus* prefers the relatively dry summers (P in July is less than about 6 mm).

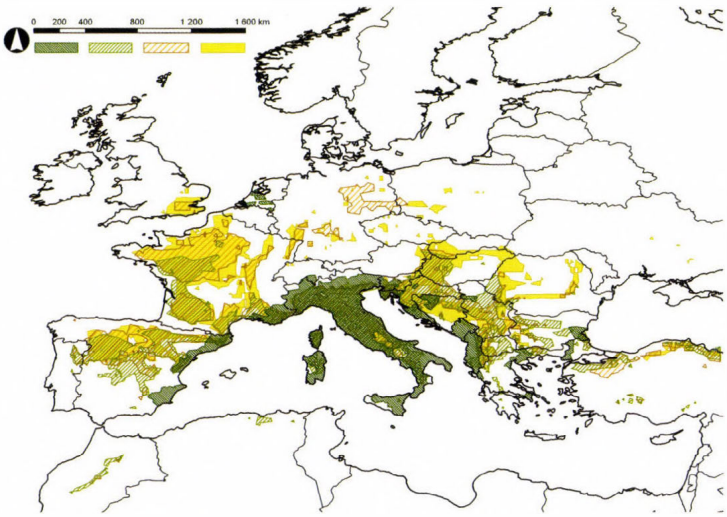

Fig. 13. The recent (2012) distribution of *A. albopictus* mosquito (dark green according to the VBORNET database), the potential distribution area for the reference period (1961–1990, light green), and the projected future distribution for the periods of 2011–2040 (orange) and 2041–2070 (yellow).

4. Discussion

The comparison of the recent and predicted future distributions of a vector and a vector-borne diseases, at first aspect, may seem to be problematic, but the recent geographical range of WNF is cannot be explained without the climate factors. The most important determinants of the spatial range of *Ae. albopictus* are climate factors according to our model.

The recent distribution of WNF suggests that climate, topographically the run of the rivers, floods, the migrating routes of birds, and the annual ontogeny of *Culex* mosquitoes together determine the occurrence of the disease.

The annual features of the epidemics suggest brief exposures in multiple focuses. In contrast to the Lyme disease occurrence in Hungary (Lyme disease is also an emerging vector-borne disease) WNF did not show constant occurrence pattern in 2008 and 2010–2012. It may explained by the fact, that in the case of Lyme disease, the parasite permanently persists in the local tick and host animal populations, while it is plausible, that birds recurring from Africa and the Mediterranean wetlands are re-introduce WNV into Hungary every year. It also explains the very low incidence of WNF in Hungary.

Our findings showed that floods have an important influence on annual WNF case number. There are differences between the major rivers, since over the larger Danube less WNF cases were observed in every year than between the smaller, but more natural rivers as Tisza and its tributaries, which have backwaters, wreaths and high amplitude water level changes. The high water level fluctuation can play an important role to create the appropriate conditions for mosquito populations (as this phenomenon is known in the case of *Anopheles darlingi* Anopheles Meigen (1818) malaria mosquitoe; *Rozendaal*, 1992) and consequently for the presence of WNF. The water level of Tisza as a characteristic representative of the rivers of the Carpathian Basin and the annual WNF case number simultaneously changed between 2007 and 2011. We studied separately the year of 2012 and we found, that the contradiction was apparent, since most of the cases occurred in Transdanubia and not in the Tisza valley thanks to the extraordinary low water level of the Tisza in this year.

According to *Epstein* (2010), the epidemic of WNF is ecologically similar to that of the St. Louis encephalitis, since these two vector-borne diseases are connected to long, hot, and dry (continental) summers with occasionally wet summers, when the case number generally is the highest. Extreme summer rainfalls are favored by WNF, and the increasing amount of extreme meteorological events are one of the consequences of climate change (*Fay et al.*, 2008; *Meehl et al.*, 2000). It may explain the observations, since the year of 2010 in Hungary was unusually wet; the total annual rainfall was two times higher than the average of the last 100 years, the 25% of the cases occurred in this year. Naturally, we cannot make conclusions based on the observations of a single year.

In the case of the *Aedes* mosquito, the connection between the climate and the geographical distribution is the clearest. The main determinants of the European distribution of *Ae. albopictus* are climatic conditions, mainly the mean temperature in July, the minimum temperature in January, and the low precipitation of the summer months (Mediterranean summers). Climatically the geographical occurrence of WNF is partly determined by the warm ambient

temperature of July and August with wet summers. According to the VBORNET (2012) database, the recent occurrence of WNF in Europe is mainly similar to the migration route of white stork from the east sub-saharan Africa (e.g., Uganda, by via Sinai) to central and eastern Europe. Although climatic factors alone cannot explain the observed occurrence of West Nile virus, they indicate that dry and warm summers, and heavy rainfalls can enhance the population density of *Culex* mosquitoes (*Reeves et al.*, 1994; *Reiter*, 2001). According to *Sellers* and *Maarouf* (1990), warm winds may carry infected mosquitoes from the dry riverbanks to northern areas. The above described extreme weather events are specific to continental climate conditions, where the disease recently occurred.

The seasonality of WNF is regular as far as it can be judged from the low case number of the last decade, it starts in late July, has a peak from August to mid-September and declines, when the weekly mean ambient temperature drops below 13–14 °C. Climate change may cause a shift in the WNF season elongating the hottest period of summer and enhancing the warmer period of the autumn season. This seasonality may correspond to the spring early summer migration of birds (*Jourdain et al.*, 2007), in the sense that time needs to ensure a sufficient number of mosquito contaminate with the virus for the chance of human transmission.

In contrast to, e.g., *Culex pipiens* or *Culex modestus, Ae. albopictus* mosquito prefers the more balanced conditions and milder winters of subtropical coasts of the Mediterranean basin. Higher summer precipitation seems to be a major limiting factor in the model for *Ae. albopictus*, which is in accordance with the study of *Alto* and *Juliano* (2001) who found that Asian tiger mosquito populations occurring in warmer regions are likely to produce more adults as long as water bodies (e.g., containers, little ponds) do not dry completely. We found, that *Ae. albopictus* does not prefer the wetter climate of the oceanic areas of Western Europe, which also matches with *Alto* and *Juliano* (2001) who found that the populations of the mosquito in cooler regions produce less amount of adults with the variability of precipitation. In the case of *Aedes* mosquito, wetlands and floodplains do not seem to be primary determinants of the distribution. Our model findings are highly in accordance with the findings of *Fischer et al.* (2011) who projected the future expansion of *Ae.albopictus* mosquito to the end of the 2060's to France, the western part of the Carpathian Basin.

The major benefit of our model is that the observed temperature requirement of the WNF peak season in Hungary is similar to the modeled temperature needs (T_{mean} of the summer months and September is more than 20 °C). Since 3 days to two weeks latency is plausible (CDC), the mosquito bites may occur at higher weekly mean temperatures.

5. Conclusions

Our study indicates that in creating a climate envelope model for a vector-borne disease or a vector, the primary concern is to consider the behavior, and the requirements of every elements of the vectorial chain. Climate can be the main determinant of the distribution, but in other cases climate itself is not sufficient to explain the observed distribution or occurrence. The predicted future warmer and dryer summer seasonal climate of the Carpathian Basin is likely to extend the northern distribution of *Ae. albopictus* and may modify the seasonality of West Nile fever. Floods has a very important role in modifying the mosquito abundance rivers which have a major water running as the river Tisza and have more or less preserved floodplains offering better conditions for mosquitos than the highly regulated rivers. Recently it is plausible, that birds re-introduce WNF into Hungary from year to year.

Acknowledgements—The authors would like to thank *Arnold Móra* MSc, the research assistant of the Balaton Limnological Research Institute of the Hungarian Academy of Sciences for the summary distribution map of Chironomidae mosquitos in Hungary. The research was supported by Project TÁMOP-4.2.1/B-09/1/KMR-2010-0005 and TÁMOP (4.2.2. A-11/1/KONV-2012-0064, 1.1). The ENSEMBLES data used in this work was funded by the EU FP6 Integrated Project ENSEMBLES (Contract number 505539) whose support is gratefully acknowledged.

References

Alto, B.W. and *Juliano, S.A.*, 2001: Precipitation and temperature effects on populations of Aedes albopictus (Diptera: Culicidae): implications for range expansion. *J. med. entomol. 38*, 646.

Bardos, V., Adamcová, J., Dedei, S., Gjini, N., Rosicky, B., and *Simkova, A.*, 1959: Neutralizing antibodies against some neurotropic viruses determined in human sera in Albania. *J. hyg. epid. microbial. immunol. 3*, 277.

Bartholy, J., Pongrácz, R.,and *Gelybó, Gy.*, 2007: A 21. század végén várható éghajlatváltozás Magyarországon. *Földrajzi Értesítő 56*, 147–168. (In Hungarian)

Bayoh, M.N. and *Lindsay, S.W.*, 2003: Effect of temperature on the development of the aquatic stages of Anopheles gambiae sensu stricto (Diptera: Culicidae). *B. entomol. res. 93*, 375–382.

Bayoh, M.N. and *Lindsay, S.W.*, 2004: Temperature-related duration of aquatic stages of the Afrotropical malaria vector mosquito Anopheles gambiae in the laboratory. *Med. veterinary entomol., 18*, 174–179.

Berthold, P., Kaatz, M., and *Querner, U.*, 2004: Long-term satellite tracking of white stork (Ciconia ciconia) migration: constancy versus variability. *J. Ornithol. 145*, 356–359.

Cannon, R.J., 2004: The implications of predicted climate change for insect pests in the UK, with emphasis on non-indigenous species. *Glob. Change Biol. 4*, 785–796.

Czúcz, B., 2010: Az éghajlatváltozás hazai természetközeli élőhelyekre gyakorolt hatásainak modellezése. PhD dissertation. Corvinus University of Budapest, Faculty of Horticultural Sciences. Budapest. (In Hungarian)

CDC: West Nile Virus (WNV) Infection: Information for Clinicians. Clinical features. http://www.cdc.gov/ncidod/dvbid/westnile/resources/fact_sheet_clinician.htm. Last accessed: 27 March 2013.

Chumakov, M.P., Belyaeva, A.P., and *Butenko, A.M.,* 1964: Isolation and study of an original virus from Hyalomma plumbeum plumbeum ticks and from the blood of a febrile patient in the Astrakhan region. *Materialy XI Nauchnoi Sessii Instituta Poliomielita i Virusnykh Encefalitov* (Moskva), 5–7.

De la Roque, S., Rioux, J.A., and *Slingenbergh, J.,* 2008: Climate change: Effects on animal disease systems and implications for surveillance and control. *Rev. Sci.t Tech. Int. Epizooties 27,* 339–354.

Dukes, J.S. and *Mooney, H.A.* (1999): Does global change increase the success of biological invaders? *Trends Ecol. Evolut. 14,* 135–139.

ECDC, West Nile fever maps 2012: Reported cases of WNF for the EU and the neighbouring countries. www.ecdc.europa.eu/en/healthtopics/west_nile_fever/West-Nile-fever-maps/Pages/index.aspx. Last accessed: 27 March 2013.

ECDC, West Nile fever maps 2011: Reported cases of WNF for the EU and the neighbouring countries. ecdc.europa.eu/en/healthtopics/west_nile_fever/West-Nile-fever-maps/Pages/index.aspx. Last accessed: 27 March 2013.

Elith, J., Leathwick, J.R., 2009: Species Distribution Models: Ecological Explanation and Prediction Across Space and Time. *An. Rev. Ecol. Evolut. Systematics 40,* 677–697.

ENSEMBLES, 2013: ENSEMBLES data archive. ensemblesrt3.dmi.dk. Last accessed: 27 March 2013.

Epinfo, 2010A: Nyugat-nílus láz megbetegedések Magyarországon és Európában. *Epinfo 17/34,* 449–452. (In Hungarian)

Epinfo, 2010B: Nyugat-nílus láz megbetegedések, Magyarországon, 2010. *Epinfo 17/36,* 417–424. (In Hungarian)

Epstein, P.R., Diaz, H.F., Elias, S., Grabherr, G., Graham, N.E., Martens, W.J., and *Susskind, J.,* 1998: Biological and physical signs of climate change: focus on mosquito-borne diseases. *B. Am. Meteorol. Soc. 79,* 409–417.

Fay, P.A., Kaufman, D.M., Nippert, J.B., Carlisle, J.D., and *Harper, C.W.,* 2008: Changes in grassland ecosystem function due to extreme rainfall events: implications for responses to climate change. *Glob. Change Biol. 14,* 1600–1608.

Fischer, D., Thomas, S.M., Niemitz, F., Reineking, B., and *Beierkuhnlein, C.,* 2011: Projection of climatic suitability for Aedes albopictus Skuse (Culicidae) in Europe under climate change conditions. *Glob. Planet. Change, 78,* 54–64.

Githeko, A.K., Lindsay, S.W., Confalonieri, U.E., and *Patz, J.A.,* 2000: Climate change and vector-borne diseases: a regional analysis. *B. WHO 78,* 1136–1147.

GISCO, 2013: GISCO - Eurostat (European Commission). epp.eurostat.ec.europa.eu/portal/page/-portal/gisco_Geographical_information_maps/popups/references/administrative_units_statistical_units_1. Last accessed: 2013.01.01

Global Register of Migratory Species. www.groms.de. Last accessed: 27 March 2013.

Global Register of Migratory Species. Ciconia ciconia. www.groms.de/groms/Ciconia_Info.html. Last accessed: 27 March 2013.

Goldblum, N., Sterk, V., and *Paderski, B.,* 1954: WNF, The clinical features op tue disease and the Isolation of West Nile Virus from the blood of nine human cases. *Am. J. Epidemiol. 59,* 89–103.

Guisan, A. and *Zimmermann, N.E.,* 2000: Predictive habitat distribution models in ecology. *Ecolog. Model. 135,* 147–186.

Hammer R.O., Harper D.A.T. and *Ryan P.D..,* 2001: PAST: Paleontological statistics software package for education and data analysis. *Paleontol Electron, 4,* 1-9.

Hannoun C, Panthier R, Mouchet J., and Eouzan Jp., 1964: Isolement En France Du Virus West-Nile 'A Partir De Malades Et Du Vecteur Culex Modestus Ficalbi. *C. R. Hebd. Seances Acad. Sci. 30,* 4170–4172.

Harvell, C.D., Mitchell, C.E., Ward, J.R., Altizer, S., Dobson, A.P., Ostfeld, R.S., and *Samuel, M.D.,* 2002: Climate warming and disease risks for terrestrial and marine biota. *Science 296,* 2158–2162.

Hijmans, R.J. and *Graham, C.H.,* 2006: The ability of climate envelope models to predict the effect of climate change on species distributions. *Glob. Change Biol. 12,* 2272–2281.

Hubálek, Z. and *Halouzka, J.,* 1999: WNF–a reemerging mosquito-borne viral disease in Europe. *Emerg. infect.dis. 5,* 643.

Hunter, P.R., 2003: Climate change and waterborne and vector-borne disease. *J. Appl.Microbiol. 94(s1)*, 37–46.

Hydroinfo. Országos vízjelző szolgálat. Archívum. Éves vízállástáblázatok. http://www.hydroinfo.hu–/Html/archivum/archiv_tabla.html. Last accessed: Last accessed: 27 March 2013.(In Hungarian)

Jourdain, E., Gauthier-Clerc, M., Bicout, D., and *Sabatier, P.*, 2007: Bird migration routes and risk for pathogen dispersion into western Mediterranean wetlands. *Emerg. Infect. Dis. 13*, 365.

Kilpatrick, A.M., Meola, M.A., Moudy, R.M., and *Kramer, L.D.*, 2008: Temperature, viral genetics, and the transmission of West Nile virus by Culex pipiens mosquitoes. *PLoS pathogens 4*, e1000092.

Krisztalovics, K., .Bán, E., Ferenczi, E., Zöldi, V., Bakonyi, T., Erdélyi, K., Szalkai, T., Csohán, Á., and *Szomor, K.*, 2011: Nyugat-nílus láz Magyarországon 2010. Epinfo, 18/9-10(6): 89–94. (In Hungarian)

Krisztalovics, K., Ferenczi, E., Molnár, Z.S., Csohán, Á., Bán, E., Zöldi, V., Kaszás, K,. 2008: West Nile virus infections in Hungary, August-September 2008. *Euro surveillance: bulletin européen sur les maladies transmissibles= European communicable disease bulletin, 13*(45), pii-19030.

KSH, 2012: Magyarország térképek. Lakónépesség 2012. január 1. http://www.ksh.hu/interaktiv/terkepek/mo/nepesseg.html. Last accessed: 27 March 2013. (In Hungarian)

Ladányi, M. and *Horváth, L.*, 2010: A review of the potential climate change impact on insect populations – general and agricultural aspects. *Appl. Ecol. Environ.Res. 8*, 143–152.

Lindegaard, C., 1995: Classification of water-bodies and pollution. The Chironomidae. 385-404. Springer, Netherlands.

Mackenzie, J.S., Gubler, D.J., and *Petersen, L.R.*, 2004: Emerging flaviviruses: the spread and resurgence of Japanese encephalitis, West Nile and dengue viruses. *Nature med. 10*, S98–S109.

Malkinson, M., Banet, C., Weisman, Y., Pokamunski, S., and *King, R.*, 2002: Introduction of West Nile virus in the Middle East by migrating white storks. *Emerg. Infect. Dis. 8*, 392.

McLean, R.G., Ubico, S.R., Docherty, D.E., Hansen, W.R., Sileo, L., and *McNamara, T.S.*, 2001: West Nile virus transmission and ecology in birds. *Ann. N Y Acad. Sci. 951*, 54-57.

Medlock, J.M., Hansford, K.M., Schaffner, F., Versteirt, V., Hendrickx, G., Zeller, H,. and *Bortel, W.V.*, 2012: A review of the invasive mosquitoes in Europe: ecology, public health risks, and control options. *Vector-Borne Zoonotic Dis. 12*, 435–447.

Meehl, G.A., Zwiers, F., Evans, J., Knutson, T., Mearns, L., and *Whetton, P.*, 2000: Trends in Extreme Weather and Climate Events: Issues Related to Modeling Extremes in Projections of Future Climate Change. *B. Am. Meteorol. Soc. 81*, 427–436.

Móra, A. and *Dévai, Gy.*, 2004: Magyarország árvaszúnyog-faunájának (Diptera: Chironomidae) jegyzéke az előfordulási adatok és sajátosságok feltüntetésével. *Acta Biol. Debr. Oecol. Hung 12*: 39.207. (In Hungarian)

Nakicenovic, N., Alcamo, J., Davis, G., de Vries, B., Fenhann, J., Gaffin, S., and *Dadi, Z.*, 2000: Special report on emissions scenarios: a special report of Working Group III of the Intergovernmental Panel on Climate Change (No. PNNL-SA-39650). Pacific Northwest National Laboratory, Richland, WA (US), Environmental Molecular Sciences Laboratory (US).

Neghina, R., Neghina, A.M., Merkler, C., Marincu, I., Moldovan R., and *Iacobiciu. I.*, 2009: Importation of visceral leishmaniasis in returning Romanian workers from Spain. *Travel Med Infect Dis. 7*, 35–39.

Rappole, J.H. and *Hubalek, Z.*, 2003: Migratory birds and West Nile virus. *J. Appl. Microbiol. 94*(s1), 47–58.

Reed, K.D., Meece, J.K., Henkel, J.S., and Shukla, S.K., 2003: Birds, migration and emerging zoonoses: West Nile virus, Lyme disease, influenza A and enteropathogens. *Clinic. Med. Res. 1*, 5–12.

Reeves, W.C., Hardy, J.L., Reisen, W.K., and *Milby, M.M.*, 1994: Potential effect of global warming on mosquito-borne arboviruses. *J. Med. Entomol. 31*, 323–332.

Reisen, W.K., Fang, Y., and *Martinez, V.M.*, 2006: Effects of temperature on the transmission of West Nile virus by Culex tarsalis (Diptera: Culicidae). *J. med. entomol. 43*, 309–317.

Reiter, P., Fontenille, D., and *Paupy, C.*, 2006: Aedes albopictus as an epidemic vector of chikungunya virus: another emerging problem? *Lancet infect. dis. 6*, 463–464.

Reiter, P., 2001: Climate change and mosquito-borne disease. *Environ. Health Perspect. 109*(S1), 141-161

Roeckner, E., Bäuml, G., Bonaventura, L., Brokopf, R., Esch, M., Giorgetta, M., Hagemann, S., Kirchner, I., Kornblueh, L., Manzini, E., Rhodin, A., Schlese, U., Schulzweida, U., and *Tompkins, A.*, 2003: The atmospheric general circulation model ECHAM 5. Part I: Model description. Max-Planck-Institut für Meteorologie, Hamburg.

Roeckner E., Brokopf, R., Esch, M., Giorgetta, M., Hagemann, S., Kornblueh, L., Manzini, E., Schlese, U., and *Schulzweida, U.*, 2004: The atmospheric general circulation model ECHAM 5. PART II: Sensitivity of Simulated Climate to Horizontal and Vertical Resolution. Max-Planck-Institut für Meteorologie, Hamburg.

Rogers, D.J. and *Randolph, S.E.*, 2006: Climate Change and Vector-Borne Diseases. *Adv. Parasitol. 62*. 345–381.

Rozendaal, J.A., 1992: Relations between Anopheles darlingi breeding habitats, rainfall, river level and malaria transmission rates in the rain forest of Suriname. *Med. veteran. entomol. 6*, 16–22.

Rueda, L.M., Patel, K.J., Axtell, R.C., and *Stinner, R.E.*, 1990: Temperature-dependent development and survival rates of Culex quinquefasciatus and Aedes aegypti (Diptera: Culicidae). *J. Med. Entomol. 27*, 892–898.

Sellers, R.F. and *Maarouf, A.R.*, 1989: Trajectory analysis and bluetongue virus serotype 2 in Florida 1982. *Can. J. Veterinar. Res. 53*, 100.

Spielman, A., 2001: Structure and seasonality of nearctic Culex pipiens populations. *Ann.N.Y. Acad. Sci. 951*, 220–234.

Teng, H.J. and *Apperson, C.S.*, 2000: Development and survival of immature Aedes albopictus and Aedes triseriatus (Diptera: Culicidae) in the laboratory: effects of density, food, and competition on response to temperature. *J. Med. Entomol. 37*, 40–52.

Thuiller, W., Araújo, M.B., and *Lavorel, S.*, 2004: Do we need land-cover data to model species distributions in Europe? *J. Biogeograph. 31*, 353–361.

Topciu, V., Roşiu, N., Arcan, P., Fufezan, V., and *Bran, B.*, 1971: The existence of arbovirus group B (Casals) disclosed by serological analysis of various animal species in the province of Banat (Rumania)]. *Arch. roumain. pathol. exp. microbial. 30*, 231.

The migration routes and staging areas of the storks. www.groms.de/groms/Ciconia_Info.html. Last accessed: 27 March 2013.

VBORNET, 2013: VBORNET maps-Mosquitoes. The current distribution of Aedes albopictus.ecdc.europa.eu/en/activities/diseaseprogrammes/emerging_and_vector_borne_diseases/Pages/VBORNET_maps.aspx. Last accessed: 27 March 2013.

Walther, G.R., Roques, A., Hulme, P.E., Sykes, M.T., Pyšek, P., Kühn, I., and *Settele, J,.* 2009: Alien species in a warmer world: risks and opportunities. *Trends Ecol. Evol. 24*, 686–693.

West Nile fever map 2012. Reported cases of the West Nile fever for the EU and the neighbouring countries. ecdc.europa.eu/en/healthtopics/west_nile_fever/West-Nile-fever-maps/Pages/index.aspx. Last accessed: 27 March 2013.

IDŐJÁRÁS

Quarterly Journal of the Hungarian Meteorological Service
Vol. 118, No. 1, January – March 2014, pp. 41–52

Impact of climate change on the potential distribution of Mediterranean pines

Ákos Bede-Fazekas[1]*, Levente Horváth[2], Márton Kocsis[3]

[1]*Corvinus University of Budapest, Faculty of Landscape Architecture, Department of Garden and Open Space Design*
Villányi út 29-43, H-1118 Budapest, Hungary
bfakos@gmail.com

[2]*Corvinus University of Budapest, Faculty of Horticultural Science, Department of Mathematics and Informatics;*
"Adaptation to Climate Change" Research Group
Villányi út 29-43, H-1118 Budapest, Hungary
levente.horvath@uni-corvinus.hu

[3]*Corvinus University of Budapest, Faculty of Horticultural Science, Department of Farm Management and Marketing*
Villányi út 29-43, H-1118 Budapest, Hungary
marton.kocsis@uni-corvinus.hu

* *Corresponding author*

(Manuscript received in final form March 27, 2013)

Abstract—The impact of climate change on the potential distribution of four Mediterranean pine species – *Pinus brutia* Ten., *Pinus halepensis* Mill., *Pinus pinaster* Aiton, and *Pinus pinea* L. – was studied by the Climate Envelope Model (CEM) to examine whether these species are suitable for the use as ornamental plants without frost protection in the Carpathian Basin. The model was supported by EUFORGEN digital area database (distribution maps), ESRI ArcGIS 10 software's Spatial Analyst module (modeling environment), PAST (calibration of the model with statistical method), and REMO regional climate model (climatic data). The climate data were available in a 25 km resolution grid for the reference period (1961–1990) and two future periods (2011–2040, 2041–2070). The regional climate model was based on the IPCC SRES A1B scenario. While the potential distribution of *P. brutia* was not predicted to expand remarkably, an explicit shift of the distribution of the other three species was shown. Northwestern African distribution segments seem to become abandoned in the future. Current distribution of *P. brutia* may be highly endangered by the climate change. *P. halepensis* in the southern part and *P. pinaster* in the western part of the Carpathian Basin may find suitable climatic conditions in the period of 2041–2070.

Key-words: Mediterranean pines, climate envelope model, CEM, potential distribution, climate change, distribution modeling, *Pinus brutia*, *Pinus halepensis*, *Pinus pinaster*, *Pinus pinea*

1. Introduction

According to the predictions for the period of 2011–2040, spatially analogue territories of Hungary – the territories with present climate similar to the future climate of Hungary – can be found in Southern Romania, Northern Bulgaria, Serbia, Macedonia, and Northern Greece (*Horváth*, 2008). Therefore, the ornamental plant assortment of Hungary – as the assortment of other central and eastern European countries – should be reconsidered (*Szabó* and *Bede-Fazekas*, 2012; *Schmidt*, 2006). This realization inspired some previous studies (*Bede-Fazekas*, 2012a,b) on whether some warm-demanding ligneous plants are able to be adapted in Hungary in the future.

By this time, regional climate models have good horizontal and temporal resolution and are reliable enough for creating some climate envelope models (CEMs) based on the current distribution of tree species. Our previous works of research were about modeling the future area of introduction of several Mediterranean ligneous plant species that can have significance in the future ornamental plant usage. Based on these former studies, it was aimed to run a new and more accurate model on four of the previously studied species. The improvement of the modeling method was achieved by statistical calibration based on an iterative error evaluation. Hence, the improved model is able to study not the future area of introduction but the future potential distribution.

We aimed to create multi-layered distribution maps with a GIS (Geographic Information System) software, displaying the predicted shift of the potential distributions. These maps can have importance not only in forestry, landscape architecture, and botany, but in visualization of the effects of climate change also for non-professionals (*Czinkóczky* and *Bede-Fazekas*, 2012). The studied species were Brutia pine (*Pinus brutia* Ten. syn. *Pinus halepensis* var. *brutia* (Ten.) A. Henry), Aleppo pine (*Pinus halepensis* Mill.), maritime pine (*Pinus pinaster* Aiton syn. *Pinus maritima* Lam.), and Italian stone pine (*Pinus pinea* L.), which are very close relatives (classified in section *Pinus*, subsection *Pinaster*) according to phylogenetic studies (*Wang et al.*, 1999; *Gernandt et al.*, 2005; *Eckert* and *Hall*, 2006).

2. Materials and methods

2.1. Climate data and distribution maps

The current (latest update was achieved in 2008) continuous distribution map of the species was derived from the EUFORGEN digital area database (*Euforgen*, 2008), while the discrete (fragmented) observations were ignored. Therefore 28 (*P. brutia*), 233 (*P. halepensis*), 23 (*P. pinaster*), and 109 (*P. pinea*) observed data were disregarded by the model. The distributions from 2008 were bound to

the reference period. This difference may not cause any problem since the pines have long life cycle and can slowly adapt to the changing climate.

The climatic data were gained from the REMO regional climate model (RCM); the grid had a 25 km horizontal resolution. The model REMO is based on the ECHAM5 global climate model (*Roeckner et al.*, 2003, 2004) and uses the IPCC SRES scenario called A1B. This scenario supposes a future world characterized by a very rapid economic growth, a global population that peaks in the mid-century, and rapid introduction of new and more efficient technologies (*Nakicenovic* and *Swart*, 2000). The reference period was 1961–1990, the two future periods of modeling were 2011–2040 and 2041–2070. The entire European continent is within the domain of REMO, we used, however, only a part of the grid (25724 of the 32300 points; *Fig. 1*).

36 climatic variables were used for the distribution modeling: monthly mean temperature (T, °C), monthly minimum temperature (M, °C), and monthly precipitation (P, mm). All climatic data were averaged in the three periods.

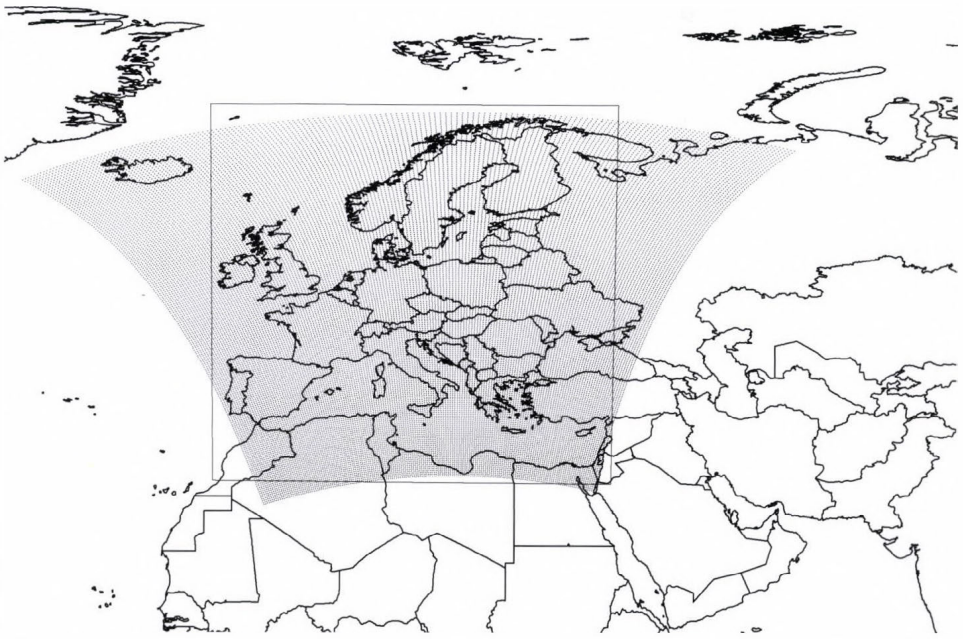

Fig. 1. The domain of climate model REMO and its part used in the study.

2.2. Climate envelope modeling

2.2.1. Modeling approach and software

ESRI ArcGIS 10 software was used for preparing climatic data, running the model, and displaying the model results. Climatic data were managed and the expressions for modeling were prepared with the assistance of Microsoft Excel 2010 program. PAST statistic analyzer software (*Hammer et al.*, 2001) was used for creating the cumulative distribution function of the climatic parameters, and getting the percentile values of the parameters (model calibration).

The impact of climate change on the distribution of selected species was modeled with climate envelope modeling (CEM; also known as niche-based modeling, correlative modeling) (*Hijmans* and *Graham*, 2006). This method is about predicting responses of species to climate change by drawing an envelope around the domain of climatic variables where the given species has been recently found, and then identifying areas predicted to fall within that domain under future scenarios (*Ibáñez et al.*, 2006). It hypothesizes that (both present and future) distributions are dependent mostly on the climatic variables (*Czúcz*, 2010) which is somewhat dubious (*Skov* and *Svenning*, 2004). Compared to mechanistic models, CEM tries to find statistical correlations between climate and distribution of species (*Guisan* and *Zimmermann*, 2000; *Elith* and *Leathwick*, 2009), and models the future temporal correspondence based on the present spatial correspondence between the variables (*Pickett*, 1989).

2.2.2. Calibration by iterative modeling

The calibration of the model has been conducted by iterative error evaluation. The model was run iteratively to determine the optimal amount of percentiles to be left from the climatic values. Cumulative distribution functions were calculated by PAST for all climatic parameters. Then 0 to 14 percentiles have been left from the lower values of a certain type of climate parameters (e.g., 12 monthly precipitations), while the maximum values were fixed and also the other 24 climatic parameters were fixed at the extreme values. In case of a certain species, 90 error evaluations were done. Two types of error values were calculated: internal (the ratio of the current distribution segment not determined by the model), and external (the ratio of area outside the current distribution, determined falsely by the model). Then the errors were summarized. The increasing accumulated error function determined the appropriate number of percentiles to left: the greatest number of percentiles was chosen which produces no more than 100% summarized error. Cohen's kappa values (*Cohen*, 1960) were estimated in two cases: without and with percentile leaving to evaluate the improvement achieved by the model calibration.

This iterative calibration technique shows several similarities with "area under the receiver operating characteristic (ROC) curve" (AUC; *Hanley* and *Mcneil*, 1982). The comments of *Lobo et al.* (2008) on AUC may also refer to the calibration method used in this research. For further error-based model calibration procedures see *Fielding* and *Bell* (1997).

2.2.3. Modeling method

First, climatic data were refined by Inverse Distance Weighted interpolation method. Then the modeling steps were as follows:

1. The grid points within the distribution were queried (a few hundred × 36 data; ArcGIS).
2. The percentile points of the 36 climatic parameters (101×36 data, PAST) were calculated.
3. The appropriate percentiles of the climatic parameters determined by the calibration were selected (2×36 data, Excel).
4. Modeling phrases (3 strings, Excel) were created by string functions for the three modeling periods.
5. Those territories were selected where all the climatic values of the certain period were between the extremes selected in step 3. (ArcGIS – Raster Calculator function).

Positive raster results were transformed to ESRI shapefile format (polygons). The order of the four layers (one observed and three modeled distributions) determines whether the result maps are able to display the northward expansion, not the retreat from the southern parts (trailing edge) of the current distribution. Therefore, two types of layer order were applied and are shown herein.

3. Results

3.1. Result of iterative modeling

Based on the iterative modeling, the optimal number of percentiles to be left was determined in case of the four species, and two extremes of the three types of climate variables (*Table 1*). The improvement of the model can be estimated by comparing the two different Cohen's kappa values. The most significant improvement can be seen in case of *P. pinaster*, while the Cohen's kappa value shows inessential increase in case of *P. pinea*.

Table 1. The result of model calibration: the number of percentiles to be left over, the Cohen's kappa value before (Ck 1) and after (Ck 2) percentile omission

Species	min(*T*)	max(*T*)	min(*M*)	max(*M*)	min(*P*)	max(*P*)	Ck 1	Ck 2
P. brutia	3	2	3	3	5	3	0.1157	0.2056
P. halepensis	9	2	9	3	3	2	0.1103	0.2474
P. pinaster	6	3	6	3	2	4	0.0862	0.2848
P. pinea	6	1	5	2	2	1	0.0805	0.1484

3.2. Modeled potential distributions

3.2.1. Brutia pine (Pinus brutia)

The current distribution of *P. brutia* (*Fig. 2a; Fig. 3a*) is focused on the eastern Mediterranean region (Turkey, Cyprus, and Malta), while the model results in a much larger potential distribution for the reference period that includes southern Portugal, southern Spain, northern Morocco, northern Algeria, Sardinia, southern Italy, and Greece. The Cyprian and Cretan distribution segments were however, not redrawn by the model. Significant northern expansion is not predicted, and Hungary is not affected by the model. Maritime distribution in Turkey seems to become partly viable for the species in the periods of 2011–2040 (near Adana) and 2041–2070 (near Denizli). The Turkish discrete distributions seem to remain climatically viable.

3.2.2. Aleppo pine (Pinus halepensis)

Segments of the observed distribution of *P. halepensis* (*Fig. 2b; Fig. 3b*) can be found in eastern Spain, southern France, Italy, southern Greece, northern Morocco, Algeria, Tunisia, and Libya. The model cannot redraw the Libyan distribution fragment. The potential distribution for the reference period seems to be larger than the observed area: southern Portugal and Spain, Italy, Corsica and Sardinia, the coast of the Aegean Sea, and greater North African territories are modeled to be suitable for the species. Future expansion is predicted in Spain, France, Italy, Croatia, Bosnia and Herzegovina, Serbia, Bulgaria, and the Crimea. The western territories seem to become suitable for living sooner, while the Balkan Peninsula and the Crimea are predicted to be affected only in the far future period. Although most of the discrete distributions in the western Mediterranean were redrawn by the model, discrete observations near Croatia, Lebanon, and Jordan were not. A large part of the distribution in North Africa seems to become abandoned in the period of 2011–2040. Also the Italian and Greek coastline may be negatively affected. Interestingly, some of the Spanish and French distribution segments are predicted to find more suitable climatic environment in the future than in the reference period.

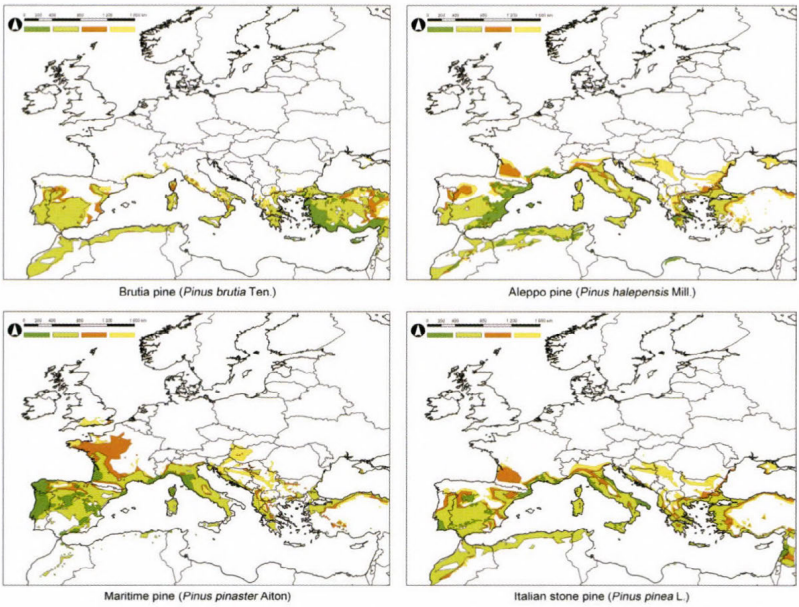

Fig. 2. Expansion: current distribution (dark green), modeled potential distribution in the reference period (light green), and modeled potential distribution in the periods of 2011–2040 (orange) and 2041–2070 (yellow) of the four studied *Pinus* species.

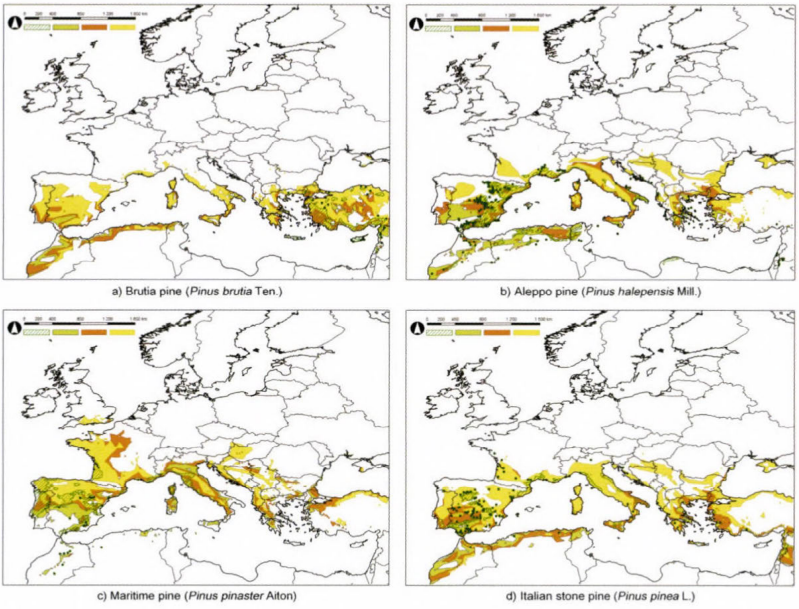

Fig. 3. Retraction: current distribution (dark green hatch and points), modeled potential distribution in the reference period (light green), and modeled potential distribution in the periods of 2011–2040 (orange) and 2041–2070 (yellow) of the four studied *Pinus* species.

3.2.3. Maritime pine (Pinus pinaster)

The current distribution of *P. pinaster* (*Fig. 2c; Fig. 3c*) is focused on the western Mediterranean (Portugal, Spain, southern France, Corsica, and northern Italy), which is well expressed by the model. The African (continuous and discrete) distribution segments are, however, not redrawn by the model. Significant northern expansion is predicted to occur in western France, southern England, the Balkans, and the western part of the Carpathian Basin. The latter areas may become suitable for the species in the far future period, while the expansion to western France seems to occur between 2011 and 2040. Maritime and southern Iberian distributions may become abandoned in the period of 2011–2040. By the end of the studied future periods the climate seems to remain suitable for the species in northern Spain and France.

3.2.4. Italian stone pine (Pinus pinea)

Apart from central Spain, *P. pinea* (*Fig. 2d; Fig. 3d*) is clearly a coastal pine: its current distribution includes maritime parts of Portugal, Spain, France, Italy, Turkey, Syria, and Lebanon. The potential distribution for the reference period is modeled to include North African coastal territories, southern Portugal and Spain, Italy, and the coastline of the eastern Mediterranean. Future northern expansion can be seen in France, Italy, and the Balkans. Only the Syrian, southern Spanish, and eastern Italian distribution segments are somewhat endangered (the latter one only in the far future period). Most of the distributions in Italy, France, and Spain seem to remain viable by the end of the studied period. Similarly to *P. halepensis*, some continuous and discrete Spanish and French distribution segments are predicted to find more suitable climatic conditions in the future than in the reference period. Discrete distributions in North Africa, Italy, Greece, and Turkey seem to remain viable at least by the period of 2011–2040.

4. Discussion

4.1. Model evaluation

Although the aforementioned predictions are obviously valuable and spectacular, there are some questions and disadvantages concerning the model applied. Opinions differ if climatic variables are by themselves sufficient or even the most important factors for explaining the real distribution of species (*Dormann*, 2007). In case of determining the potential distribution of plant species, edaphic characteristics found within their current distribution area seem to be the only parameters that may be as important as climatic factors are. The studied conifers are, however, tolerant to the alkalinity/lime content of the soil in an extent that they are able to be planted as ornamentals in their predicted future potential distribution

area. Nevertheless, it must be noted that the previously presented model results should, in botanical point of view, not to be acknowledged without considering edaphic characteristics. It should also be noted that extremes and absolute climatic values (rather than averages) may better explain the limits of distribution (*Kovács-Láng et al.*, 2008). The input climate data were obtained from RCM, which differ from the observed meteorological data. No bias correction was applied on the modeled climate data, since the bias correction should have been used in the same way in case of the reference and future periods and, therefore, no remarkable difference could have been evolved. The applied model calibration technique seems to result in a realistic and supportable model, since

1. the differences between the potential and observed distributions are not unacceptably large;
2. iterative model calibration resulted in doubled Cohen's kappa values in case of three of the four studied species; and
3. ornamental plantings of these pines in central and western Europe have proven that the predictions are not overestimations.

Various other ways can be found to determine the climate envelope, including simple regression, distance-based methods, genetic algorithms for rule-set prediction, and neural nets (*Ibáñez et al.*, 2006). Our subsequent aim is to develop a program module for ArcGIS that implements the artificial intelligence algorithm artificial neural network (ANN) for modeling the future distribution of Mediterranean tree species.

The model results for the reference period show the least difference to the observed distribution in case of *P. halepensis* and *P. pinaster*, while the model performed worst in case of *P. pinea* (*Table 2*).

Table 2. The points of grid are within the observed distribution; the ratio of modeled and observed points in the reference period; the expansion from the reference period to the near future period; and the expansion from the reference period to the far future period in case of the four studied species

Species	Observed points	Model/observation (%)	Expansion 2011–2040 (%)	Expansion 2041–2070 (%)
P. brutia	236	591.10	14.41	30.04
P. halepensis	326	380.06	22.28	56.98
P. pinaster	352	351.14	31.55	48.95
P. pinea	176	849.43	23.88	53.98

4.2. Shift of distributions

Our former research found that the extent of future shift of area of introduction is much larger. That model was, however, inaccurate. The results of this improved model show clearly and spectacularly the impacts of the predicted

climate change on the distribution of Mediterranean pines. The most affected territories may be France and the Balkans. By comparing the model results of the reference period to the results of the future periods (*Table 2*) it can be concluded that the greatest absolute expansion is predicted to occur in case of *P. pinaster*, the greatest relative expansion may occur in case of *P. halepensis* and *P. pinea*, while the distribution of *P. brutia* seems to be nearly unchanged. Although the current distribution of *P. halepensis* and *P. pinea* differs remarkably, the predictions are almost the same, which originates from the similar climatic demand and tolerance of the two species. The northwestern African coastline was predicted to be suitable for *P. brutia*, *P. halepensis*, and *P. pinea*. By 2070, the climate of western and southern Hungary seems to become suitable for *P. pinaster*. In the far future period, *P. halepensis* is predicted to occur in the southern part of the Carpathian Basin, while *P. pinea* and *P. brutia* seem to stay out of the basin. Nevertheless, it must be noted that *P. halepensis* is better adapted to drought but less adapted to cold than *P. brutia* (*Fady et al.*, 2003). Hence, the latter species is able to serve as ornamental plant in the near future period (when frost is limiting factor) and in moist (irrigated) plots in the far future period.

Some plant species originating from a certain part of the Mediterranean Basin and introduced to other parts of it seem to become particularly invasive (*Groves*, 1991), and are better to be treated as potentially invasive species in the territories predicted to become climatically suitable for them. *P. halepensis* is known to be invasive (*Acherar et al.*, 1984; *Trabaud et al.*, 1985; *Lepart* and *Debussche*, 1991). Other species, such as *P. brutia* in southern Anatolia (*Quézel et al.*, 1990), can effectively be established where they had been introduced and even expand in some extent but without becoming really invasive (*Le Floc'h*, 1991). The phenomena of plant invasion is now under revision in ecology, since some of the species treated to be invasive may become important elements of the natural vegetation due to climate change (*Walther et al.*, 2009).

It must be mentioned that the original distribution area of *P. pinea* is obscure, since it was extensively planted around the Mediterranean throughout historical times by Etruscans, Greeks, Romans, and Arabs because of its edible seeds. (*Groves*, 1991; *Barbéro et al.*, 1998; *Fady et al.*, 2004). The differentiation of autochthonous and non-autochthonous stands is, as also in the case of *P. pinaster*, controversial (*Alía* and *Martín*, 2003).

5. Conclusion

Mediterranean pines are potentially able to expand the ornamental plant assortment of the Carpathian Basin. Although some specimens of the four studied conifers can be found in arboreta of Hungary, they are susceptible to frost and, therefore, not widely introduced. In this research we aimed to examine whether these pines will be able to be planted without frost protection in the

future by modeling the future potential distributions. The result of CEM shows that *P. halepensis* in the southern part and *P. pinaster* in the western part of the Carpathian Basin may find similar climatic conditions in the period of 2041–2070 than the observed distributions of these species were living within in the reference period. Therefore, landscape architecture, dendrology, forestry, and botany should think of these pines as potential ornamental plants or even as potential plants of natural vegetation in the future in Hungary.

Acknowledgements—Special thanks to *Levente Hufnagel* (Corvinus University of Budapest, Department of Mathematics and Informatics) for his assistance. The research was supported by Project TÁMOP-4.2.1/B-09/1/KMR-2010-0005. The ENSEMBLES data used in this work was funded by the EU FP6 Integrated Project ENSEMBLES (Contract number 505539), whose support is gratefully acknowledged.

References

Acherar, M., Lepart, J., Debussche, M., 1984: La colonisation des friches par le pin d' Alep (Pinus halepensis, Miller) en Languedoc mediterraneen. *Acta Oecol. 5*, 179–189. (in French)

Alía, R., Martín, S., 2003: *EUFORGEN* Technical Guidelines for genetic conservation and use for *Maritime pine (Pinus pinaster)*. International Plant Genetic Resources Institute, Rome, Italy.

Barbéro, M., Loisel, R.,Quézel, P.,Richardson, D.,Romane, F., 1998: Pines of the mediterranean basin. In (Ed. *Richardson, D.M.*): Ecology and Biogeography of Pinus. Cambridge University Press, Cambridge, UK.

Bede-Fazekas, Á., 2012a: Melegigényes díszfák telepíthetőségi területének előrejelzése a 21. századra. Thesis, Corvinus University of Budapest, Faculty of Landscape Architecture, Budapest, Hungary. (in Hungarian)

Bede-Fazekas, Á., 2012b: Methods of modeling the future shift of the so called Moesz-line. *Appl. Ecol. Environ. Res. 10*, 141–156.

Cohen, J., 1960: A coefficient of agreement for nominal scales. *Edu. Psychol. Meas. 20*, 37–46.

Czinkóczky, A. and *Bede-Fazekas, Á.,* 2012: Visualization of the climate change with the shift of the so called Moesz-line. In (Eds. *Buhmann, E., Ervin, S., Pietsch, M.*): Peer Reviewed Proceedings of Digital Landscape Architecture 2012 at Anhalt University of Applied Sciences. Herbert Wichmann Verlag, Berlin, Germany.

Czúcz, B., 2010: Az éghajlatváltozás hazai természetközeli élőhelyekre gyakorolt hatásainak modellezése. PhD dissertation. Corvinus University of Budapest, Faculty of Horticultural Sciences, Hungary. (in Hungarian)

Dormann, C.F., 2007: Promising the future? Global change projections of species distributions. *Basic Appl. Ecology 8*, 387–397.

Eckert, A.J. and *Hall, G.D.,* 2006: Phylogeny, historical biogeography, and patterns of diversification for Pinus (*Pinaceae*): Phylogenetic tests of fossil-based hypotheses. *Mol. Phylogenet. Evol. 40,*, 166–182.

Elith, J., Leathwick, J.R., 2009: Species Distribution Models: Ecological Explanation and Prediction Across Space and Time. *Ann. Rev. Ecol. Evol. Systemat. 40*, 677–697.

EUFORGEN, 2008: Distribution maps. Bioversity International, Rome, Italy. Online: www.euforgen.org/distribution_maps.html. Last accessed: 2013.01.01.

Fady, B., Semerci, H., and *Vendramin, G.G.,* 2003: EUFORGEN Technical Guidelines for genetic conservation and use for Aleppo pine *(Pinus halepensis)* and Brutia pine *(Pinus brutia)*. International Plant Genetic Resources Institute, Rome, Italy.

Fady, B., Fineschi, S., and *Vendramin, G.G.,* 2004: EUFORGEN Technical Guidelines for genetic conservation and use for Italian stone pine *(Pinus pinea)*. Int. Plant Genetic Res.Institute, Rome, Italy

Fielding, A.H. and *Bell, J.F.,* 1997: A review of methods for the assessment of prediction errors in conservation presence/absence models. *Environ. Conservat. 24,* 38–49.

Gernandt, D.S., Geada López, G., Garcia, S.O., and *Liston, A.,* 2005: Phylogeny and classification of Pinus. *Taxon 54,* 29–42.

Groves, R.H., 1991: The biogeography of mediterranean plant invasions. In (Eds. *Groves, R.H., Di Castri, F.*) Biogeography of Mediterranean Invasions. Cambridge University Press, Cambridge, UK.

Guisan, A. and *Zimmermann, N.E.*, 2000: Predictive habitat distribution models in ecology. *Ecolog. Model. 135*, 147–186.

Hammer, Ř., Harper, D.A.T., and *Ryan, P.D.*, 2001: PAST: Paleontological statistics software package for education and data analysis. *Palaeontologia Electronica. 4*, 9.

Hanley, J.A. and *McNeil, B.J.*, 1982: The meaning and use of area under a receiver operating characteristics (ROC) curve. *Radiology 143*, 29–36.

Hijmans, R.J. and *Graham, C.H.*, 2006: The ability of climate envelope models to predict the effect of climate change on species distributions. *Glob. Change Biology 12*, 2272–2281.

Horváth, L., 2008: Földrajzi analógia alkalmazása klímaszcenáriók elemzésében és értékelésében. PhD dissertation, Corvinus University of Budapest, Budapest, Hungary. (in Hungarian)

Ibáñez, I., Clark, J.S., Dietze, M.C., Feeley, K., Hersh, M., Ladeau, S., Mcbride, A., Welch, N.E., and *Wolosin, M.S.*, 2006: Predicting Biodiversity Change: Outside the Climate Envelope, beyond the Species-Area Curve. *Ecology. 87*, 1896–1906.

Kovács-Láng, E., Kröel-Dulay, Gy., and *Czúcz, B.*, 2008: Az éghajlatváltozás hatásai a természetes élővilágra és teendőink a megőrzés és kutatás területén. *Term. Közl. 14*, 5–39. (in Hungarian)

Le Floc'h, E., 1991: Invasive plants of the Mediterranean Basin. In (Eds. *Groves, R.H., Di Castri, F.*): Biogeography of Mediterranean Invasions. Cambridge University Press, Cambridge, UK.

Lepart, J. and *Debussche, M.*, 1991:. Invasion processes as related to succession and disturbance. In (Eds. *Groves, R.H., Di Castri, F.*): Biogeography of Mediterranean Invasions. Cambridge University Press, Cambridge, UK.

Lobo, J.M., Jimenez-Valverde, A., and *Real, R.*, 2008: AUC: a misleading measure of the performance of predictive distribution models. *Glob. Ecol. Biogeogr. 17*, 145–151.

Nakicenovic, N. and *Swart, R. (eds.)*, 2000: Emissions Scenarios. Cambridge University Press, Cambridge, UK.

Pickett, S.T.A., 1989: Space-for-time substitution as an alternative to long-term studies. In (Ed. *Likens, G.E.*): Long-Term Studies in Ecology: Approaches and Alternatives. Springer, New York, USA.

Quézel, P., Barbéro, M., Bonin, G., and *Loisel, R.*, 1990: Recent plant invasions in the Circum-Mediterranean region. In (Eds. *Di Castri, F., Hansen, A.J., Debussche, M.*) Biological Invasions in Europe and the Mediterranean Basin. *Monographiae Biologicae 65.*

Roeckner, E., Bäuml, G., Bonaventura, L., Brokopf, R., Esch, M., Giorgetta, M., Hagemann, S., Kirchner, I., Kornblueh, L., Manzini, E., Rhodin, A., Schlese, U., Schulzweida, U., and *Tompkins, A.*, 2003: The atmospheric general circulation model ECHAM 5. Part I: Model description. Max-Planck-Institut für Meteorologie, Hamburg, Germany.

Roeckner E., Brokopf, R., Esch, M., Giorgetta, M., Hagemann, S., Kornblueh, L., Manzini, E., Schlese, U., and *Schulzweida, U.*, 2004: The atmospheric general circulation model ECHAM 5. PART II: Sensitivity of Simulated Climate to Horizontal and Vertical Resolution. Max-Planck-Institut für Meteorologie, Hamburg, Germany.

Schmidt, G., 2006: Klíma- és időjárás-változás és a fás szárú dísznövények. In: (Eds. Csete, Nyéki) Klímaváltozás és a magyarországi kertgazdaság. „AGRO-21" Kutatási Pr.iroda, Bp. (in Hungarian)

Skov, F. and *Svenning, J.C.*, 2004: Potential impact of climatic change on the distribution of forest herbs in Europe. *Ecography. 27*, 366–380.

Szabó, K. and *Bede-Fazekas, Á.*, 2012: A forgalomban lévő fásszárú dísznövénytaxonok szárazságtűrésének értékelése a klímaváltozás tükrében. *Kertgazdaság 44*, 62–73. (in Hungarian)

Trabaud, L., Michels, C., and *Grosman, J.*, 1985: Recovery of burnt Pinus halepensis mill. forests. II. Pine reconstruction after wildfire. *Forest Ecol. Manage. 13*, 167–179.

Walther, G-R., Roques, A., Hulme, P.E., Sykes, M.T., Pyšek, P., Kühn, I., Zobel, M., Bacher, S., Botta-Dukát, Z., Bugmann, H., Czúcz, B., Dauber, J., Hickle, T., Jarošik, V., Kenis, M., Klotz, S., Minchin, D., Moora, M., Nentwig, W., Ott, J., Panov, V.E., Reineking, B., Robinet, C., Semenchenko, V., Solarz, W., Thuiller, W., Vila, M., Vohland, K., and *Settele, J.*, 2009: Alien species in a warmer world: risks and opportunities. *Trends in Ecol. Evolut. 24*, 686–693.

Wang, X.-R., Tsumura, Y., Yoshimaru, H., Nagasaka, K., and *Szmidt, A.E.*, 1999: Phylogenetic relationships of Eurasian pines (*Pinus, Pinaceae*) based on chloroplast rbcL, matK, rpl20-rps18 spacer, and trnV intron sequences. *Amer. J. Bot. 86*, 1742–1753.

IDŐJÁRÁS

Quarterly Journal of the Hungarian Meteorological Service
Vol. 118, No. 1, January – March, 2014, pp. 53–77

Sensitivity analysis of microscale obstacle resolving models for an idealized Central European city center, Michel-Stadt

Anikó Rákai[1*], **Gergely Kristóf**[1], and **Jörg Franke**[2,3]

[1]*Department of Fluid Dynamics, Budapest University of Technology and Economics, Bertalan L. u. 4-6, H-1111 Budapest, Hungary*
E-mails: rakai@ara.bme.hu, kristof@ara.bme.hu

[2]*University of Siegen, Institute of Fluid- and Thermodynamics, 56068 Siegen, Germany*

[3]*Vietnamese-German University (VGU), Binh Duong New City, Vietnam, joerg.franke@vgu.edu.vn*

**Corresponding author*

(Manuscript received in final form March 8, 2013)

Abstract—Microscale meteorological models with obstacle resolving grids are an important part of air quality and emergency response models in urban areas providing the flow field for the dispersion model. The buildings as bluff bodies are challenging from the discretization point of view and have an effect on the quality of the results. In engineering communities the same topic has emerged, called computational wind engineering (CWE), using the methods of computational fluid dynamics (CFD) calculating wind load on buildings, wind comfort in the urban canopy, and pollutant dispersion. The goal of this paper is to investigate the sensitivity of this method to the discretization procedure used to resolve the urban canopy with meshes which are of operational size, i.e., which can be run on a single powerful computer of a design office as well. To assess the quality of the results, the computed mean and rms (root mean square) velocity components are compared to detailed wind tunnel results of an idealized Central European city center, Michel-Stadt. A numerical experiment is carried out where the numerical sensitivity of the solution is tested by additional solutions on different grid resolutions (at least 3 stages of grid refinement), unrelated grid types (tetrahedral, polyhedral, Cartesian hexahedral, and body fitted hexahedral, all automatically generated), and different discretization schemes. For an objective qualitative judgment two metrics are investigated, the well know hit rate and another metric that does not depend on threshold values. The quality of the meshes is investigated with correspondence to the numerical stability, CPU-time need, and grid quality metric. It is shown that the solution with the best resulting metric is not necessarily the most suitable for operational purposes and almost 20% difference in the hit rate metric can result from different discretization approaches.

Key-words: microscale air quality models, obstacle resolving, urban flow, polyhedral mesh, snappyHexMesh, OpenFOAM®

1. Introduction

Prognostic microscale obstacle resolving meteorological models and computational wind engineering (CWE) models deal with the common fields of wind and pollutant dispersion modeling inside the urban canopy. *Baklanov* and *Nuterman* (2009) show that these models with increasing computational capacity can be the final scale in a nested multi-scale meteorological and dispersion model. *Mészáros et al.* (2010) have also shown a coupled transport and numerical weather prediction system for accidental pollutant releases. They say that a microscale resolved model is also needed and investigated resolving obstacles at the smallest scale with a computational fluid dynamics (CFD) model in *Leelőssy et al.* (2012).

Stull (1988) defines microscale in meteorology being a few kilometers or less where the typical phenomena include mechanical turbulence caused by the buildings. *Britter* and *Hanna* (2003) suggest the following length-scales: regional (up to 100 or 200 km), city scale (up to 10 or 20 km), neighborhood scale (up to 1 or 2 km), and street scale (less than 100 to 200 m). The two last correspond to the microscale definition of *Stull* and are used in this paper.

Baklanov (2000) showed the possibilities and weaknesses of using CFD for air quality modeling and concluded that they have a good potential. *Balczó et al.* (2011) showed a real life test case of dispersion studies of motorway planning around Budapest, carried out with the code MISKAM®, compared to wind tunnel measurements. That was an extensive example of using microscale meteorological and dispersion models for operational purposes and also showed its difficulties. To be able to use these models with confidence for operational purposes in air quality forecasting or emergency response tools, without using additional experiments, a detailed knowledge on their quality is necessary.

There are several research groups dealing with this field who have issued best practice guidelines, mainly based on validation studies compared with wind tunnel measurements of fairly simple cases. Wind tunnel models are used because of the well defined boundary conditions and the relative ease of high resolution measurement points compared to full scale field models. In these microscale validation studies usually steady state flow models are used, assuming neutral stability and neglecting the Coriolis forces. The two most thorough guidelines are from the Architectural Institute of Japan (*Tominaga et al.*, 2008), and from a COST project, Quality assurance of microscale meteorological models (*Franke et al.*, 2011). The German Engineering Community has also a standard on validation of microscale meteorological models for urban flows with a database of simple building configurations (*VDI*, 2005).

Several studies have dealt with the problem of defining inflow conditions for the atmospheric boundary layer, the most influential being *Richards* and *Hoxey* (1993). There was a considerable effort on defining inflow conditions

which are maintained throughout the computational domain if no buildings are inside, i.e., aiming for lateral homogeneity, see *Blocken et al.* (2007a), *Yang et al.* (2007), *Parente et al.* (2010), *O'Sullivan et al.* (2011), and *Balogh et al.* (2012).

Another huge effort was made for developing turbulence models which are the best for the purpose of Computational Wind Engineering. Since buildings are bluff bodies, the stagnation point anomaly revealed by *Durbin* (1996) gives a challenge for the turbulence models. There were attempts to improve the linear approach of the Boussinesq assumption and choose the best model; a wide comparison of the possibilities is shown in *Tominaga et al.* (2004) and *Yoshie et al.* (2005). Nonlinear turbulence models were also considered for flow around a single cube obstacle by *Erhard et al.* (2000) and *Wright* and *Eason* (2003), and for topographical features by *Lun et al.* (2003).

The numerical discretization procedure has less focus but it can also have a significant effect on the quality of computations. In engineering communities, dealing with computational fluid dynamics (CFD), quality assurance, verification and validation, and numerical uncertainty analysis are becoming more and more important; see e.g., *Roache* (1997) , *Oberkampf* and *Trucano* (2002), and *Franke* (2010).

This paper shows different numerical discretization possibilities for a test case called Michel-Stadt. This is an idealized Central European city center investigated in a wind tunnel with detailed measurement results publicly available. When meshing a complex urban geometry, several approaches are possible, with different quality in performance and results, and with different cost in the meshing and computing procedure. *Franke et al.* (2012a) and *Hefny* and *Ooka* (2009) are the only ones to the knowledge of the authors who compared different mesh types when investigating microscale meteorological or air quality models. *Franke et al.* (2012a) compared a block-structured hexahedral meshing approach to an unstructured hexahedral and an unstructured hybrid mesh which consists of tetrahedral and prism elements, the latter comprising of 3 layers around the geometries. They investigated simple block geometries and rows of blocks, thus simpler urban arrangements than the one presented in this paper. Their findings about the quality of the results of mean velocity components compared to experiments showed that the unstructured meshes yield often better metrics which they attributed to the higher resolution of those meshes. In this paper different resolution is used for each mesh to enable to compare similar resolutions. For the geometry of rows of blocks, *Franke et al.* (2012a) found that second order simulations with unstructured meshes are unstable, which is similar to the findings of this paper. *Hefny* and *Ooka* (2009) compared hexahedral and tetrahedral elements only for a simple block geometry, and they compared the results of dispersion to each other. In their findings the hexahedral mesh had the best performance regarding estimated numerical error, but they did not compare the results to

experimental values. There is no comparison for the flow field in their paper either, which determines the results of the dispersion essentially. The study presented here gives important additional information to these two papers in several points. The geometry used is more complex, information about the computational cost is given qualitatively for the mean and turbulent velocity components as well (dispersion studies will be carried out in the next stage of the research), and the stability of the numerical solution is also addressed in a systematic way. Apart from the hexahedral and tetrahedral meshes, here a polyhedral mesh type is also used.

In the present paper, four mesh types are compared from the points of view mentioned above, a tetrahedral, a polyhedral, a Cartesian hexahedral, and a body fitted hexahedral mesh. At least 3 spatial resolutions and 3 discretization approaches of the convective term are considered for each mesh. For the calculations the open source CFD code, OpenFOAM® was used. It was already validated by *Franke et al.* (2012a) for simple obstacle geometries and by *Rakai* and *Kristof* (2010) for the Mock Urban Setting Test used in the COST Action 732. The test-case used in this study was also already calculated and compared to results of ANSYS® Fluent by *Rakai* and *Franke* (2012), which is a widely used industrial CFD code for CWE, and the results were similar with the two different codes.

The goal of the paper is to show the change in computational cost and quality of the results via statistical metrics of the mean and rms (root mean square) velocity components measured inside the urban canopy.

In Section 2, the numerical experiment is described with a detailed description of the case study, the numerical discretization methods, and the metrics used for comparison. In Section 3, results are shown from different viewpoints and conclusions are drawn in Section 4 with an outlook to future work.

2. *Numerical experiment*

2.1. Case study

The chosen case study is an idealized Central European city centre, Michel-Stadt. It was chosen as it is a complex geometry with detailed measurement results available (*Fischer et al.*, 2010). In the COST Action 732 (*Schatzmann et al.*, 2009) on the Quality assurance of microscale meteorological models, a more simple (Mock Urban Setting Test, simple rows of identical obstacles) and a more complex (a part of Oklahoma city) test-case was used, and it was found that an in-between complexity would be beneficial. In the COST Action ES 1006 on the Evaluation, improvement and guidance for the use of local-scale emergency prediction and response tools for airborne hazards in built environments (http://www.elizas.eu/), the Michel-Stadt case is used for the first evaluations.

Two component LDV (laser doppler velocimeter) measurements were carried out in the Environmental Wind Tunnel Laboratory of the University of Hamburg. They are part of the CEDVAL-LES database (http://www.mi.uni-hamburg.de/Data-Sets.6339.0.html), which consists of different complexity datasets for validation purposes. This case, Michel-Stadt, is the most complex case of the dataset. There are two versions of it, one with flat roofs and another with slanted roofs. In this paper the flat-roof case is used. 2158 measurement points are available for the flow field; they can be seen in *Fig. 1*. They consist of 40 vertical profiles (10–18 points depending on location for each), 2 horizontal planes (height 27 m and 30 m, 225 measurement points for each), and 3 so-called street canyon planes (height 2 m, 9 m and 1 m, 383 measurement points for each), which are located inside the urban canopy.

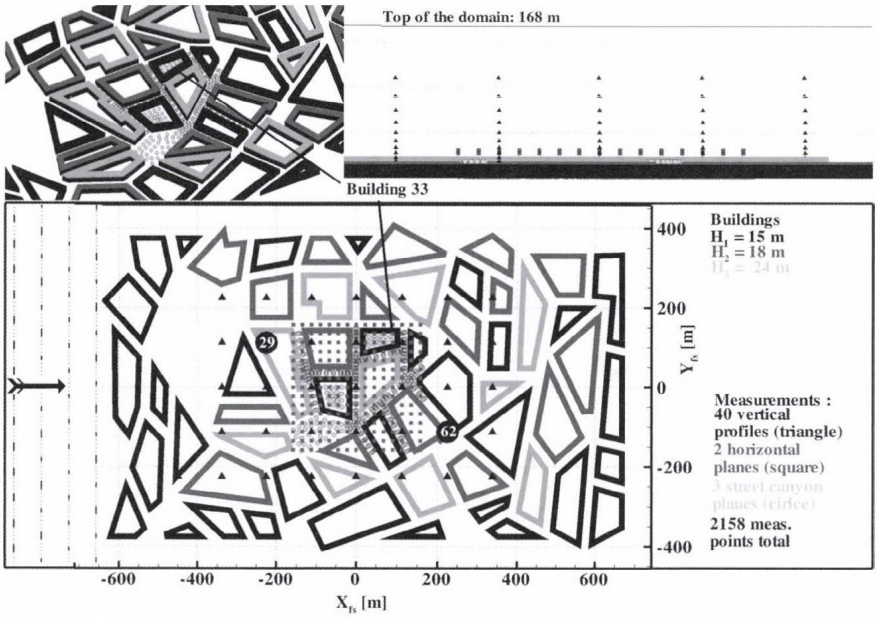

Fig. 1. Michel-Stadt with measurement points, Building 33 highlighted, the location of the roughness elements is just illustration, not exact.

The two available components are the streamwise and lateral velocity components, and time series are available for each of them. The dataset also contains the statistically evaluated mean (U_{mean}-streamwise, V_{mean}-lateral), rms (U_{rms}-streamwise, V_{rms}-lateral), and correlation values for comparison with steady state computations.

Approach flow data are provided from 3 component velocity measurements. The approach flow is modeled as an atmospheric boundary layer in the wind tunnel with the help of spires and roughness elements.

2.2. Computational model and boundary conditions

The computational domain was defined to correspond with the COST 732 Best Practice Guideline (*Franke et al.*, 2007) (*Fig. 1*), which resulted in a 1575 m × 900 m × 168 m domain, with a distance of the buildings of 11 H_3 from the inflow, 9.4 H_3 from the outflow, and at least 6 H_3 from the top boundaries, where H_3=24 m is the highest building's height. The computations were done in full scale, while the experiment was done at a scale of 1 : 225. The dependence of the results on this scale change was investigated by *Franke et al.* (2012b) using both full scale and wind tunnel scale simulations, and only a small difference in the statistical validation metrics was observed.

As *Roache* (1997) explains, the governing partial differential equations (PDE) and their numerical solution both add up to the total error of the simulation. To have a better view of the effect of the numerical discretization (and the resulting numerical error), the governing PDEs were kept the same during all the numerical experiments.

As inflow boundary condition, a power law profile (exponent 0.27, with a reference velocity U_{ref}=6.11 m/s defined at z_{ref}=100 m) fitted to the measured velocity values was given. This corresponds to a surface roughness length z_0=1.53 m. *Britter* and *Hanna* (2003) define this as a very rough or skimming approach flow. The turbulent kinetic energy and its dissipation profiles were calculated from the measured approach flow values by their definition and equilibrium assumption. At the top of the domain the measurement values corresponding to that height were fixed. The lateral boundaries were treated as smooth solid walls, as the computational domain's extension is the same as the wind tunnel width. The floor, roughness elements, and buildings were also defined as smooth walls. Standard wall functions were used. As the roughness elements are included in the domain, there is no need to use rough wall functions for the approach flow, and also the problem of maintaining a horizontally homogeneous ABL (atmospheric boundary layer) profile, which is reported (*Blocken et al.*, 2007b) to be problematic for this kind of modeling, is avoided. *Franke et al.* (2012b) have shown in a further investigation that this is not necessary as the flow is governed by interacting with the first buildings. They compared the modeling of the roughness elements explicitly and implicitly and found little influence on the results.

The Reynolds Averaged Navier-Stokes Equations were solved with standard k-ε turbulence model and the SIMPLE (semi-implicit method for pressure linked equations) method was used for pressure-velocity coupling (*Jasak,* 1996).

2.3. Discretization of the governing PDFs

As was stated before, numerical discretization has an effect on the results of the solution due to numerical error. In complex geometries its exact quantification is difficult as no analytical solution of the governing equations exists, but with a numerical experiment the effect can be investigated. In the following the mesh type, spatial resolution and the convective term discretization used for Michel-Stadt is explained. All the meshes were generated automatically which is a necessity for using this model for operational purposes and general building configurations.

2.3.1. Spatial discretization

Four mesh types are compared; their visual appearance is illustrated always for Building 33, highlighted in *Fig. 1*:

- *Unstructured full tetrahedral Delauney mesh generated with ANSYS® Icem.*

For the creation of the Delauney volume cells, first an Octree mesh was created and kept only at the surfaces, the Delauney mesh was grown from that surface mesh (*Fig. 2a*). The coarsening of the meshes was carried out by scaling the defined minimum length scales in ANSYS® Icem by 1.6. Resolution of buildings was given by the minimum face and edge size on each building. The maximum allowed expansion ratio was given for the Delauney algorithm.

- *Unstructured full polyhedral mesh created by ANSYS® Fluent from the tetra mesh.*

The polyhedral meshes were converted from the original tetrahedral meshes by ANSYS® Fluent. Each non-hexahedral cell is decomposed into sub-volumes called duals which are then collected around the nodes they belong to in order to form a polyhedral cell (see *Ansys*, (2009) for more details). The refinement ratio is thus kept very similar to the one in case of the tetra meshes(*Fig. 2b*).

- *Cartesian hexahedral mesh created with snappyHexMesh of OpenFOAM®.*

As the main research tool for these investigations is OpenFOAM®, its open source meshing tool is also used for mesh generation. This is done first by creating a Cartesian castellated mesh by refining around a given file in STL format and deleting cells inside the geometry. This mesh was also investigated in the studies (Fig. 2c), as the generation process for this one in much faster than for any of the other meshes mentioned. Building resolution cannot be given explicitly, only the resolution of the starting domain and the number of refinement iteration cycles can be defined.

- *Body fitted hybrid mesh with mostly hexahedral elements meshed with snappyHexMesh of OpenFOAM®.*

The Cartesian mesh is snapped to the edges of the geometry (*Fig. 2d*) as a next step, which takes approximately 10 times more time as the creation of the Cartesian mesh.

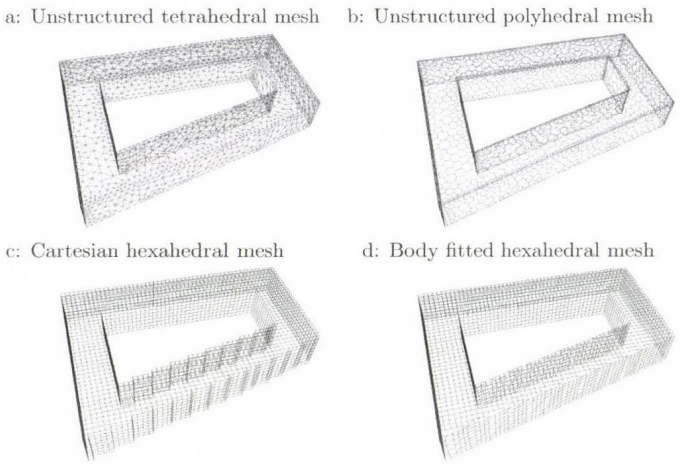

Fig. 2. Coarsest surface meshes on Building 33.

The grid convergence performance of the meshes was also investigated; at least 3 different resolutions were used for each mesh type. This makes it possible to use them for numerical uncertainty estimation at a later stage of the study.

The cell numbers of the investigated meshes can be found in *Table 1*. To have a better idea of the resolution of urban area and the buildings, in *Table 2* the number of faces on Building 33 is shown. This building was chosen as it is in the measured area close to other buildings, thus it is an indicator of street canyon resolution. The entire surface area of this building is approximately 12 000 m^2.

As it can be seen, the resolution on the building for different mesh types is not in linear relation with the total cell numbers of that mesh. See, e.g., in *Table 1* that the coarsest polyhedral mesh has 1.7 million cells and 4038 faces on the building, while the coarsest tetrahedral mesh has 6.65 million cells and 4317 faces on the building.

Table 1. Cell numbers (million cells) of the investigated meshes

	coarsest				**finest**
polyhedral	1.73	–	3.21	–	6.17
tetrahedral	6.65	–	13.17	–	26.79
Cartesian hexahedral	2.39	3.97	8.04	14.23	27.52
body fitted hexahedral	2.40	3.97	8.04	14.23	27.52

Table 2. Face numbers on Building 33

	coarsest				**finest**
polyhedral	4038	–	7455	–	12293
tetrahedral	4317	–	8934	–	15987
Cartesian hexahedral	3600	5486	11780	19879	36525
body fitted hexahedral	3416	5217	11180	18854	34660

2.3.2. Mesh quality

If we would like to resolve complex geometries properly, a compromise in mesh quality is unavoidable. This can cause a decrease both in numerical accuracy and stability of the computations, for more detail see *Jasak* (1996).

Some general measures on mesh quality to keep in mind when creating a mesh are the following:

- *Cell aspect ratio*

  Ratio of longest to shortest edge length is best to keep close to 1.

- *Expansion ratio/cell volume change*

Ratio of the size of two neighboring cells is best to keep under 1.3 in regions of high gradients (*Franke et al.*, 2007).

- *Non-orthogonality*

Angle α between the face normal $\underline{S}$ and PN vector connecting cell centers P and N is best to keep as low as possible, see in *Fig. 3.*

- *Skewness*

Distance between face centroid and face integration point is best to keep as low as possible, see $\underline{m}$ in *Fig. 3.* In OpenFOAM® this value is normalized by the magnitude of the face area vector $\underline{S}$.

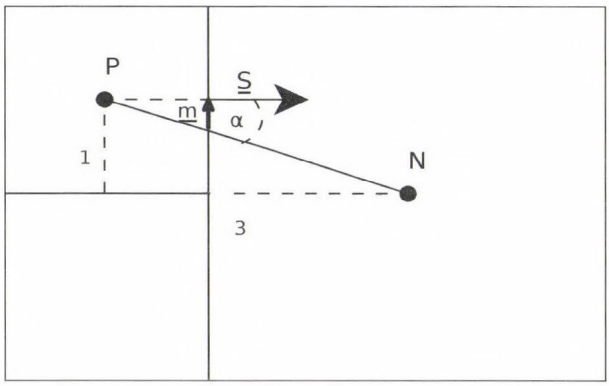

Fig. 3. Non-orthogonality and skewness.

2.3.3. Discretization of the convective/advective term

The discretization of the convective/advective terms of the transport equations solved is an important source of numerical discretization error. Upwind schemes use the values of the upwind cell as face value for the flux calculation (*Jasak*, 1996).

Central differencing uses a linear interpolation of the upwind and downwind cell value for the face value, which is of higher accuracy but may be unstable. Other schemes are defined as combination of the two for an optimal compromise between accuracy and stability (*Jasak,* 1996), like linearUpwind (a first/second order, bounded scheme) in OpenFOAM® (*OpenCFD Limited*, 2011) or second order upwind in ANSYS® Fluent (*Ansys*, 2009).

Different schemes can be used for the different variables, and to reach convergence, the following was found to be useful in OpenFOAM®:

- Initialize the solution domain with a potential flow solution.
- Use full upwind schemes for all convective terms.
- Use linearUpwind for momentum equation convective terms, upwind for the turbulence equations.
- Use linearUpwind for all convective terms.

The discretization of the pressure equation used to enforce mass conservation and all other gradients was approximated with the linear Gauss scheme. This can also add up to the instability of the solution.

It is important to note here that using higher order schemes of the convective/advective terms for meteorological models is not straightforward. E.g., in the MISKAM® model, which is a microscale operational model for urban air pollution dispersion problems, only upwind-differences are used for the discretization of the advection terms in the momentum equations (*Eichhorn,* 2008). *Janssen et al.* (2012) also shows that for certain meshes the use of higher order terms can cause convergence problems, so users may be forced to use lower order discretization. They suggest a not automatically generated hexahedral mesh to avoid this problem.

2.4. Validation metrics

With all the modeling and numerical errors inherent in the simulations, it is of vital importance to compare the simulation results to measurements. This way one can gain more information on the performance of the model. In case of wind engineering, the simulations are usually compared to wind-tunnel experiments as they are more controllable than field experiments with regard to boundary/meteorological conditions and have smaller measurement uncertainties, see *Schatzmann* and *Leitl* (2011) and *Franke et al.* (2007).

The most straightforward and inevitable part of the comparison is visual comparison with the aid of vertical profiles, contour and streamline plots, scatter plots, etc. It is also important, however, to quantify the differences in the models, for which reason validation metrics are used.

- *HR*

The most widespread metric in CWE (see, e.g., *VDI* (2005), *Schatzmann et al.* (2009), and *Parente et al.* (2010)) for wind velocity data is hit rate, which can be defined as in Eq. (1), where S_i is the prediction of the simulation at measurement point *i*, E_i is the observed experimental value, and W is an allowed absolute deviation, based on experimental uncertainty. N is the total number of measurement locations.

$$HR = \frac{1}{N}\sum_{i=1}^{N}\delta_i \,, \tag{1}$$

$$\delta_i \begin{cases} 1 for \left|\frac{S_i - E_i}{E_i}\right| \leq 0.25 \vee |S_i - E_i| \leq W \\ 0 for else \end{cases} .$$

The allowed relative deviation in Eq. (1) was used as 25% first in the VDI guideline (*VDI*, 2005), and from thereon this value is used by the CWE community. A disadvantage of the hit rate metric is that it takes into

consideration only the experimental uncertainty and it is sensitive to the used allowed experimental uncertainty (W) value. More detail on this can be found in the Background and Justification Document of the COST ES1006 Action (*COST ES1006,* 2012). When comparing different simulations with the same allowed threshold values, differences can equally be seen.

For the investigated Michel-Stadt case, the allowed absolute uncertainty was defined by *Efthimiou et al.* (2011) only for the streamwise and lateral normalized velocity components (0.033 for U_{mean}/U_{ref} and 0.0576 for V_{mean}/U_{ref}), so the calculation of the metric would only be possible for those variables. However, as time dependent measurement series are available and statistical results are also provided by the *EWTL*, it is beneficial to compare also the Reynolds stress components. Here the normalized diagonal components are shown as they are used to calculate turbulent kinetic energy, which will be of vital importance for the dispersion simulations.

For the allowed absolute uncertainty in the hit rate metric, different values were tested. It was found that the relation of metrics to each other is independent of the chosen value, so 0.003 are used for both U_{rms}/U_{ref} and V_{rms}/U_{ref}, which were found to be appropriate to have sensible values between 0 and 1 for the hit rate metric.

- *L2 norm*

Using matrix norms for comparison is also possible. With *L2* norm, the negative values of velocity components are not problematic. This metric can be seen as a normalized relative error of the whole investigated dataset.

$$L2 = \frac{\sqrt{\sum_{i=1}^{N}(E_i - S_i)^2}}{\sqrt{\sum_{i=1}^{N} E_i^2}}. \tag{2}$$

Finally, it is important to note that the most recent papers dealing with numerical uncertainty suggest metrics incorporating both experimental and numerical uncertainties in validation metrics as validation uncertainty, see, e.g., *Eca* and *Hoekstra* (2008). It is an important part of the quality assurance process and will be regarded in a separate publication.

3. Results and discussion

3.1. Mesh quality evaluation

The grid quality measures explained in Section 2 are investigated first for the mesh types used for the computations. The values of the quality metrics are shown in *Fig. 4* as a function of the number of cells. They were computed by the checkMesh utility of OpenFOAM®.

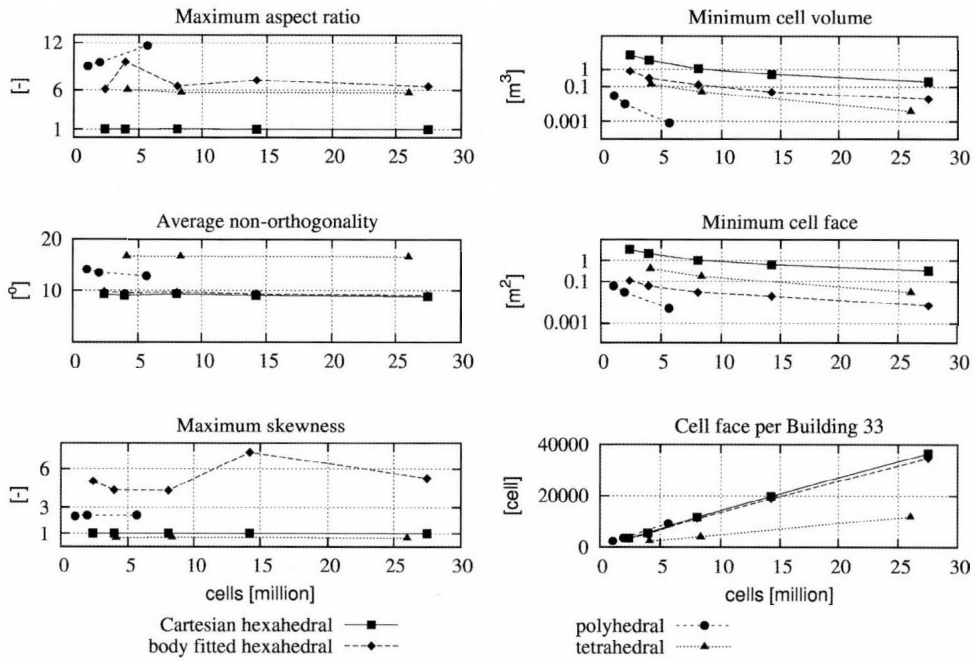

Fig. 4. Mesh quality as a function of cell number, in view of metrics explained in Section 2.3.2.

Maximum aspect ratio is highest for the polyhedral mesh, the tetrahedral and body fitted hexahedral ones are approximately half of it, while the Cartesian hexahedral mesh has an average aspect ratio of 1 as it can be expected.

The non-orthogonality is highest for the tetrahedral meshes, followed by the polyhedral ones, while all hexahedral based meshes have a constant value of 10°. Although these meshes are mainly Cartesian where 0° value is expected, by halving the cells this rule is broken for different sized neighbors. In *Fig. 3* it can be observed, how this affects the non-orthogonality. The angle for a transition of this kind in 2D can be computed as the ratio of the edges, 1 : 3 as can be seen in *Fig. 3* (angle α). This is an angle of approximately 20° which is averaged with the rest 0° values resulting in this 10° average.

Maximum skewness is the highest for the body fitted hexahedral mesh. For this metric no average value is given by the utility, it shows only the values of the worst quality cells. In that mesh, cells with skewness vector 3 times greater than the face area vector occur.

Minimum cell volume and face area decrease vary rapidly with the increase of resolution. The creation of polyhedral mesh is done by splitting the tetrahedral first, so smaller volumes and face areas occur in case of the polyhedral meshes. This can also be seen in *Fig. 2*.

About the expansion ratio it can be said, that it was set to maximum 1.3 in case of the tetrahedral meshes. For the snappyHexMesh meshes, neighboring cells can differ by a factor of 2 in edge length due to halving cells when refining locally. For unstructured meshes, the cell volume change in neighboring cells is a more useful indicator of the smoothness of transition between smaller and larger cells than expansion ratio. In case of the tetrahedral meshes, the majority of this cell volume change is below 2, while for the polyhedral meshes 6–8% of the neighbors have a cell volume change more than 10. For the hexahedral meshes, the cell volume change is below 2 in 90% of the neighbors and a jump appears around 7–8 due to the refinement method of cell halving which is expected in 3D.

3.2. Convergence

Reaching convergence in complicated geometries and low quality meshes is not always trivial, and in case of this test case, the first computations were often not successful. The best way to reach convergence for all of the cases was explained before. In cases of tetra- and polyhedral meshes, the simulations were unstable also with the described method with default relaxation factors (0.3 for p and 0.7 for the other variables). The cases had to be drastically underrelaxed to reach convergence (0.1 for p and 0.3 for the other variables). In the Best Practice Guideline for ERCOFTAC (European Research Community On Flow, Turbulence and Combustion) special interest group "Quality and Trust in Industrial CFD" (*ERCOFTAC*, 2000) it is suggested to increase the relaxation factors at the end of the solution to check if the solution holds, thus we checked it for one of the converged underrelaxed simulations. It is important also because *Ferziger* and *Peric* (2002) has shown that the optimum relation between the underrelaxation factors for velocities (uf_u) and pressure (uf_p) is $uf_p = 1 - uf_u$. With raising the relaxation factors each time by 0.1, the combination of 0.2 for p and 0.6 for the other variables were reached, but with the default combination the computation crashed again. For this reason, results with the low underrelaxation factors were investigated in the paper.

The difference between the convergence behavior of the hexahedral and polyhedral based meshes is not only their stability. Residual history is smoother for the hexahedral meshes, which makes them a more suitable tool for regulatory purpose simulations, where robustness is a big advantage and can save a lot of time for the operator.

It is an important question what may cause the instability of the tetrahedral and in one case also the polyhedral simulations. Looking at the quality metrics of the meshes, one similar behavior was found for the non-orthogality of the meshes, which can be seen in *Fig. 4*. It is clear that the tetrahedral meshes have the highest non-orthogonality followed by the polyhedral meshes, what can cause the instabilities. This indicates that gradient discretization is also

problematic. *Ferziger* and *Peric* (2002) show that in the discretization of non-orthogonal grids of the general transport equation mixed derivatives arise for the diffusive term. They say that if the angle between gridlines is small and aspect ratio is large, the coefficients of these mixed derivatives may be larger than the diagonal coefficients, which can lead to numerical problems. The checkMesh utility of OpenFOAM® reports the number of cells above the non-orthogonality threshold, which is given as 70° as a default. Although the tetrahedral meshes have higher averages of non-orthogonality, their maximum values never reached this threshold. For the polyhedral ones on the other hand, there were around 10 highly non-orthogonal cells in each mesh.

The convergence behavior of the meshes in general is explained in *Table 3*, where the necessary number of iterations is shown for each mesh, separately for the first order initialization (full upwind-11)/linearUpwind for momentum, first order for turbulence variables (mixed-21)/all higher order (full linearUpwind-22) variations. Convergence is considered when a plateau is reached in the residuals for all variables, see *Fig. 5*. For the meshes where the residuals were not smooth, other variables were also checked to stay stable.

Table 3. Necessary iterations for convergence (full upwind-11/mixed-21/full linearUpwind-22)

	coarsest				**finest**
polyhedral-11	500	–	5000	–	3000
polyhedral-21	+2500	–	+2500	–	+2500
polyhedral-22	+2500	–	+3000	–	+3000
tetrahedral-11	2000	–	2000	–	3000
tetrahedral-21	+1500	–	+1500	–	+2500
tetrahedral-22	+3500	–	+4500	–	+2500
Cartesian hexahedral-11	500	2500	2000	2500	3000
Cartesian hexahedral-21	+1000	+1000	+1000	+1000	+1500
Cartesian hexahedral-22	+500	+2000	+1000	+1000	+1500
body fitted hexahedral-11	1000	1500	1500	2000	2000
body fitted hexahedral-21	+500	+500	+1000	+1000	+1000
body fitted hexahedral-22	+1000	+1000	+1000	+1000	+1000

It can be observed that more iteration is necessary for more cells to reach the first converged state than the expected iterations for linear solvers. The outstanding value of 5000 for the medium polyhedral mesh can be explained by the instability of the computation which made heavy underrelaxation necessary.

In general, the iteration numbers are of the same order of magnitude for all of the meshes. The most orderly results are given by the snapped hexahedral meshes, which underlines again their robustness for operational simulations.

No big difference can be seen between the snapped and Cartesian hexahedral meshes, but in some cases periodic oscillation occurred using a Cartesian mesh. This reduced for the higher order computations, see *Fig. 5*.

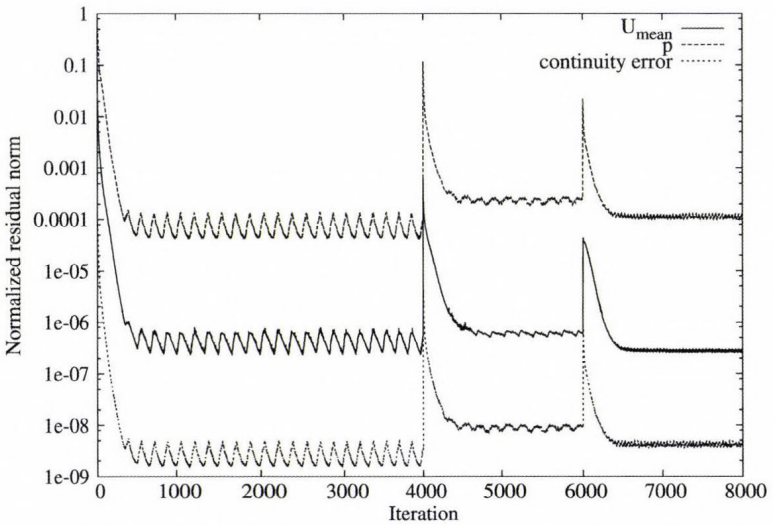

Fig. 5. Residual behavior of a Cartesian mesh.

Turning to the value of the residual norm and its drop from the beginning of the computation we observed, that this case is too complex and values do not reach the machine accuracy in single precision mode. The lowest drop is found in each case for the Poisson equation for the pressure, followed by the lateral and vertical mean velocity components. Another general observation is that all values drop below 10^{-5} for the first order calculations except for the pressure, while for the linearUpwind, only for the momentum equation this drop is usually smaller, followed by a drop below 10^{-5} again for the full linearUpwind computations. The continuity error had a similar behavior, but the first drop was usually below 10^{-8} (see *Fig. 5* for graphical explanation).

This behavior can be explained by the categorization of *Menter* (2012), who states that the classical example of a globally unstable flow is the flow past bluff bodies (like the buildings). Because of this unsteadiness, periodical changes in the residuals are appearing even if the boundary conditions are steady, like in our case.

3.3. Computational cost analysis

One of the main goals of the paper is to compare the models from a regulatory purpose point of view. When carrying out simulations for, e.g., a government, it is usually not possible to wait several days until the simulation is finished on a cluster, and stability is of high importance. For this reason, the computational costs are also evaluated.

The results of this analysis for all of the meshes can be seen in *Fig. 6*. It is apparent, that the memory usage scales linearly for all of the meshes, and the difference in the mesh types can be explained by the relative number of cell faces, i.e., the polyhedral mesh uses more memory for a given number of cells, while the tetrahedral mesh uses less. There is no significant difference between the two kinds of hexahedral meshes, but it is important to note that the solver itself takes no benefit from the fact that one of them is Cartesian.

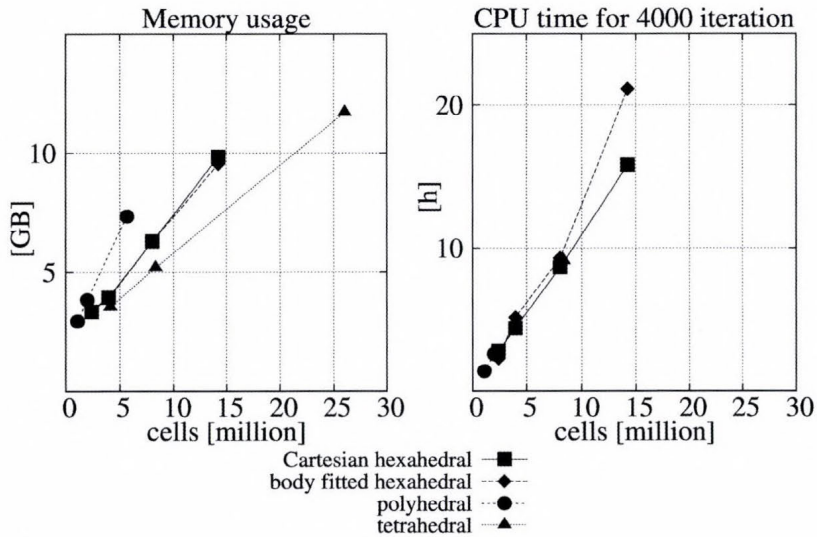

Fig. 6. Computational cost of the simulations for the full upwind simulations, 4000 iterations.

For the comparison of the CPU time, only the relative values are interesting, and it can be seen that the CPU time demand scales linearly with the number of cells, and there is no significant difference in the mesh types. These comparative simulations were carried out on the new cluster of the University of Siegen (http://www.uni-siegen.de/cluster/index.html?lang=en), run for 4000 iterations with first order upwinding for all variables on 24 cores. As a rule of thumb for this setup it can be said, that a simulation result can be obtained in

1 hour/1 million cells. Those meshes which were unstable with the default relaxation factors are omitted from the CPU-time graph.

3.4. Sensitivity to discretization in view of different metrics

Metrics are unavoidable when comparing a lot of different variations, but it is better to check with different metrics to reveal if one of them is biased. The metrics described in Section 2 are used to compare the performance of 4 mesh types, 3–5 spatial resolutions, and 3 discretization scheme combinations for the convective term of the transport equations. Hit rate results for all the cases investigated are shown in *Fig. 7* as a function of the number of cells. The metric based on *L2* normalization can be seen in *Fig. 8* also as a function of the number of cells.

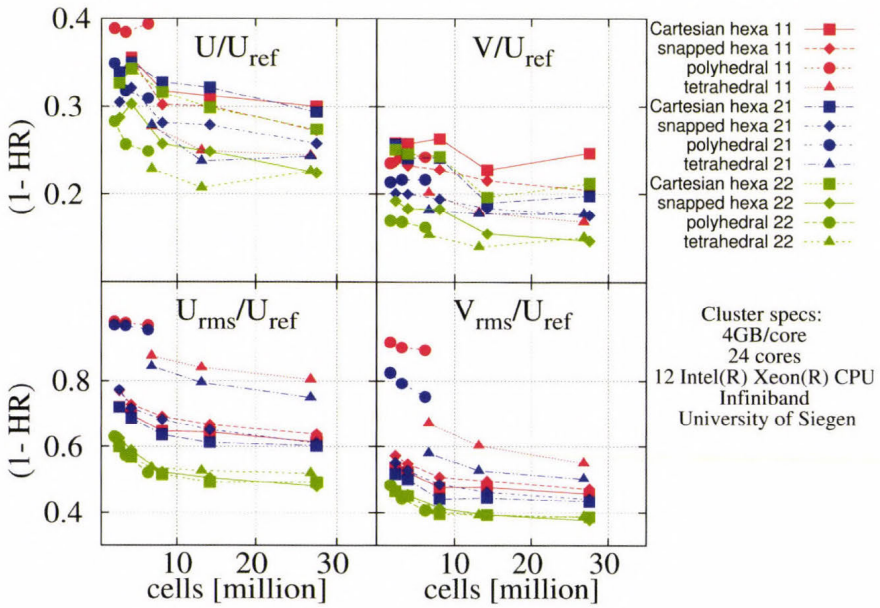

Fig. 7. Sensitivity to discretization, hit rate metric (full upwind-11/mixed-21/full linearUpwind-22).

Comparing the hit rate metric results in *Fig. 7* and the *L2* norm metric results in *Fig. 8* it is important to note, that in case of the hit rates, an "1 – *HR*" is shown to make them visually similar. Thus, on both figures the smaller is the better. However, the interpretation is very different. In case of the hit rate figure, a smaller value means that more points became "hits", the difference between simulation and experiment getting to the acceptable range. Once a point is in this

range, the hit rate will not improve even if the results get closer to each other. On the other hand, for the *L2* norm metric, a smaller value means that the difference between simulation and experiment got smaller.

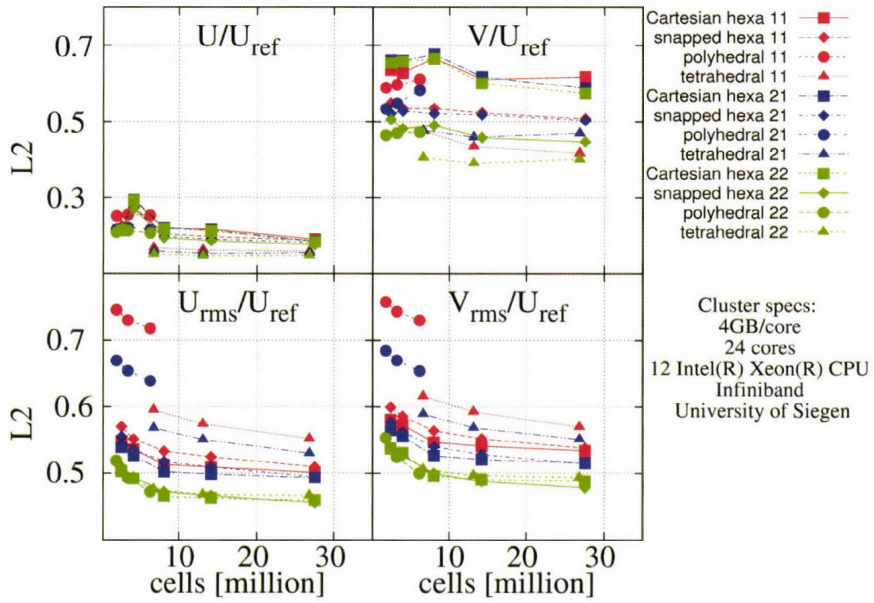

Fig. 8. Sensitivity to discretization, *L2* metric (full upwind-11/mixed-21/full linearUpwind-22).

For the absolute value of the hit rate metric for the mean velocity values it can be said, that these high hit rates are good results for this complex case. Similar values were found by *Efthimiou et al.* (2011) for two other codes, Andrea® and Star-CD®, and by *Franke et al.* (2012b) and *Rakai* and *Franke* (2012) for the ANSYS® Fluent code for the mean velocities. No further exact comments can be made for the turbulent quantities, as the threshold value was chosen arbitrarily and not based on measurement uncertainties. In the VDI guideline (*VDI*, 2005) an acceptable HR value is given for certain test cases, thresholds, and measurement points, but it is not easily transferable to a totally different case.

The absolute value of the *L2* norm metrics can be interpreted as a kind of relative error, showing that for the streamwise velocity results, where the values are essentially higher, the metric is smaller than for all the other variables. For the conclusions drawn later, the absolute value of this metric is not considered.

The conclusions which can be drawn from *Fig. 8* of the *L2* metric norm are the following:

1. For streamwise velocities, tetrahedral meshes perform outstandingly better.

From theoretical point of view, the smallest numerical error is expected from the hexahedral meshes. The reason for this is shown by *Juretic* and *Gosman* (2010): because the hexahedral mesh is aligned with the flow, the errors in fluxes cancel. Explanation for the superior performance of the same mesh size for the tetrahedral meshes in this case can be that those were made with the Delauney algorithm, so they are not "wasting" so many cells in the middle of the domain where there is no geometric feature to disturb the flow, so the gradients are small and do not make high mesh resolution necessary. In case of the hexahedral meshes, the underlying original mesh block has a quite high density. This can be seen in the two coarse meshes compared in *Fig 9*. It is also seen that the transition of tetrahedral cells is smoother from the fine to the coarse cells, and above the canopy where there are still strong gradients, the hexahedral meshes are not resolved enough. See *Fig. 10* for the visualization of these gradients above the urban canopy. A line is shown in *Fig. 9* below which high gradients occur in the solution.

Franke et al. (2012b) used also a block-structured hexahedral mesh for their investigations with ANSYS® Fluent and had better performance also in the mean velocities. That mesh is not automatically generated and has very different mesh quality metrics than the automatic snappyHexMesh meshes (average non-orthogonality 2.64, maximum skewness 1.47, and smooth cell volume transition). The worse results of the automatic hexahedral meshes can be explained by their larger and lower quality cells in the most important regions shown in *Fig. 9*.

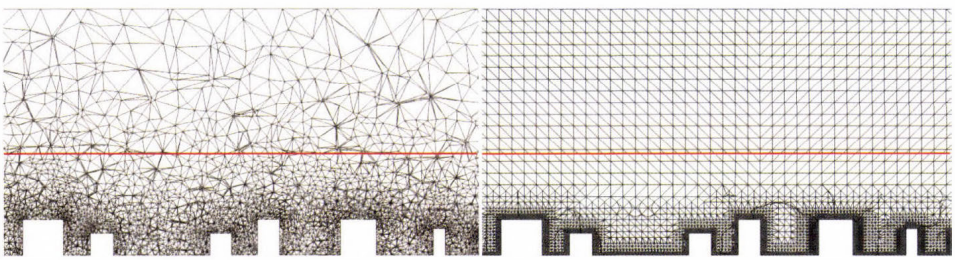

Fig. 9. Tetrahedral (6.65 $\times 10^6$ cells) and hexahedral (8.0 $\times 10^6$ cells) mesh cross sections (diagonal lines are just visualization tool specific features in the hexahedral mesh).

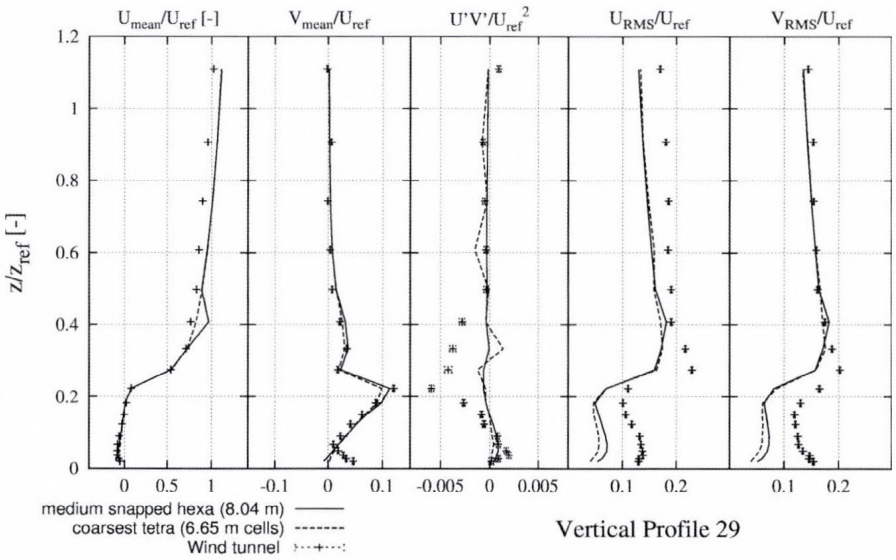

Fig. 10. Profile 29 of one tetrahedral (6.65 $\times 10^6$) and one hexahedral (8.0 $\times 10^6$) mesh (full linearUpwind solution).

2. Better performance of the tetrahedral meshes is not so apparent for lateral velocity, and disappears for the rms values.

To better understand this phenomenon, *Fig. 10* shows the profiles compared at location 29 (see *Fig. 1*) which is in the yard of an 18 m high building. In the non-dimensional scale 0.18 is the top of the building and it can be observed that changes in streamwise mean velocity reach 0.4, while for the other values the maximum is 0.3. So the smoother transition of the tetra mesh can help to better resolve the streamwise velocity, but for the other values it is not so important. The oscillations on the profiles for the tetra meshes can be found on other profiles computed with OpenFOAM® as well. They may be a consequence of the instability of the simulations, however, for the ANSYS® Fluent results they do not appear. This phenomenon needs further investigation.

3. Full second order solutions perform better already for the mean values, but that difference competes with the CPU-time cost of the results. For the turbulent quantities, however, full second order solutions are outstanding.

Theoretically this is obvious as higher order terms are more accurate, but on the other hand, this can amplify the errors in the modeling assumptions. In the Michel-Stadt case the higher order results for the simulation always compare better to the experimental values. It must be kept in mind that not all

micrometeorological models use higher order advective terms. As the turbulent quantities are used for the dispersion calculations, it can have a significant effect and higher order terms are suggested.

4. Polyhedral meshes have very low performance compared to all the other cases if not full second order discretization is used.

This can be a result of the larger volumes in those meshes and the large cell volume changes explained, strengthening the numerical errors. It is suggested to use polyhedral meshes only with higher order convective/advective terms, as those metrics are comparable with the other mesh types.

5. The Cartesian hexahedral meshes have lower performance in the mean velocities, but this disappears for the turbulent statistics.

More comparable results for rms value prediction need further investigation. This can be caused by the generally wrong rms predictions for all mesh types and by the numerical errors canceling the modeling errors.

6. There is a jump of low performance for the second coarsest hexahedral meshes which is visible both in the hit rate metric and *L2* norm metric.

This is a sign that mesh refinement does not always lead to improved solutions because of the error cancellation explained above. Also the importance of investigation of mesh dependency on more meshes must be noted.

4. Conclusions and outlook

Sensitivity of four different metrics to compare experimental and simulation results was investigated for a test case of an idealized Central European city center, Michel-Stadt. The numerical discretization approaches were compared with four different mesh types, at least 3 resolutions for each of them, and different discretization procedures of the convective/advective term in a numerical experiment.

It was found that snappyHexMesh meshes are more stable computationally. so they are more appropriate for operational purposes, although their metric performance is not as good as that of the tetrahedral meshes. The lower validation metric performance is not true in general for all hexahedral meshes, more time consuming block-structured meshes with higher mesh quality metrics can be generated which are both stable and more accurate.

For diagonal components of the Reynolds stresses, i.e., the rms values in experimental results, discretization schemes of the convective terms have a striking but expectable effect which must be kept in mind for dispersion studies where their value effects turbulent diffusion. Numerical discretization differences can cause almost 20 % change in the hit rate metric.

There are still many open questions to be further investigated, e.g., the oscillation in the tetrahedral profiles, correspondence between stability and mesh quality of the different mesh types, and the generation of the polyhedral mesh to explain their low upwind validation metrics. This will be carried out through further more detailed analyses of the datasets.

The work with Michel-Stadt continues in the framework of COST Action ES 1006 with numerical uncertainty estimation and dispersion studies for continuous and puff passive scalar sources. The Action involves several research groups who use different codes, including prognostic microscale obstacle resolving meteorological models, diagnostic flow models, and operational Gaussian type plume models. After investigations of the setup shown in this paper, a blind test will be carried out to evaluate the use of local-scale emergency prediction and response tools for airborne hazards in built environments.

Acknowledgement–This research was financed by a scholarship of the Hungarian Government and the project Talent Care and Cultivation in the Scientific Workshops of BME. The project is supported by the grant TAMOP-4.2.2/B-10/1-2010-0009. It is also related to the scientific programme of the project Development of Quality-Oriented and Harmonized R+D+I Strategy and the Functional Model at BME, the New Hungary Development Plan (Project ID: TAMOP-4.2.1/B-09/1/KMR-2010-0002), and the K 108936 ID project of the Hungarian Scientific Research Fund. Collaboration of the authors was possible thanks to two DAAD (German Academic Exchange Service) research grants, number A/10/82525 and A/11/83345.

References

Ansys®, 2009: Ansys Fluent 14.0 Theory Guide. Canonsburg, Pennsylvania.

Baklanov, A. and *Nuterman, R.B.*, 2009: Multi-scale atmospheric environment modelling for urban areas. *Adv. Sci. Res. 3,* 53–57.

Baklanov, A., 2000: Application of CFD methods for modelling in air pollution problems: possibilities and gaps. *Environ. Monit. Assess. 65,* 181–189.

Balczó, M., Balogh, M., Goricsan, I., Nagel, T., Suda, J., and *Lajos, T.*, 2011: Air quality around motorway tunnels in complex terrain – computational fluid dynamics modeling and comparison to wind tunnel data. *Időjárás 115,* 179–204.

Balogh, M., Parente, A., and *Benocci, C.*, 2012: RANS simulation of ABL flow over complex terrains applying an Enhanced k-ε model and wall function formulation: Implementation and comparison for fluent and OpenFOAM®. *J. Wind Eng. Ind. Aerod. 104–106,* 360–368.

Blocken, B., Stathopoulos, T., and *Carmeliet, J.*, 2007a: CFD evaluation of wind speed conditions in passages between parallel buildings – effect of wall-function roughness modifications for the atmospheric boundary layer flow. *J. Wind Eng. Ind. Aerod. 95,* 941–962.

Blocken, B., Stathopoulos, T., and *Carmeliet, J.*, 2007b: CFD simulation of the atmospheric boundary layer: wall function problems. *Atmos. Environ. 41,* 238–252.

Britter, R.E. and *Hanna, S.R.*, 2003: Flow and dispersion in urban areas. *Annu. Rev. Fluid Mech. 35,* 469–96.

COST ES1006, 2012: COST ES1006 Background and Justification Document. *COST. Action ES 1006: Evaluation, improvement and guidance for the use of local-scale emergency prediction and response tools for airborne hazards in built environments.*

Durbin, P.A., 1996: On the k- ε stagnation point anomaly. *Int. J. Heat Fluid Flow 17,* 89–90.

Eca, L. and *Hoekstra, M.*, 2008: Testing Uncertainty Estimation and Validation Procedures in the Flow Around a Backward Facing Step. In *Proceedings of the 3rd Workshop on CFD Uncertainty Analysis.*

Efthimiou, G.C., Hertwig, D., Fischer, R., Harms, F., Bastigkeit, I., Koutsourakis, N., Theodoridis, A., Bartzis, J.G., and *Leitl, B.*, 2011: Wind flow validation for individual exposure studies. In *Proceedings of the 13th International Conference on Wind Engineering (ICWE13)*, Amsterdam, The Netherlands.

Ehrhard, J., Kunz, R., and *Moussiopoulos, N.*, 2000: On the performance and applicability of nonlinear two equation turbulence models for urban air quality modelling. *Environ. Monit. Assess. 65*, 201–209.

Eichhorn, Dr. J., 2008: MISKAM manual for version 5. Spielplatz 2 55263 Wackernheim.

ERCOFTAC, 2000: Best Practice Guidelines. *ERCOFTAC Special Interest Group on "Quality and Trust in Industrial CFD".*

Ferziger, J.H. and *Peric, M.*, 2002: Computational Methods for Fluid Dynamics. Springer, Berlin Heidelberg New-York

Fischer, R., Bastigkeit, I., Leitl, B., and *Schatzmann, M.*, 2010: Generation of spatio-temporally high resolved datasets for the validation of LES- models simulating flow and dispersion phenomena within the lower atmospheric boundary layer. In *Proceedings of The Fifth International Symposium on Computational Wind Engineering (CWE2010)*, Chapel Hill, North Carolina, USA.

Franke, J., Hellsten, A., Schlünzen, H., and *Carissimo, B.*, 2007: Best Practice Guideline for the CFD Simulation of Flows in the Urban Environment. *COST Action 732: Quality Assurance and Improvement of Microscale Meteorological Models.*

Franke, J., 2010: A review of verification and validation in relation to CWE. In *Proceedings of the Fifth International Symposium on Computational Wind Engineering (CWE2010)* Chapel Hill, North Carolina, USA, May 23–27, 2010.

Franke, J., Hellsten, A., Schlunzen, K.H., and Carissimo, B. 2011. 2011 The COST 732 Best Practice Guideline for CFD simulation of flows in the urban environment: a summary. *International Journal of Environment and Pollution, 44(1–4), 419–427.*

Franke, J., Sturm, M., and *Kalmbach, C.*, 2012a: Validation of OpenFOAM® 1.6.x with the German VDI guideline for obstacle resolving microscale models. *J. Wind Eng. Ind. Aerod. 104–106*, 350–359.

Franke, J., Laaser, A., Bieker, B., and *Kempfer, T.* 2012b: Sensitivity analysis of RANS simulations for flow and dispersion in the generic European City Centre Michel-Stadt. In *Proceedings of Conference on Modelling Fluid Flow.* Budapest, Hungary, Sept 4–7 2012.

Hefny, M.M. and *Ooka, R.*, 2009: CFD analysis of pollutant dispersion around buildings: Effect of cell geometry. *J. Build. Environ. 44*, 1699–1706.

Janssen, W.D, Blocken, B., and *van Hoof, T.* 2012: Pedestrian wind comfort around buildings: comparison of wind comfort criteria based on whole-flow field data for a complex case study. *J. Build. Environ. accepted for publication.*

Jasak, H., 1996: Error Analysis and Estimation for the Finite Volume Method with Application to Fluid Flows. *PhD. Thesis, Imperial College of Science, Technology and Medicine.*

Juretic, F. and *Gosman, A.D.*, 2010: Error Analysis of the Finite-Volume Method with respect to Mesh Type. *Num. Heat Transfer 57*, 414–439.

Leelőssy, Á., 2012: Baleseti kibocsátásból származó szennyezőanyagok lokális skálájú terjedésének modellezése. *M.Sc. thesis, Eötvös Lóránd Univ. Dep. Meteorology.* (In Hungarian)

Lun, Y.F., Mochida, A., Murakami, S., Yoshino, H., and *Shirasawa, T.*, 2003: Numerical simulation of flow over topographic features by revised k – ε models. *J. Wind Eng. Ind. Aerod. 91*, 231–245.

Menter, F.R., 2012: Best Practice: Scale-Resolving Simulations in ANSYS® *CFD. ANSYS®*, Germany.

Mészáros, R., Vincze, Cs., and *Lagzi, I.*, 2010: Simulation of accidental release using a coupled transport (TREX) and numerical weather prediction (ALADIN) model. *Időjárás 114*, 101–120.

Oberkampf, W.L., and *Trucano, T.G.*, 2002: Verification and validation in computational fluid dynamics. *Prog. Aerospace Sci, 38.* 209–272.

OpenCFD Limited, 2011: OpenFOAM® User Guide – Version 2.0.0. OpenCFD Limited.

O'Sullivan, J.P., Archer, R.A., and *Flay, G.J.,* 2011: Consistent boundary conditions for flows within the atmospheric boundary layer. *J. Wind Eng. Ind. Aerod. 99,* 65–77.

Parente, A., Gorlé, C., van Beeck, J., and *Benocci, C.* 2010: A Comprehensive Modelling Approach for the Neutral Atmospheric Boundary Layer: Consistent Inflow Conditions, Wall Function and Turbulence Model. *Bound-Lay. Meteorol. 140,* 411–428.

Rakai, A. and *Franke, J.,* 2012: Validation of two RANS solvers with flow data of the flat roof Michel-Stadt case. In *Proc. 8th International Conference on Air Quality – Science and Application,* Athens, Greece.

Rakai, A., and *Kristóf, G.,* 2010: CFD Simulation of Flow over a Mock Urban Setting Using OpenFOAM®. In Gépészet 2010: *Proceedings of the Seventh Conference on Mechanical Engineering.* Budapest, Hungary.

Richards, P.J. and *Hoxey, R.,* 1993: Appropriate boundary conditions for computational wind engineering models using the k – turbulence model. *J. Wind Eng. Ind. Aerod. 47,* 145–153.

Roache, P.J., 1997: Quantification of Uncertainty in Computational Fluid Dynamics. *Annu. Rev. Fluid Mech. 29,* 123–60.

Schatzmann, M., Olesen, H., and *Franke, J.* 2009: COST 732 Model Evaluation Case Studies: Approach and Results. *COST Action 732: Quality Assurance and Improvement of Microscale Meteorological Models.*

Schatzmann, M. and *Leitl, B.,* 2011: Issues with validation of urban flow and dispersion CFD models. *J. Wind Eng. Ind. Aerod. 99,* 169–186.

Stull, R.B., 1988: An Introduction to Boundary Layer Meteorology. Kluwer Academic Pub.

Tominaga, Y., Mochida, A., Yoshie, R., Kataoka, H., Nozu, T,, Kazuyoshi, Y,, M., and *Shirasawa, T.,* 2008: AIJ guidelines for practical applications of CFD to pedestrian wind environment around buildings . *J. Wind Eng. Ind. Aerod. 96,* 1749–1761.

Tominaga, Y., Mochida, A., Shirasawa, T., Yoshie, R., Kataoka, H., Harimoto, K., and Nozu, T., 2004: Cross Comparison of CFD Results of Wind Environment at Pedestrian Level around a High-rise Building and within a Building Complex. *J. Asian Arch. Build. Engin., 3.*

VDI., 2005: Environmental Meteorology – Prognostic microscale wind field models – Evaluation for flow around buildings and obstacles, *VDI guideline 3783, Part 9.*

Wright, N.G., and *Easom, G.J.,* 2003: Non-linear k – turbulence model results for flow over a building at full scale. *Appl. Math. model. 27,* 1013–1033.

Yang, Y., Gu, M., Chen, S., and *Jin, X.,* 2007: New inflow boundary conditions for modeling the neutral equilibrium atmospheric boundary layer in computational wind engineering. *J. Wind Eng. Ind. Aerod. 97,* 88–95.

Yoshie, R., Mochida, A., Tominaga, Y., Kataoka, H., and *Yoshikawa, M.,* 2005: Cross Comparison of CFD Prediction for Wind Environment at Pedestrian Level around Buildings Part 1-2. In *Proceedings of the 6th Asia-Pacific Conference on Wind Engineering (APCWE-VI).*Seoul, Korea, September 12–14, 2005.

IDŐJÁRÁS

Quarterly Journal of the Hungarian Meteorological Service
Vol. 118, No. 1, January – March, 2014, pp. 79–92

Facts about the use of agrometeorological information in Hungary and suggestions for making that more efficient

Zoltán Varga

Department of Agrometeorology, Faculty of Agricultural and Food Sciences,
University of West Hungary,
Vár 2, H-9200 Mosonmagyaróvár, Hungary
e-mail: varzol@mtk.nyme.hu

(Manuscript received in final form February 15, 2013)

Abstract–Demands on use of information upon relationship between meteorological conditions and agricultural production were from the beginning of meteorology and from the beginning of human civilization. The sudden development of natural sciences during the 19th and 20th centuries opened up a new prospect in producing meteorological information which was of use to food processing. On the other hand, contemporary agricultural development needed supply of more detailed and more practical agrometeorological information. Increasing importance of ecological agriculture at the expense of intensive farming systems and uncertain effects of climate change did not reduce the want for agrometeorological information; in fact, they extended the needs for those in the last decades. But positive tendencies of domestic agrometeorological research and information service in the second half of the 20th century declined till the 1990s, and there is no reason to be optimistic on the grounds of current situation.

This work attempts to review not only possibilities and results of agrometeorological information supply, but also interdisciplinary factors, such as factors of economical development and regulation, education, agricultural-advisory system, etc., which set back the development of this area. The base of our investigations is a SWOT analysis which is a strategic planning method of economical sciences used to evaluate strengths, weaknesses, opportunities, and threats involved in a project. This way we try to answer the following questions:

- Why is agrometeorology no longer an important economical factor in Hungary?
- How could we make agrometeorological research and information service become a productive economical factor again?

Key-words: agrometeorological information, agrometeorological research, SWOT analysis, climate change, decision-making

1. Introduction

The agrometeorological use of information started after the cold event called as Younger Dryas. The climate shock – a drastic warming - following that event caused a significant rise in sea level, and it changed the coastlines and topography of continents. But after that neither the sea level (topography), nor the climatic conditions changed enormously, so it helped the mankind to develop from hunter-gatherer to agricultural societies in the early Holocene (*Behringer,* 2010). According to *Bernal* (1963), it is important to make a distinction between prescientific stage of cognition and stages of history of science. Those early attempts to come to know and to influence the environmental (meteorological) effects on agricultural production belonged to the previous one of course. The ancient ploughmen awaked to their dependence on their environment and especially on weather and climate. Namely, they discovered that more sunshine and higher temperature accelerated development of plants and more rainfall caused higher yields. Results of observations about relationship between meteorological conditions and development, growth, and yields of crops came down from father to son, but this kind of knowledge could not have been quantified. People tried to influence natural forces, but it happened in a superstitious and mystificated way as they were not able to discover causal relationships. Anyhow, these efforts were the first – although not scientific – attempts to use agrometeorological information (*Varga*, 2010).

A new approach, which supposed that the world around us could have been discovered and which focused on understanding the causal relationships between phenomena of that world, rose in the first millennia BC and it helped scientific thinking to improve. It was a beneficial method also for meteorological and applied (agro)meteorological studies. Several findings and ideas – including some erroneous ones – of that era were undisputed and unsurpassable knowledge of the given area of science for the following two thousand years. The only way for gathering information was the theoretical (speculative) one, as instrumental measurements still were not possible. It obstructed to define numerically the processes and attributes of atmosphere and relationships of climate-agriculture-soil system, respectively. Consequently, use of agrometeorological information was not able to develop for further centuries.

The sudden development of natural sciences during the 19th and 20th centuries opened up a new prospect in producing meteorological information which was of use to food processing. On the other hand, contemporary agricultural development needed supply of more detailed and more practical agrometeorological information. The science of agrometeorology developed parallel with agriculture, and it worked as a prerequisite of agricultural production in those decades.

That period can be considered as the days of glory for using agrometeorological information. The well-organized agrometeorological

information supply system met the demand of intensive crop production better and better. To make the first move for this a network of phenological stations for observing the development of field crops was organized – under the direction of Zoltan Varga-Haszonits – by the Hungarian Meteorological Institute (now: Hungarian Meteorological Service). To help this work, a monograph (manual) was published (*Varga-Haszonits,* 1967), then observers working in collective farm systems were drawn into the phenological network. That study used also the database collected by the National Institute for Agricultural Quality Control (now: Central Agricultural Office). The most comprehensive Hungarian phenological database – especially for the period 1955–2000 – can be built up by unification of those two databases organized by the National Institute for Agricultural Quality Control and Hungarian Meteorological Service, respectively. The phenological data for field crops collected by the observational network of Hungarian Meteorological Service were stored at and used by the Department of Agricultural Information Supply and later by the Department of Agrometeorological Forecasting. The agrometeorological information service using those data worked under the direction of Zoltan Varga-Haszonits, after that it was organized by Sándor Dunay. Agroclimatological model-based crop yield forecasts were done for decades on behalf of the agricultural ministry.

Increasing importance of ecological agriculture at the expense of intensive farming systems and uncertain effects of climate change did not reduce the want for agrometeorological information; in fact, they extended the needs for those in the last decades. But positive tendencies of domestic agrometeorological research and information supply in the second half of the 20th century declined till the 1990s and there is no reason to be optimistic on the grounds of current situation.

This way we try to answer the following questions:

- Why – and what kind of - agrometeorological information is important for agricultural production?
- Why is agrometeorology no longer an important economical factor in Hungary?
- How could we make agrometeorological research and information service become a productive economical factor again?

2. The SWOT analysis of agrometeorological information service

Position, possibilities, and problems of agrometeorological information service were surveyed by the help of SWOT (sometimes SLOT) analysis. This method is a strategic planning used to evaluate strengths, weaknesses (or limitations), opportunities, and threats involved in a project. The internal and external factors which are favorable or unfavorable to achieve the objective can be determined (*Székely,* 2000). Identification of SWOTs is important, because they can inform

later steps in planning to achieve the objective. The usefulness of this method is not limited to profit-seeking organizations. SWOT analysis may be used in any decision-making situation when a desired objective has been defined (URL[1]). The objective of our examined area is to help agricultural decisions and to raise food production a higher level. So it seemed to be reasonable to estimate the internal advantageous and disadvantageous characteristics of agrometeorological research and information supply, as well as the external opportunities and threats of those by means of this generally accepted method.

Table 1 summarizes the SWOTs of agrometeorological information service.

Table 1. The SWOTs of agrometeorological information service

	Helpful (+)	**Harmful (-)**
Internal origin	***Strengths:***	***Weaknesses/Limitations:***
	– the agricultural production's need for agrometeorological information	– stochastic relationships of soil-atmosphere-agriculture system
	– domestic agrometeorological research includes all important approaches of that science	– over-emphasizing the importance of individual factors
	– information supply can be based on results of former agrometeorological research	– sometimes meteorological effects are treated as background noise by farmers
	– interdisciplinary nature of agrometeorology	– inexact data and information supply
		– the biological respects are usually in the rough in climate scenarios
External origin	***Opportunities:***	***Threats:***
	– growing need for interdisciplinary research	– current academic structures do not foster interactions between biological and physical scientists
	– more attention should be payed to investigation of agricultural impacts of global warming	– problems of educational and agricultural-advisory systems
	– former favorable experiences suggest that agrometeorological information supply can work in Hungary	– financial problems
	– the potential to handle data and information by computers and exchange them globally is growing	– legal and economical regulation of agricultural production does not always inspire use of agrometeorological information
	– high-level food production and food security need adequate information supply	– problems of observational networks
		– tendency for senescence of agrometeorological experts

2.1. Strengths

It can be stated that a permanently high level agriculture which always tries to make the best of its environmental potential can not be realized without using agrometeorological information. The must for agricultural information supply is

explained by multiple influences of atmosphere on agricultural production. In support of this, let us have a short review of relationship between meteorological factors and crop production.

The atmosphere can be considered as a system of terms and conditions for plant production. The climate fundamentally determines:

- which plants can not be grown in a given area (see the failed attempts for growing orange or cotton in Hungary in the 1950s),
- which species and varieties can be planted there, and
- in which period of the year are those plants able to grow (it could be basically decided if we compared the length of actual growing season of crops to beginning and end of potentially available growing season (in weather and climate respect)).

The atmosphere means also system of resources for agriculture. Plants are not able to produce organic matter without climatic resources (energy and substances) which come from – or through – the surrounding atmosphere. Amounts of factors which are required for both photosynthesis and respiration, such as water (precipitation), carbon dioxide, oxygene, carbohydrates, temperature, and photosyntheticallay active radiation, are significantly influenced by weather and climate.

The atmospheric factors work as a system of affecting factors for plants. Crops are constantly influenced by (meteorological) factors of their environment during the whole growing season. Intensity of life processes continually changes as a result of favorable or unfavorable, development accelerating or delaying, yield increasing or yield decreasing effects. More unfavorable values of meteorological elements cause more serious anomalies of life processes. Influences of meteorological elements below the lower or above the upper threshold values can be considered as damaging effects. The frequency of those marks production risk of varieties and hybrids. That is why the atmospheric relations are risk factors for farming as well (*Varga-Haszonits* and *Varga,* 1999).

There is a continuous must for decision-making in agricultural practice. The quality of decision-making determines the level of farming.

Decisions can be divided into two groups on the base of term of their implication. Strategic decisions are fundamental, directional, and over-arching. They affect long term goals. Tactical (or operational) decisions affect the day-to-day implementation of strategic decisions and are for short term. Strategy defines the "what" is to be done and tactics define the "how". Decision-making always needs information, but information requirements depend on kind of decision. Both tactical and strategic decisions of farming demand agrometeorological information. Tactical decisions need information about weather and short term forecast, however, strategic planning needs climatic information and long term forecast.

Farming success basically depends on the base of decision-making. Effectiveness of planning is influenced by thoroughness of the decision-maker. In this respect, decisions can be divided into the following groups: intuition-based decisions, past experience-based decisions, and decision based on professionally collected and processed data and scientific information. Intuition means instinctive and unconscious knowing without deduction or reasoning. This first group also includes decisions based on information of doubtful origin. Effectiveness of these decisions is low, but it is not zero. So we can make even good intuition-based decisions, but in this case we can not know why it works. All farming decisions without agrometeorological information belong to this group.

For the most part of past experience-based decisions, recent experiences are used. It is because of the fact that memory of bygone days fades from our minds. However there is no guarantee for similar meteorological conditions or effects of consecutive years. Sometimes climatic features of distant time periods are analogous. That is why this kind of decision is also a hazardous one. A further problem is that individual experiences are not able to give enough information for a complex approach of agrometeorological problems.

That complex approach is assured only by decisions based on professionally collected and processed data and scientific information. Scientific information supply developed from individual experiences by making those more objective, integrated, and verifiable (*Varga*, 2010). In the case of those decisions we also know probability of effectiveness for different alternatives. Effectiveness of these decisions is in general high, but it is not 100 %. So we can make even inexact scientific information-based decisions, but in this case we can search the source of the problem and it helps to make better decisions in the future.

For this reason, good agrometeorological decisions require exact data and information supply. The appropriate data come from professional agrometeorological observation networks or from laboratory or field experiments. The other two principal elements of agrometeorological information service are theoretical and methodical research and information service itself. These three elements have to be in close connection with each other, and all of them must depend largely on the agricultural requirements (*Varga-Haszonits,* 1983, 1997). Some typical characteristics of a functional agrometeorological information service are described in the following.

The basic element of the system is data collection. The efforts in various countries led to the recognition of a need for combining and coordinating phenological and meteorological observations. Data of professional network of meteorological observations combined with data from additional measurements of soil properties (temperature, moisture etc.) and with data from phenological and other agricultural observations provide an integrated database for research of atmosphere-soil-plant system. Agrometeorological information service can use all available observed or measeured data of controlled origin.

The data must be elaborated and analyzed. The detected false data have to be corrected or excluded from the database. Data analysis is a process of cleaning and transforming data. Afterwards, the analyzed data should be transformed into agricultural research or directly into agricultural information service. The goal of this process is highlighting useful agrometeorological information, suggesting conclusions, and supporting decision-making. It is important to send not data, but helpful information for users. This is the task – and strength – of agrometeorological service.

The objective of agrometeorological research is to study and numerically determine the influence of meteorological elements on plant development and yield of crops. The investigations in this field consist of the following research areas: agroclimatological studies, agromicrometeorological model research, elaboration of new agrometeorological forecasting methods, and verification of new results. The investigations include analysis of databases, field experiments, and laboratory experiments (*Varga-Haszonits,* 1983).

The data measured in these experiments are much more detailed than that of observational network, because those are measured by special instruments. Therefore, on the basis of these data, the atmosphere-(soil)-crop basic relationships can be elaborated and can be used as fundamental knowledge for agroclimatological modeling. The obtained relationships between meteorological factors and life processes of crops are fundamental knowledge for agrometeorological information service. The results have to be expressed in objective, mathematically exact terms which do not depend on the person giving information.

We can change mainly characteristics of plants and agricultural production technologies – as input parameters - in the case of field experiments, however, also modified weather conditions can be studied in laboratory experiments (in plastic tunnels or houses, greenhouses, climate chambers, or phytotrones). Therefore, field experiments allow examining the current agricultural production and laboratory experiments are suitable for also simulating and giving information about the future conditions of plant production.

The analysis of agroclimatological databases is based on long-term data series. These studies include investigations of climatic conditions of crop production and relationship between climate and agricultural production, as well as determination of regions or zones with different agroclimatologic characteristics and conditons. These surveys can use much longer but less detailed dataseries than that of agroclimatological experiments. In the case of building an agroclimatological database, it is very important to check the reliability of data sets of different origin.

Methodological investigations – including models for forecasting soil moisture, actual evapotranspiration, plant development, crop yield, etc. - allow detailed analysis of climate-agriculture relationship and help decision-making on the base of verified information.

The verification of methods means that we compare the values obtained by elaborated methods with the actual measured or observed values. The accuracy of results is measured by error of estimation – that is the difference between calculated and measured value – and then by studying the frequency of these errors. Verification is needed for determining the effectiveness of methods and effectiveness of decisions based on these proceedings. The practical objective of verification process is to improve the information quality and to reduce the probability of false decisions.

The practical importance of agrometeorology depends on quantity and quality of information presented for agricultural producers. But agrometeorological information service could not be qualified as not satisfactory if its results are not used in practical decisions. It is because the use of information devolves on producers. To supply information to agriculture, it is necessary to analyze the biological and meteorological data and transform them into agricultural information. In the process of analysis, numerical characteristics of meteorological and phenological elements are calculated, tables and figures are prepared. In the process of preparation of information, the knowledge obtained from data analysis is drafted into answers concerning the meteorological effects on agricultural operations and on crop life (*Dmitrenko*, 1971). Information service can include information about past, present, and expected future meteorological effects on agricultural production. The answers can be published in rather different forms: orally or in writing, in television, in radio, on internet, in newspapers, in agrometeorological bulletins etc.

There are some criteria for servicing directly applicable information. The most important ones are the following:

- An information is more valuable than others if it has not only more accuracy, but also longer time interval between the date of issue and the beginning of practical use of information.
- The information must be drafted in agricultural terms as it is used by agricultural producers.
- The probability of decision alternatives should be known.

If we suppose that:

- a given problem of agricultural production depends on weather conditions, and
- required information is provided by agrometeorological information service, and
- we have methods for problem solving,

then we could choose one of the three possibilities:

- adapting agricultural production to meteorological conditions, or
- mitigating the unfavorable meteorological effects, or
- modification of meteorological factors.

Adaptation is the type of decision when we try to avoid plant damages. Several examples can be mentioned for this. Agricultural production can be adapted to climatic conditions by cautious choosing of:

– plant species, varieties, hybrids,

– cultivation area,

– date of sowing or planting, and

– agrotechnical processes

of agricultural production.

Mitigation means reducing unfavorable effects of environmental factors. If we are not able to prevent susceptible crop from meeting extreme meteorological effects (by the help of adaptation techniques), then we should try to minimize the damages suffered. Two kinds of mitigation can be mentioned from agrometeorological point of view: prevention of direct and indirect effects of meteorological elements. Damages can be caused by single meteorological elements (e.g., frost) and by combined meteorological effects (e.g., drought). They exert a harmful influence on plants directly, therefore, they are called damaging factors with direct effect. There are cases when the meteorological factors cause loss to the agricultural production indirectly, that is when meteorological conditions are favorable for those factors (e.g., plant diseases) which reduce productivity (*Varga-Haszonits*, 1983). Both types of mitigation can be applied only based on agrometeorological information.

Modification means effectively influencing meteorological factors to make those more favorable for cultivated crops. Theoretically, modification of meteorological conditions can be achieved in three levels: macro-, meso-, and microscale meteorological elements can be changed. But because of lack of energy and lack of exact information about feedbacks of the system, it is impossible to modify macroclimate. Opportunities for successful mesoclimatic modifications are also limited, but use of shelterbelt planting or preventing hail can be mentioned in this field. Methods for modification of micrometeorological environment, such as using various reflective materials, changing orientation and width of the crop rows, companion planting system, etc., are commonly used in agricultural practice. Using all kinds of controlled-environment facilities, such as greenhouses, phytotrones, etc., means an effective form of modification. These plant-growth chambers would provide the most ideal conditions also for commercial production, but these facilities function primarily as research tools.

It should be emphasized that all the environmental factors are interrelated; therefore, any attempt to modify one parameter may influence the others as well; for example the higher air humidity conditions of irrigated fields are favorable for plant diseases. This is the reason why quality of information should be important in decision-making. Without decisions based on professionally collected and processed data and scientific

information, only schematic farming with higher risk can be realized which ignores actual variability of weather conditions and effects.

Advances in weather forecasting and computer technology have improved the potential of farmers to prepare and adjust farming operations in response to climatic variations. For this potential to be realized, the complexity of decision-making in agricultural systems needs to be acknowledged, and the challenges facing farmers in accessing and learning to apply agrometeorological information need to be addressed (*Mavi* and *Tupper,* 2004).

Hungarian agrometeorological research includes all important approaches of this science: agroclimatology, agromicrometeorology approached in an inductive way, and agromicrometeorology approached in an analytic and deductive way (*Szász,* 1997). In addition, research activity of different agrometeorological departments concerns different ecological conditions of our country. This complexity of domestic agrometeorological research can be considered as strength.

2.2. Weaknesses, limitations

Sometimes it is quite difficult to give the required agrometeorological information for producers because of the stochastic relationships of soil-atmosphere-agriculture system. The farming is exposed to random effects among which the meteorological factors have an important role. In the agricultural production it can not be foreseen, whether we can achieve the wanted purpose or not, and if we can, with what kind of accuracy. Weather factors can cause a wide fluctuation in the yield, so that the role of random effects is very important in every case. The yield fluctuations of improved varieties or hybrids are greater than that of traditional varieties. The year-to-year differences in yield of improved varieties are sometimes greater than the total yield value of old varieties (*Varga-Haszonits* and *Varga*, 1999).

The further specific feature of the soil-atmosphere-agriculture system is its exposure to synchronous effect of different external and internal factors. The productivity of plants is influenced by biological, genetical properties, applied agrotechnical methods, soil and weather conditions. These complex synchronical effects are realized by direct and indirect processes. Therefore, it is difficult to separate the effect of a single factor. Another special biological feature, the so-called seasonality makes agrometeorological information supply more difficult. It means that crops respond differently to meteorological effects during various phenological stages (*Varga-Haszonits,* 1983).

Over-emphasizing the importance of individual factors of production levels defined by de Wit (*de Wit* and *van Keulen*, 1987; *Goudrian* and *van Laar*, 1994) and leaving the stochastic relationships of soil-atmosphere-agricultural production system out of consideration also may cause problems. This way, agrometeorological information could be considered unnecessary.

According to *Cousens* and *Mortimer* (1995), many farmers regard meteorological conditions as unpredictable and beyond their control. Yearly variations are usually treated as background noise and are ignored.

As we mentioned before, the good agrometeorological decisions require professionally gathered data and data-based information supply. It suggests that if:

– used data or information are of unchecked source, or

– farmers use their own (agro)meteorological data schematically (to reduce costs of production), or

– information supply is independent from the agricultural requirements, or

– data are not transformed into agricultural information,

then agricultural decisions would not be able to use agrometeorological information actually.

The biological respects are usually in the rough in climate scenarios, which are the main tools for the assessment of future developments in the complex climate-agriculture system. It is often ignored that not only the atmospheric conditions but also the agricultural ones could be dynamically changing systems when analyzing hypothetical relationships between climate and agriculture. Therefore, yield responds on climatic changes should be interpreted circumspectly (*Kocsis* and *Anda,* 2010). It also emphasizes that an agrometeorologist have to be fluent in both the biological and physical sciences and have to look at the world from a different and wider perspective than the physical and biological scientist does (*Mavi* and *Tupper*, 2004). That is why we can state that the interdisciplinary nature of agrometeorology – and agrometeorological information supply – is both its greatest strength and its greatest weakness (*Hollinger*, 1994).

2.3. Opportunities

As we could see earlier, agrometeorological research and agrometeorological information supply are in strong relationship with each other. Information supply about effects of a dynamically changing atmospheric system on a constantly developing farming system can be done only on the base of continuous agrometeorological research activities. It is the reason why it is practical to review the opportunities of agrometeorological research and information service jointly.

In recent decades, interdisciplinar research became more and more important, because problems may cut right across the borders of any discipline *(Popper,* 1963). The interdisciplinar approach of agrometeorology is well-known, and it can be advantageous in this respect.

The study of climate change can be identified as research priority because of its global impacts. It is like enough that more attention should pay to investigation of agricultural impacts of global warming in the future.

Moreover, favorable experiences of agrometeorological information service during 1967–1990 suggest that it can work again in Hungary.

The potential to handle data and information by computers and exchange them globally via the internet is growing continuously.

Progressing food production supported rise and development of human civilization. High-level food production and food security need adequate information supply – especially when environmental conditions are changing, resources are limited, and human population growth is increasing.

2.4. Threats

Agrometeorological information supply has to face several problems which originate from its external relations.

- There is no need for B.Sc. or M.Sc. degree in agricultural science for farming in Hungary. It can cause problems in the quality of decision-making.
- Most of domestic agricultural BSc and MSc courses do not contain agrometeorological studies. Therefore, not even a qualified agronomist can realize the importance of using agrometeorological information.
- Neither Hungarian agricultural-advisory system includes agrometeorological information supply.
- Legal and economical regulation of agricultural production does not always inspire use of agrometeorological information.
- Hungarian farmers are not interested in agrometeorological information service because of their financial problems.
- Current academic structures do not foster interactions between biological and physical scientists.
- Both the Hungarian Meteorological Service and the agricultural faculties including agrometeorological departments or groups have financial problems.
- Financial problems influence also observational (meteorological and phenological) networks.
- There is not any gradual or postgradual course in agrometeorology in Hungary.

All the above threats originate in financial and organizational problems.

Average age of Hungarian agrometeorologists is about 54.5 years, two-third of them are over 50, one-third of them are over 60 years according to a

study written by Anda for the Agrometeorological Committee of Hungarian Academy of Sciences (URL[2]). This tendency for senescence is also a threat of agrometeorological research and information supply. It could be compensated by agrometeorological training programs, but it is far from a solution yet.

3. Summary

Agricultural production and human civilization developed in parallel in the Holocene. The intense farming activities of our early agrarian ancestors improved food supply, and thus, opened up a new prospect for social processes (*Behringer*, 2010). *Ruddiman* (2003) – modifying Crutzen`s "anthropocene" theory (*Crutzen et al.,* 2000 cit. *Behringer,* 2010; *Crutzen* and *Steffen,* 2003) – thinks that human-induced changes in greenhouse gases did not begin in the eighteenth century with advent of coal-burning factories and power plants of the industrial era, but date back to 8,000 years ago, triggered by increasing agricultural production. These theories suggest that the relationships between climate, agriculture, and society are more complex than we supposed it before. Agriculture needs meteorological information not only for increasing productivity, but also for reducing environmental damages.

The global warming tendency means both opportunity and threat for us. *Behringer* (2010) distinguishes between warm and cold periods of the Holocene and highlights the ability of agricultural production to adapt to climatic changes. He rates warm periods positively and cold periods negatively. On the other hand, climate change forces adaptation of farming for it. It is expected that modern farming systems should produce big amount and high quality yields under changing climatic conditions – in an economically reasonable and sustainable way. Adaptation strategies require professionally gathered meteorological and phenological data and data-based information supply.

In this study, advantageous and disadvantageous internal features and external relations of agrometeorological information service were analyzed by means of a SWOT analysis. It was found that several and significant strengths and opportunities enable agrometeorological research and information supply to help agricultural decision-making effectively.

Weaknesses originate in complex and stochastic nature of the atmosphere-soil-plant system, that makes difficult to give the required agrometeorological information, and in inadequate working of agrometeorological information supply. Threats include educational, organizational, and financial problems.

Acknowledgement–The author would like to thank for the support of TÁMOP-4.2.2A-11/1/KONV-2012-0003 project.

References

Behringer, W., 2010: A klíma kultúrtörténete. Corvina Kiadó, Budapest. (in Hungarian)

Bernal, J.D., 1963: Tudomány és történelem. Gondolat Kiadó, Budapest. (in Hungarian)

Cousens, R. and *Mortimer, M.*: 1995: Dynamics of weed populations. Cambridge University Press, Cambridge.

Crutzen, P.J. and *Steffen, W.*, 2003: How long have we been in the Anthropocene Era? *Climatic Change 61*, 251–257.

de Wit, C.T. and *van Keulen, H.*, 1987: Modelling production of field crops and its requirements. *Geoderma 40*, 253–265.

Dmitrenko, V.P., 1971: Features of agrometeorological service (in Russian). *Trudi UNIGMI. 109*, 37–49.

Goudrian, J. and *van Laar, H.H.*, 1994: Modelling potential crop growth processes. Textbook with exercises. Kluwer Academic Publishers, Dordrecht.

Hollinger, S.E., 1994: Future directions and needs in agricultural meteorology/climatology and modeling. *Agr. Forest Meteorol. 69*, 1–7.

Kocsis, T. and *Anda, A.*, 2010: A légköri nyomgázok hatása: az üvegházhatás és fokozódásának következményei. In (eds.: *Anda, A., Kocsis, T.*): Agrometeorológiai és klimatológiai alapismeretek. Mezőgazda Kiadó, Budapest. 36–74. (in Hungarian)

Mavi, H.S. and *Tupper, G.J.*, 2004: Agrometeorology: principles and applications of climate studies in agriculture. Food Products Press, London.

Ministry of Agriculture and Food Administration, Hungarian Meteorological Service 1974: Agroclimatology and plant production. Budapest.

Popper, K.R., 1963: Conjectures and refutations: the growth of scientific knowledge. Routledge and Kegan Paul, New York.

Ruddiman, W.F., 2003: The Anthropogenic Greenhouse Era began thousands of years ago. *Climatic Change 61*, 261–293.

Szász, G., 1997: A mikroklíma fogalma. In (eds: *Szász, G., Tőkei, L.*) Meteorológia mezőgazdáknak, kertészeknek, erdészeknek, Mezőgazda Kiadó, Budapest, 264–342. (in Hungarian)

Székely, Cs., 2000: Stratégia és tervezés. In: (eds.: *Buzás, Gy., Nemessályi, Zs., Székely, Cs.*) Mezőgazdasági üzemtan I., Mezőgazdasági Szaktudás Kiadó, Budapest. 237–271. (in Hungarian)

Varga, Z. 2010: Az agrometeorológiai információk hasznosításának alapjai. In (eds.: *Anda, A., Kocsis, T.*): Agrometeorológiai és klimatológiai alapismeretek. Mezőgazda Kiadó, Budapest, 291–314. (in Hungarian)

Varga-Haszonits, Z., 1967: Útmutatás kulturnövényfenológiai megfigyeléskre. OMI. Budapest.(In Hungarian)

Varga-Haszonits, Z., 1983: Agroclimatology and agrometeorological forecasting. Lecture notes. Budapest.

Varga-Haszonits, Z., 1997: Agrometeorológiai információk és hasznosításuk. In (eds: *Szász, G., Tőkei, L.*) Meteorológia mezőgazdáknak, kertészeknek, erdészeknek, Mezőgazda Kiadó, Budapest. 651–679.

Varga-Haszonits, Z. and *Varga, Z.*, 1999: Agroklimatológia (Climate and crop production). Lecture notes. Mosonmagyaróvár. (in Hungarian)

URL[1]: http://en.wikipedia.org/wiki/SWOT_analysis

URL[2]: http://www.mettars.hu/wp-content/uploads/2010/09/Anda100831.pdf

INSTRUCTIONS TO AUTHORS OF *IDŐJÁRÁS*

The purpose of the journal is to publish papers in any field of meteorology and atmosphere related scientific areas. These may be

- research papers on new results of scientific investigations,
- critical review articles summarizing the current state of art of a certain topic,
- short contributions dealing with a particular question.

Some issues contain "News" and "Book review", therefore, such contributions are also welcome. The papers must be in American English and should be checked by a native speaker if necessary.

Authors are requested to send their manuscripts to

Editor-in Chief of IDŐJÁRÁS
P.O. Box 38, H-1525 Budapest, Hungary
E-mail: journal.idojaras@met.hu

including all illustrations. MS Word format is preferred in electronic submission. Papers will then be reviewed normally by two independent referees, who remain unidentified for the author(s). The Editor-in-Chief will inform the author(s) whether or not the paper is acceptable for publication, and what modifications, if any, are necessary.

Please, follow the order given below when typing manuscripts.

Title page: should consist of the title, the name(s) of the author(s), their affiliation(s) including full postal and e-mail address(es). In case of more than one author, the corresponding author must be identified.

Abstract: should contain the purpose, the applied data and methods as well as the basic conclusion(s) of the paper.

Key-words: must be included (from 5 to 10) to help to classify the topic.

Text: has to be typed in single spacing on an A4 size paper using 14 pt Times New Roman font if possible. Use of S.I. units are expected, and the use of negative exponent is preferred to fractional sign. Mathematical formulae are expected to be as simple as possible and numbered in parentheses at the right margin.

All publications cited in the text should be presented in the *list of references*, arranged in alphabetical order. For an article: name(s) of author(s) in Italics, year, title of article, name of journal, volume, number (the latter two in Italics) and pages. E.g., *Nathan, K.K.,* 1986: A note on the relationship between photo-synthetically active radiation and cloud amount. *Időjárás 90,* 10-13. For a book: name(s) of author(s), year, title of the book (all in Italics except the year), publisher and place of publication. E.g., *Junge, C.E.,* 1963: *Air Chemistry and Radioactivity.* Academic Press, New York and London. Reference in the text should contain the name(s) of the author(s) in Italics and year of publication. E.g., in the case of one author: *Miller* (1989); in the case of two authors: *Gamov* and *Cleveland* (1973); and if there are more than two authors: *Smith et al.* (1990). If the name of the author cannot be fitted into the text: *(Miller,* 1989); etc. When referring papers published in the same year by the same author, letters a, b, c, etc. should follow the year of publication.

Tables should be marked by Arabic numbers and printed in separate sheets with their numbers and legends given below them. Avoid too lengthy or complicated tables, or tables duplicating results given in other form in the manuscript (e.g., graphs).

Figures should also be marked with Arabic numbers and printed in black and white or color (under special arrangement) in separate sheets with their numbers and captions given below them. JPG, TIF, GIF, BMP or PNG formats should be used for electronic artwork submission.

Reprints: authors receive 30 reprints free of charge. Additional reprints may be ordered at the authors' expense when sending back the proofs to the Editorial Office.

More information for authors is available: journal.idojaras@met.hu

Published by the Hungarian Meteorological Service

Budapest, Hungary

INDEX 26 361

HU ISSN 0324-6329